ABSTRACT

Title of Dissertation: EXPERIMENTAL VALIDATION OF TRAC-RELAP ADVANCED COMPUTATIONAL ENGINE (TRACE) FOR SIMPLIFIED, INTEGRAL, RAPID-CONDENSATION-DRIVEN TRANSIENT

Anthony Gerard Pollman, Doctor of Philosophy, 2011

Dissertation directed by: Professor Marino di Marzo
Department of Fire Protection Engineering

The purpose of the present work is to experimentally validate the TRACE (TRAC-RELAP Advanced Computational Engine) plug-in of the Nuclear Regulatory Commission's (NRC's) Symbolic Nuclear Analysis Package (SNAP) for rapid condensation transients. These transients are challenging for the code.

The experimental phase began by constructing and calibrating a simplified, integral, condensation-driven transient apparatus named the UMD-USNA Near One-dimensional Transient Experimental Assembly (MANOTEA). Then, a series of 5 well-defined transients were run. Data from the facility included: pressure, differential pressure, and temperature, all as a function of time. Using the data, mass and energy balances were closed for each experiment. Some of the relevant characteristics of the data included: inverted thermal stratification and nozzle dependent transients controlled by an energy partition. A common transient sequence was identified and served as the fundamental comparison to evaluate TRACE.

The second phase began by developing a 1-dimensional Base TRACE Model. Output from the Base Model was found to over-estimate the pressures and temperatures observed in the experiment. This Model always predicted that the condenser pipe would fill, and that transients would terminate with a non-physical discontinuity. In an effort to improve the model, a list of phenomena was generated and then mapped to TRACE parameters. The goal was to find unique ways to capture the energy partition and prevent the condenser from filling. Over 250 TRACE cases were run, and the effective and physically justifiable parameters were incorporated into a 3-dimensional Final TRACE Model. The Final Model incorporated non-condensable gases, which provided a mechanism to terminate the transients smoothly. Replacing the PIPE component with a VESSEL component provided a way to model the energy partition. The Final Model under-predicted trends observed in the experiments. Thus, the two models were able to bracket the experimental data.

Comparing TRACE output to the data led to the conclusion that the code's condensation model is over-stated. TRACE's predecessors were also known to have over-stated condensation models. As a result, TRACE will over-predict condensation-induced fluid motion when modeling several thermal-hydraulic situations important to safe nuclear reactor operation. Future work could focus on developing a NOZZLE component for TRACE, comparing the subsequent output to MANOTEA data and improving the TRACE condensation model.

EXPERIMENTAL VALIDATION OF TRAC-RELAP ADVANCED COMPUTATIONAL ENGINE (TRACE) FOR SIMPLIFIED, INTEGRAL, RAPID-CONDENSATION-DRIVEN TRANSIENT

by

Anthony Gerard Pollman.

Dissertation submitted to the Faculty of the Graduate School of the
University of Maryland, College Park, in partial fulfillment
of the requirements for the degree of
Doctor of Philosophy
2011

Advisory Committee:

Doctor Marino di Marzo, Chair
Doctor Karen Vierow
Doctor Amr Baz
Doctor Ken Kiger
Doctor Gary Pertmer, Dean's Representative

TABLE OF CONTENTS

LIST OF TABLES

LIST OF FIGURES

LIST OF SYMBOLS

Symbols

Bi	Biot number
c	specific heat
D	diameter
E	energy
f	participating fraction
H	enthalpy
h	specific enthalpy
K, k	nozzle proportionality constant
L, *l*	length
m	mass
P, p	pressure, ratio of pressures
q	heat transfer per unit mass
R	gas constant
Ra	Rayleigh number
T	temperature
t	time
U	internal energy

Subscripts

D	diameter
f	final
g	gas
i, o	initial
L, *l*	liquid
m	metal
P	pipe
sat	saturated
sp	spray
v	vapor

Greek

Δ	change (final - initial value)
Λ	$h_f - h_g$
χ	proportionality constant

Abbreviations

1D	1 dimensional
3D	3 dimensional
BC	boiler centerline
BS	boiler surface
BWR	boiling water reactor
CC	condenser centerline
CCDPHE	counter-current, double-pipe heat exchanger
CS	condenser surface
DP	differential pressure
DPHE	double-pipe heat exchanger
EZNFXXYY	EZNF: Bete nozzle designator, XX: diameter, YY: spray characteristic
ID	inner diameter
LOCA	loss of coolant accident
MANOTEA	UMD-USNA Near One-dimensional Transient Experimental Assembly
NRC	Nuclear Regulatory Commission
PWR	Pressurized Water Reactor
RELAP	Reactor Excursion and Leak Analysis Program
SETS	Stability Enhancing Two-step Techniques
SNAP	Symbolic Nuclear Analysis Program
TRAC	Transient Reactor Analysis Code
TRACE	TRAC-RELAP Advanced Computational Engine
TRAC-B	TRAC-BWR
TRAC-P	TRAC-PWR
UMD	University of Maryland
USNA	U. S. Naval Academy
WYSIWYG	what you see is what you get

Chapter 1: Introduction

Significance of Present Study

The purpose of the present work was to experimentally validate the TRAC(Transient Reactor Analysis Code)/RELAP (Reactor Leak Analysis Program) Advanced Computational Engine (TRACE) plug-in for the NRC's Symbolic Nuclear Analysis Package (SNAP) for a rapid condensation transient on a simplified, integral apparatus with behaviour similar to those found in reactor systems. SNAP is the "flagship" code of the U.S. Nuclear Regulatory Commission (NRC) and the sole tool used to perform analysis and to certify new reactor designs (NRC, 2011b). The TRACE plug-in is designed to analyze thermal-hydraulic system transients in light water reactors (NRC, 2011b). The challenges that integral, condensation-driven transients have posed to thermal-hydraulic codes provided the motivation for the present work. The present work is particularly relevant because many of the proposed passive safety systems found in next generation reactors rely on rapid condensation for operation or accident mitigation. Although clearly a "beyond design basis accident", the recent sequence of events at the Fukushima Power Plant in Japan highlights the continued relevance of reactor safety research efforts and accident mitigation in general.

Approach and Objectives

The present work was undertaken in two phases: an experimental and modeling phase. Data from the experimental phase was compared to output from a

TRACE model. Discrepancies between the data and the code output were used to identify potential problem areas in the code. Recommendations for potential ways to improve the code were then made based on this analysis.

In order to implement this approach, the following objectives were identified:

- Construct, instrument and calibrate an integral, condensation-driven transient apparatus.
- Run a series of scoped experiments on the apparatus in order to identify transient mechanisms and build a database.
- Develop a TRACE model of the transient apparatus.
- Make recommendations for code improvement by comparing experimental data to TRACE output.

Dissertation Organization

This dissertation is organized into two main parts. Prior to the first part, Chapter 2 is a literature review and introduces relevant topics. The first part encompasses Chapters 3-8 and presents the details of the experimental portion of the present work. The second part outlines efforts to model the experiment with TRACE and encompasses Chapters 9-14. The final chapter draws conclusions from the experimental and modeling portions, and makes recommendations based on these conclusions.

Chapter 2: Literature Review

Integral Transients

Over the years, the study of nuclear power plant accidents has evolved and matured from hypothetical scenarios, which were defined by imposed assumptions, to accident development sequences which maintain a physically coherent sequence of events. Some of these sequences were later characterized as the "design basis accidents." Abramson (1985) generalized the information available about Small Break- Loss of Coolant Accidents (SB-LOCAs) by suggesting a sequence of physical events, complete with descriptions, which can be expected for transients during which primary inventory is gradually lost. In a similar manner, Duffey and Sursock (1987) traced the progression of an SB-LOCA in terms of system flow characteristics. As part of the U.S. NRC's Integral Systems Test (Young and Sursock, 1987), Di Marzo and co-workers (1988) showed that a portion of an SB-LOCA is controlled by rapid condensation occurring near saturation conditions. The definition of rapid condensation usually includes the requirement that the induced fluid motion be limited by fluid inertia rather than by the heat transfer rate (Block, 1980). These works highlight the integral nature of an SB-LOCA, meaning the current state is the cumulative result of all the previous states encountered in sequence. Furthermore, the fundamental parameter characterizing each state is how much inventory has left the system.

Rapid Condensation

Rapid condensation induced fluid motion is not limited to SB-LOCAs, but occurs in numerous other accidents sequences and operating situations. Block (1987), Bankoff (1980), and Kirchner and Bankoff (1985) each wrote overview papers summarizing condensation induced fluid motion relevant to nuclear reactors. As outlined in these papers, typical examples include: water slug delivery in an annular downcomer, steam discharge into large pools of subcooled water like those found in a suppression tank, cold leg oscillations induced by an Emergency Core Cooling (ECC) injection, "reflux" condensation oscillations in U-tube steam generators, and the condensation induced oscillations due to combined injection of ECC liquid into both the hot and cold legs. These transient event sequences are complicated to analyze because they involve 2-phase flow and 3-dimensional geometry coupled with the integral effects. Historically, these multi-phase, multi-dimensional, integral transients have proven challenging for thermal-hydraulic computer codes such as those used for design certification (Wang, 1992).

Rapid Condensation in Generation III+ Reactors

The U.S. Department of Energy (DOE) classifies the evolution of nuclear reactor designs in terms of "generations" (Nuclear, 2002). Generation I reactors were the early prototypes (Shippingport, Dresden, Fermi I, and Magnox). Developed during the 1950s and 60s, these reactors were typically smaller-scale, proof-of-concept, research reactors. Lessons learned from these reactors paved the way for the development of large-scale, commercial, power generation reactors in the 1970s. These reactors are classified as Generation II and comprise all 104

commercial reactors currently operating in the United States (Nuclear Energy Institute, 2011). Generation III reactors were developed in the 1990s. Primarily built in East Asia, this generation of reactors modified Generation II designs to improve safety and efficiency (Nuclear, 2002). Generation III+ reactors are those currently under development and expected to be built in the near-term. This generation includes the Advanced Passive 1000 Reactor (AP1000) and Economic Simplified Boiling Water Reactor (ESBWR). Some details of these particular reactors are outlined below. Generation IV reactors are those that the Department of Energy would like to develop in partnership with 9 other countries coming together as the Generation IV International Forum (GIF). The goal of the GIF is to develop proliferation resistant, highly economical reactors with enhanced, passive safety features and minimal waste. Such reactors are not intended to meet the immediate need for power production, but rather to serve as the next generation (Nuclear, 2002). The Westinghouse AP1000 and General Electric ESBWR are two generation III+ reactors that incorporate rapid condensation passive safety features.

Westinghouse AP1000

The Westinghouse Advanced Passive 1000 (AP1000) is a pressurized water reactor designed to generate 1000 $MW_{electric}$ from 3415 $MW_{thermal}$. It contains many features not found in current operating reactors. The most significant improvement is use of safety systems that employ passive means such as gravity, natural circulation, condensation and evaporation heat transfer, and stored energy for accident mitigation. These passive systems perform safety injection, residual heat removal, and containment cooling functions (Schulz, 2006).

Based on analysis of the design with SNAP, the NRC issued a final design certification for the AP1000 in January of 2006. To date, 14 combined operating licenses applications have been received by the NRC for construction of AP1000 units in the U.S. Numerous reactors have also been ordered for construction in China (NRC, 2011b).

General Electric ESBWR

The General Electric-Hitachi Economic Simplified Boiling Water Reactor (ESBWR) is designed to operate at 4500 $MW_{thermal}$. The design builds on experience gained from the company's Advanced Boiling Water Reactor (ABWR) which was issued a final design certification by the NRC in 1997 (NRC, 2011b). The new design contains many features not found in current operating reactors to include the use of natural circulation for normal operations. The ESBWR also uses passive means for accident mitigation (Beard, 2006).

General Electric-Hitachi submitted an application for standard design certification to the NRC in 2005. The NRC is currently reviewing and analyzing the design. In anticipation of design approval, 3 combined operating license applications have already been received by the NRC. Overseas interest in this design is expected to be great (NRC, 2011b).

Integral Experiments and Code Development

In the wake of Three Mile Island, reactor safety research took on a new sense of urgency. The Nuclear Regulatory Commission (NRC) began placing greater emphasis on operator training and human factors, emergency planning, plant operating histories, and severe, non-design basis accidents resulting from small

equipment failures. Due to the nature of the Three Mile Island Accident, major effort was dedicated to investigation of SB-LOCAs in particular (NRC, 2011b). This renewed interest provided the motivation for a period of concentrated reactor safety research, which is still relevant today.

The NRC has funded multiple experiments to classify and quantify steady state and transient behavior in reactor systems. Data from facilities like Semiscale (Loomis, 1987), Flecht-Seaset (Hochreiter, 1985), PKL (Hass, 1982), LOFT (Nalezny, 1985), MIST (Geissler, 1987), and the UMCP Thermal-hydraulic Loop (Hsu, 1987) were used to develop, modify, and validate thermal-hydraulic reactor safety codes. These codes included, but were not limited to, the Reactor Excursion and Leak Analysis Program (RELAP) and Transient Reactor Analysis Code (TRAC), both of which focused on thermal-hydraulic analysis.

Since their inception, improvement and development of these analysis codes has been continuous. The NRC distributes the latest versions of its codes as the Symbolic Nuclear Analysis Package (SNAP). The package consists of an integrated, interoperable series of "plug-in" applications that are designed to simplify engineering analysis of reactor systems. These plug-ins were developed from legacy codes such as RELAP and TRAC (which were merged into a single thermal-hydraulic code and renamed TRAC-RELAP Advanced Computational Engine or TRACE). Other legacy codes such as the Purdue Advanced Reactor Core Simulator (PARCS) and Systems Analysis Programs for Hands-on Integrated Reliability (SAPHIRE) were also included in the package. Through the use of these plug-ins, SNAP is able to

analyze and synthesize all aspects of reactor operations. The package is the sole analysis tool used in modeling the behavior of new reactor designs (NRC, 2011b).

Since design certification is performed solely by computer code, it is of the upmost importance that the code be able to accurately predict steady state and transient behaviors in reactor systems. Inability of the codes to properly model reactor behavior has serious implications and hinders our ability to properly train operators, regulate, and address safety concerns. To ensure the analysis tools are of the highest quality and can be used with the strictest confidence, the NRC encourages users to challenge the code by comparing its predictions to data from a wide range of applications to include novel designs and non-nuclear apparatus (NRC, 2011a). Regular challenges and identification of areas for improvement ensure the code is adequate to perform the certification mission. The present work is meant to challenge the code for condensation transients. This work is useful because many new features found in Generation III+ reactors rely on condensation.

Reactor behavior is extremely complex. To capture elements of this behavior, a simplified apparatus has been constructed. The design of this apparatus is outlined in Chapter 3. Due to its simplicity, the apparatus is easier to model with TRACE, but still has behaviors similar to those of the more complex reactor system. If TRACE can properly predict the behavior of the simplier facility, it lends confidence to the code's abilities to properly predict reactor behavior.

PART 1: EXPERIMENT

Chapter 3: Facility Description

Apparatus

Figure 1 is a schematic drawing of the University of **M**aryland-United States Naval **A**cademy **N**ear **O**ne-dimensional **T**ransient **E**xperimental **A**pparatus (MANOTEA). MANOTEA was constructed at the United States Naval Academy during the summer of 2010. The facility consists of a boiler pipe, counter-current double-pipe heat exchanger, condenser pipe, and appropriate data acquisition and data logging systems (not shown in Figure 1).

The boiler pipe (6.40 *m* tall, 76.2 *mm* ID, 82.6 *mm* OD) is constructed from 2 commercially available, 3.05 *m*, schedule 40, carbon steel pipes held together by a threaded coupling and capped at the ends with threaded flanges. Blanks were machined for instrumentation and other fittings. These blanks were then bolted to the top or bottom flanges, respectively. High temperature O-rings ensure a proper seal. The exterior of the pipe is insulated with 50.8-*mm*-thick, fiberglass pipe insulation. A 1.00 *kW* ohmic heater is mounted in the bottom flange. The boiler pipe contains 3 centerline and 3 exterior surface thermocouples located at 0.30 *m*, 3.35 *m*, and 6.10 *m* (nominally: 1', 11', and 21' or axial locations 1, 11, and 21 on Figure 1) from the bottom flange, respectively. A pressure transducer is mounted to a T-valve (Valve A) in the top flange. The three-way valve allows the boiler to be vented to the atmosphere or connected to the transducer. The top flange also contains an opening for filling the apparatus with water. The bottom flange contains a valve (Valve X)

and copper tubing which allows water to be moved back and forth between the boiler and condenser pipes or for the system to be drained.

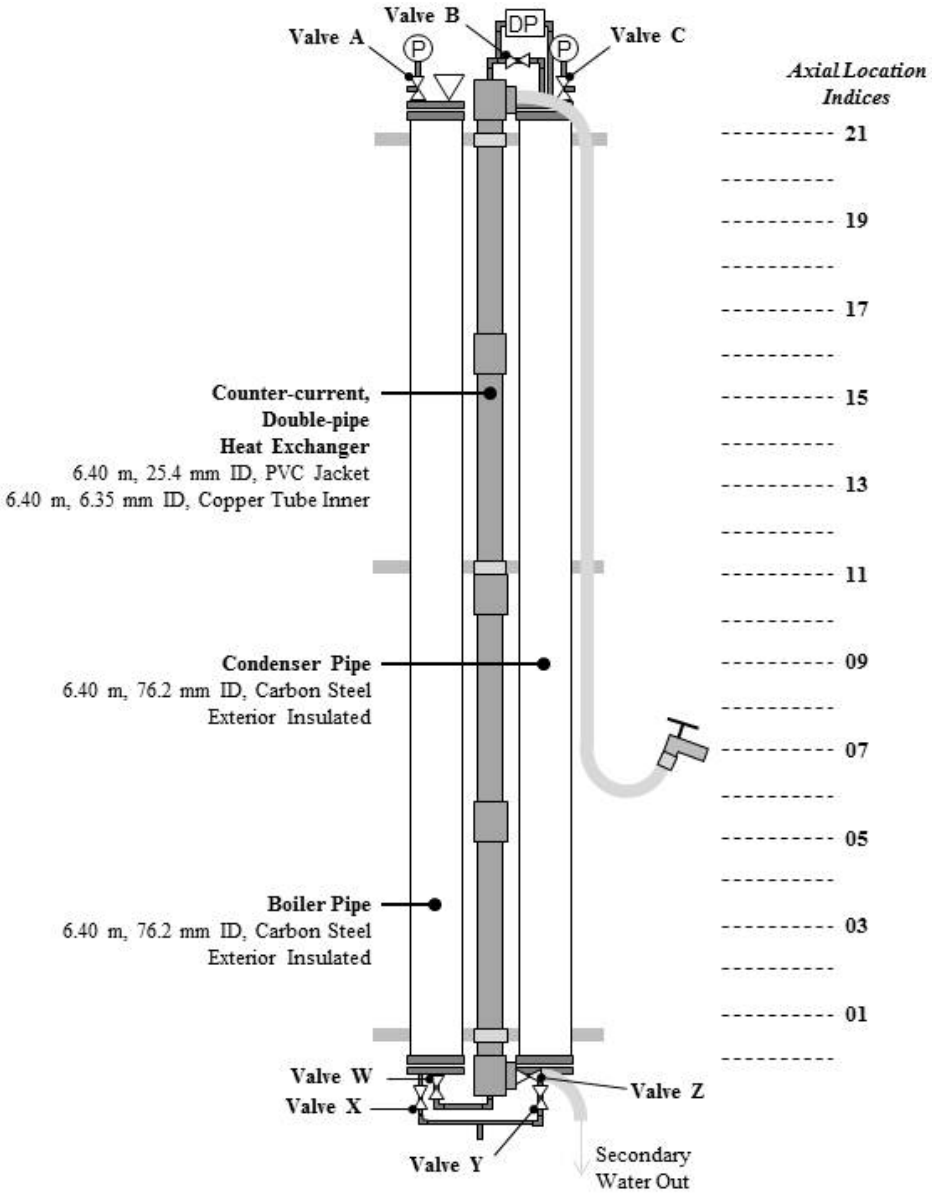

Figure 1. Schematic drawing of the University of Maryland – United States Naval Academy Near One-dimensional Transient Experimental Apparatus (MANOTEA).

The counter-current double-pipe heat exchanger (DPHE) is constructed of PVC (25.4 *mm*, schedule 80) and copper tubing (6.35 *mm* ID). Tap water enters the secondary side through the top of the PVC outer pipe and exits through the bottom into a drain. Warm water from the boiler enters the primary side through the bottom via copper tubing and exits at the top through a solenoid valve (Valve B) on its way to a nozzle in the vapor space of the condenser pipe. A thermocouple measures the temperature of the primary fluid as it exits the DPHE. The heat exchanger is sufficiently long with a secondary flow rate that ensures the primary fluid exits as highly sub-cooled liquid ($\sim 20^{o}C$). A differential pressure cell (annotated as "DP" on Figure 1) with one tap in the copper tubing as it exits the DPHE and one tap in the vapor space of the condenser provides a means for measuring primary inventory flow rate at the nozzle.

The condenser pipe is nearly identical to the boiler pipe – except it contains 11 centerline and 11 exterior surface thermocouples and the fill hole is replaced by one of the differential pressure cell taps. The first thermocouple pair is located at 0.30 *m* from the bottom flange and each successive pair advances up the length of the pipe in 0.61 *m* increments (axial locations 1, 3, 5…17, 19, 21, respectively). Scoping experiments revealed that MANOTEA transients are condensation-controlled and that a denser distribution of thermocouples would be required in the condenser to adequately capture the relevant phenomena. The condenser and boiler pipes have an aspect ratio of 84.

MANOTEA is not scaled to an actual reactor system or a feasibility study for a future design. Rather, it is designed to be a simplified, integral, rapid condensation

transient device. Such transients have been a challenge to reactor safety codes. Yet, condensation controlled phenomena are found in current and proposed reactor safety systems. Reactors systems are extremely complex. MANOTEA is simple enough that human reasoning and simple models can still capture its behavior, yet it still has behaviors and features that tie it to the more complex reactor systems, namely: it is integral in nature (this will be discussed more in a later section). Its simplicity implies that it will be easier to model with a code like TRACE. All coding difficulties have been eliminated, and thereby the code should have no problem predicting MANOTEA behavior. Facility design and operating parameters were chosen with the code in mind and with the intent of maximizing condensation effects. Due to the simplicity of the MANOTEA facility, this experimental effort may prove useful as a benchmark for next generation code development as well.

Facility Operation

Experiment preparation begins by filling the boiler pipe completely. The tee at the lowest point of the apparatus is capped, and Valves X and Y are opened to allow water to flow from the boiler to the condenser pipe, which results in each pipe being half full. Roughly 3.8 *L* of water is measured out and added to the total inventory. This additional water is required to ensure that neither of the heaters becomes uncovered during the experiment. Both heaters (one at the bottom of the boiler and one at the bottom of the condenser pipe) are turned on and the inventory is allowed to heat up and boil for a minimum of 3 hours with Valves A and C in the top flanges vented to the atmosphere. This process strips out the non-condensable gases. Non-condensable gases are undesirable because they hinder the condensation process that will occur during the actual experiment. After 3 hours, three-way Valve C in the

top of the condenser pipe is aligned to connect the vapor space to the pressure transducer and the heater in the bottom of the boiler is turned off. Pressure in the condenser builds up and moves liquid inventory to the boiler. Once a small amount of water leaks out of Valve A at the top of the boiler, three-way Valve A is aligned to connect the boiler vapor space to the pressure transducer, the boiler heater is turned on again, the condenser heater is turned off, the boiler and condenser are isolated from each other by closing Valves X and Y in the lower flanges, Valve W is opened to allow boiler inventory to flow into the primary side of the DPHE, and DPHE secondary water is turned on. The condenser is allowed to cool, this cooling takes place by natural circulation and heat loss from the exposed top and bottom flange, until the pressure in the condenser is roughly 101 kPa. While the condenser cools, the pressure in the boiler is allowed to increase to roughly 121 kPa. The pressure difference ensures all flow losses in the DPHE primary pipe are overcome and that the transient will initiate. The preparation phase ends when the initial conditions are achieved (see Table 1).

	Boiler	Condenser
Initial Pressure (kPa)	121	101
Bulk Temperature (^oC)	105	100
Initial Inventory (L)	29.2	3.8

Table 1. Initial experimental conditions.

The transient is initiated, and the actual experiment begins, by opening the solenoid valve (Valve B) at the top of the DPHE that leads to the condenser. This allows primary liquid inventory to flow out of the boiler via the copper tubing, up through the DPHE, and into the condenser pipe through a nozzle at the end of the

copper tubing in the vapor space. Sub-cooled liquid inventory enters the condenser at the temperature of the secondary water (~20.0 ^{o}C). The transient, movement of liquid inventory from the boiler to condenser via the DPHE, is driven by a pressure differential that results from rapid condensation as the cool water enters the condenser pipe. Scoping experiments revealed that the boiler pipe always provides sufficient liquid by flashing adequate steam in the vapor space, never hindering the transient. The duration of the transient and amount of liquid inventory transferred varies depending on the nozzle size and geometry. The transient (movement of liquid inventory from boiler to condenser via the double-pipe heat exchanger) is started by the small pressure differential, but sustained by rapid condensation. How much condensation occurs is controlled by a competition between condensation in the vapor space, evaporation at the wall and liquid interface, and stored energy in the walls of the condenser.

Figure 2 is a pictorial representation of the progress from setup (only selected setup steps are shown) to transient termination.

A detailed, step-by-step checklist of procedures to prepare the facility and run a transient is given in the appendix.

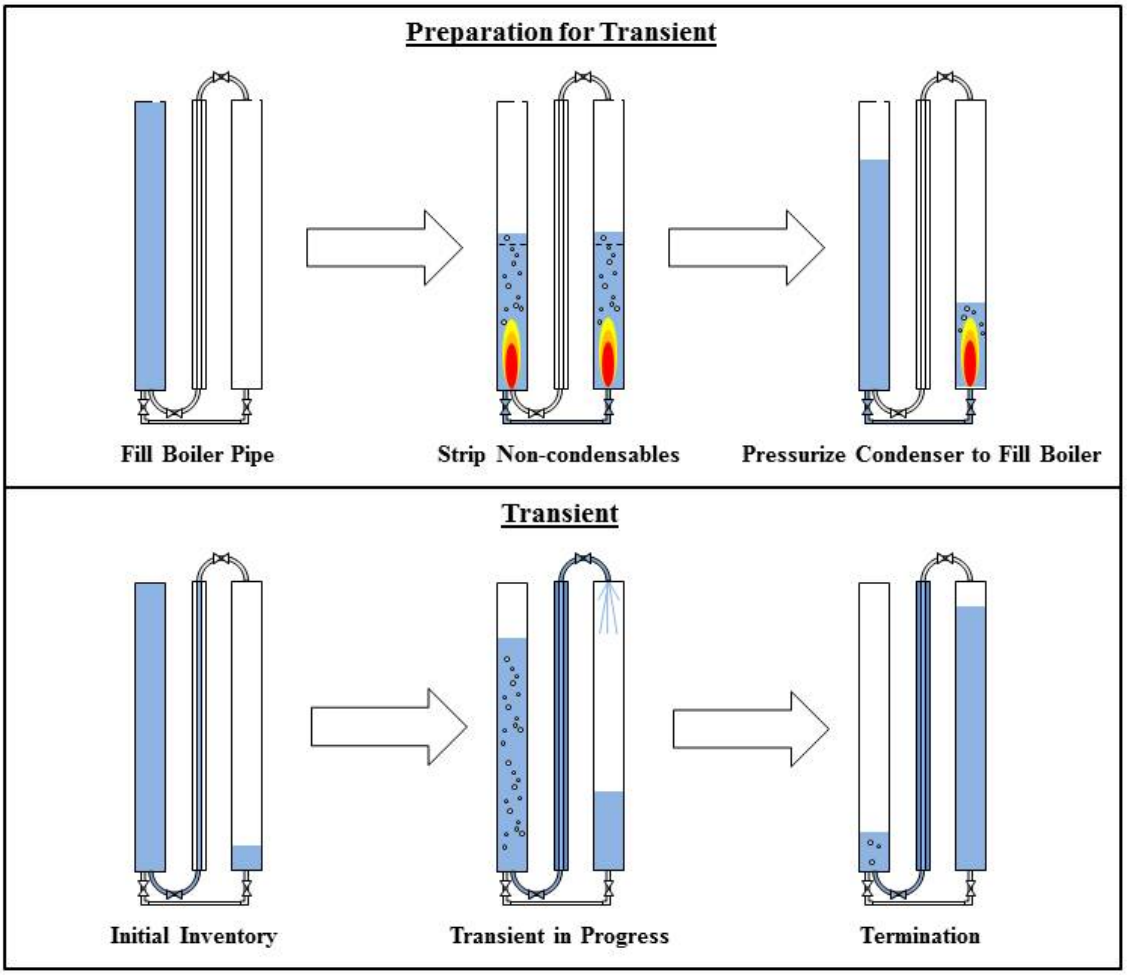

Figure 2. Schematic drawing illustrating selected preparation steps and transient progression from initial conditions to termination.

The experimental parameters can be inferred from the facility description, operating procedures, and initial conditions – namely: pressure, temperature, liquid inventory, and nozzle geometry. The following section discusses the rational behind certain parameters, procedures, and the initial conditions.

Facility Parameters Discussion

Pressure

Experimental setup begins at atmospheric pressure because it makes de-gassing the water easier. Non-condensable gasses are undesirable because they hinder heat transfer/suppress condensation. Thus, the boiler and condenser are open to the atmosphere to allow the non-condensable gasses to escape after being liberated from the water by boiling. However, in spite of efforts to rid the system of non-condensable gases, a small quantifiable fraction remains in the DPHE. These gases will be discussed in more detail later.

The transient begins with a differential pressure (boiler pressure - condenser pressure) of 21.0 *kPa*. This value insures there is sufficient pressure to overcome loss (in the copper tubing, valves, tees, and orifices) and initiate the transient when the solenoid valve is opened. It should be noted that this differential pressure only starts the transient, but rapid condensation sustains it. Higher pressure implies more vapor which means diminished condensation for the same amount of cooling spray entering the condenser. Choosing an initial pressure of 101 *kPa* in the condenser means condensation effects will be maximized. With the condenser pressure set at 101 *kPa* and the pressure differential set at 21.0 *kPa*, transient initiation temperatures follow since the boiler and condenser are always at a saturation condition.

Temperature

As discussed above, initial condenser pressure is 101 *kPa* meaning initial temperature is 100 ^{o}C on average. However, due to the setup process, there is a

temperature gradient with the bottom of the condenser being warmer due to its proximity to the heater. This is possible because the liquid above presses on the liquid below, making the saturation condition for lower liquid different from that of the higher. These inverted thermal gradients are a direct consequence of the setup process. A pressure differential of 21.0 *kPa* sets the boiler temperature at 105 ^{o}C on average at transient initiation, but has a gradient for the reason just outlined. These temperature gradients become important when performing an energy balance.

The secondary water comes from the tap at about 20.0 ^{o}C (varying from 16-22.0 ^{o}C with season) and flow is sufficient to insure primary liquid enters the nozzle in the condenser at 20.0 ^{o}C. Thus, flow exiting the boiler is at a saturation condition and flow entering the condenser is single-phase. Highly sub-cooled liquid was desired because it ensures single phase liquid enters the condenser via the nozzle. Two-phase flow is much more complex and less understood. As a result, two-phase flow has historically been more difficult for the code. Single-phase liquid provides a simple means for measuring flow through the nozzle and should be easy for TRACE to capture. Secondary water exits to a drain and final temperature is not measured or desired.

Initial Liquid Inventory

An initial condenser inventory of 3.8 *L* ensures that the heater stays covered during experiment preparation. Beginning the transient with the boiler full means less pressure head needs to be overcome in order for the liquid inventory to go over the top of the DPHE as it enters the condenser pipe. This translates to lower

operating temperatures and increased condensation for a given amount of cool spray entering the condenser.

Nozzle Geometry

The shape and size (diameter) of the nozzle, which is the only thing that was varied between experiments, dictates whether sub-cooled liquid entering the condenser hits the pipe walls or falls predominantly into the vapor space. Sub-cooled liquid flowing through a fan nozzle will hit the wall and collapse less vapor. Sub-cooled liquid flowing through a jet nozzle will fall predominantly into the vapor space, collapsing more vapor and doing more pressure-volume work. A small diameter nozzle means less primary liquid enters during a given time interval. In this case, the metal masses (stored energy) will dominate heat transfer and can actually prevent the transient from beginning properly. For a mid-sized nozzle, sufficient inventory can enter the condenser pipe and condensation rate will drive the transient. If a large diameter nozzle is used, flashing rate in the boiler pipe could constrain and control the transient. Although theoretically possible, an experiment - ran as part of our scoping matrix - without a nozzle at all (open copper end) revealed that flashing controlled transients are not possible on the MANOTEA. Thus, large-nozzle MANOTEA transients are condensation controlled. Larger diameter nozzles allow more cool liquid to enter during a given time, resulting in shorter transients. By varying nozzle geometry and size, different transients can be obtained. Thus, intuitively nozzle size and geometry will effect transient duration and amount of liquid inventory.

A test matrix outlining the nozzle used during the current work is outlined in Chapter 5. The results of the present work, outlined in a later Chapter 6, confirm the analysis outlined in the preceding paragraph.

Operating Domains

From the operating parameters, and the discussion in the proceeding section, it can be inferred that transient behavior can be classified into 3 operating domains. Depending on whether the incoming inventory (spray) interacts with the pipe wall and how much inventory enters (nozzle diameter), transients controlled by the metal mass, condensation rate, flashing rate, or a combination of these are possible. These operating domains are summarized with the parameter tree shown in Figure 3. Again, flashing controlled MANOTEA transients are not possible. Overall transient outcome can be viewed as a competition between these operating domains.

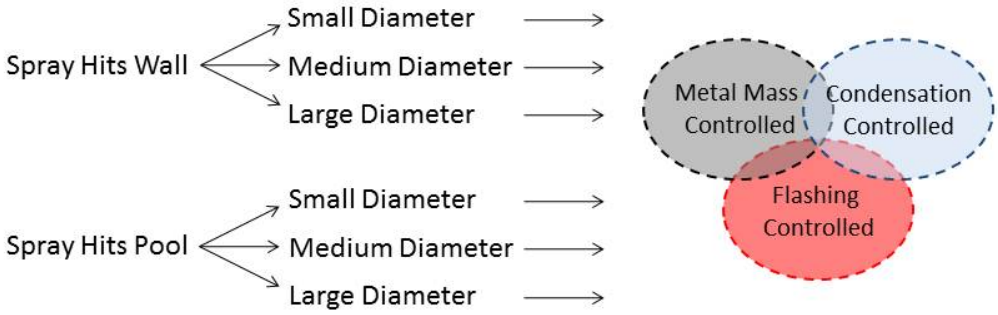

Figure 3. Parameter tree showing operating domains.

In Chapter 7, the concept of an energy partition is introduced. The energy partition builds on the concept of operating domains to delineate how much of the

incoming (spray) enthalpy goes to collapsing vapor and how much goes to cooling the pipe wall. The energy partition concept can then be used to derive a “back of the envelope” integral energy balance equation.

Chapter 4: Instrumentation

After MANOTEA was constructed, a series of scoping and shakedown experiments were conducted. The shakedown experiments verified that the facility was working properly and could produce repeatable and meaningful data. As part of the scoping evolution, calibration procedures and techniques were established. This chapter outlines how instrumentation in the MANOTEA facility was calibrated or verified for accuracy. The results of the scoping experiments were used to generate an experiment matrix that will be outlined in Chapter 5 and discussed in Chapter 7.

Differential Pressure Cell

A differential pressure (DP) cell (annotated as "DP" on Figure 1) with one tap in the sub-cooled liquid as it exits the DPHE and one tap in the vapor space of the condenser provided a means for measuring primary inventory flow rate and closing the mass balance. A commercially available Omega PX409-015WDUV differential pressure transducer with 5 point factory calibration was used to obtain differential pressure as a function of time. Error was estimated at +/- 0.5% of full scale on average (never to exceed +/- 1.0% of full scale), or about +/- 500 *Pa*. How the mass balance was closed with a DP reading will be outlined in detail in Chapter 7. The mass balance was verified against results obtained with the DP cell by using a novel buoyant rod apparatus. These results were then double-checked with the aid of drain

curves. Final inventory values obtained with the 3 methods differed by about 0.50 *L* on average, and rarely more than 1.0 *L*.

Buoyant Rod Apparatus

Figure 4 is a schematic drawing of the apparatus which will be referred to as "floats" or "the floats". A high-temperature plastic rod runs the entire length of the boiler and condenser pipes (one apparatus is in each pipe) and penetrates the lower and upper blanks. The lower end of the rod feeds into a cylindrical port that allows the rod to slide up and down while preventing liquid inventory from leaking out. The upper penetration is shown in detail in the figure. Standard cast iron pipe fittings maintain the system boundary. The high-temperature plastic rod is connected to the free end of a tempered-steel beam. The fixed end of the beam is secured in a 1/2" pipe-size NPT cap. Two strain gauges are placed at the root of the bending beam, one on the top and one on the bottom. In this configuration, the strain reading is temperature independent. Strain readings for known inventories, such as with the pipes full and empty, provide boundary conditions or calibration points. With this information liquid level in the pipe (which causes the beam to deflect up or down) can be correlated to a strain reading. Keeping track of strain readings with respect to time provides an alternate means of obtaining liquid inventory in the boiler and condenser. Figure 5 is a graph comparing the liquid inventory obtained with the differential pressure cell to that obtained with the floats. The floats give confidence to the flow rate and subsequent liquid inventory data obtained with the DP cell.

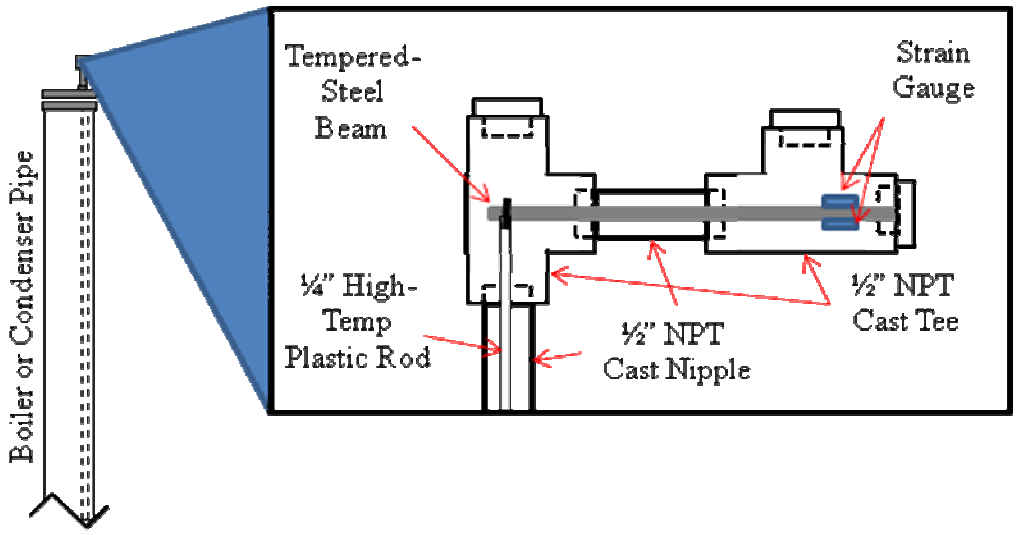

Figure 4. Schematic of liquid inventory measuring apparatus (floats).

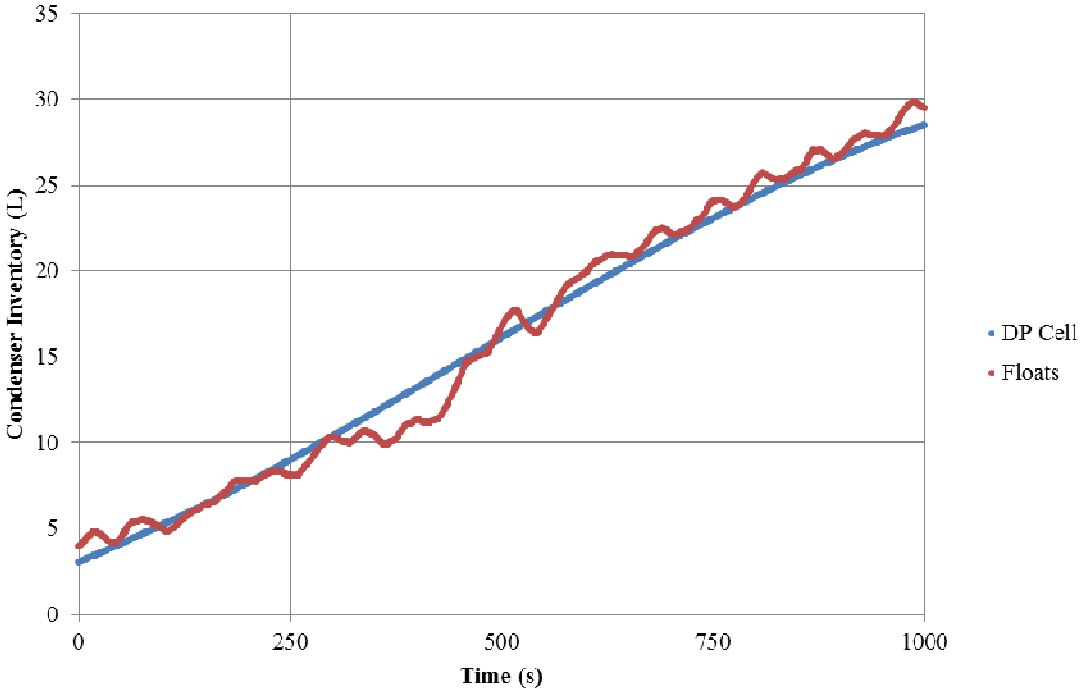

Figure 5. Comparison of liquid inventory obtained with the differential pressure cell to that obtained with the floats for an EZNF3000 transient.

Drain Curves

A second method to reverify the mass balance was performed with the aid of drain curves. The boiler and condenser pipes were each filled to known volumes. The time to drain each pipe (separately - with the vent valve at the top of each pipe open to the atmosphere) was subsequently monitored. Figure 6 is a plot of this data with a least squares fit line applied. At the end of each experiment, the boiler and condenser pipes were drained separately and the time to drain recorded. Adjusting drain times for temperature (viscosity) yielded a good final inventory check and also served to reinforce the validity of the mass balance obtained with the differential pressure cell.

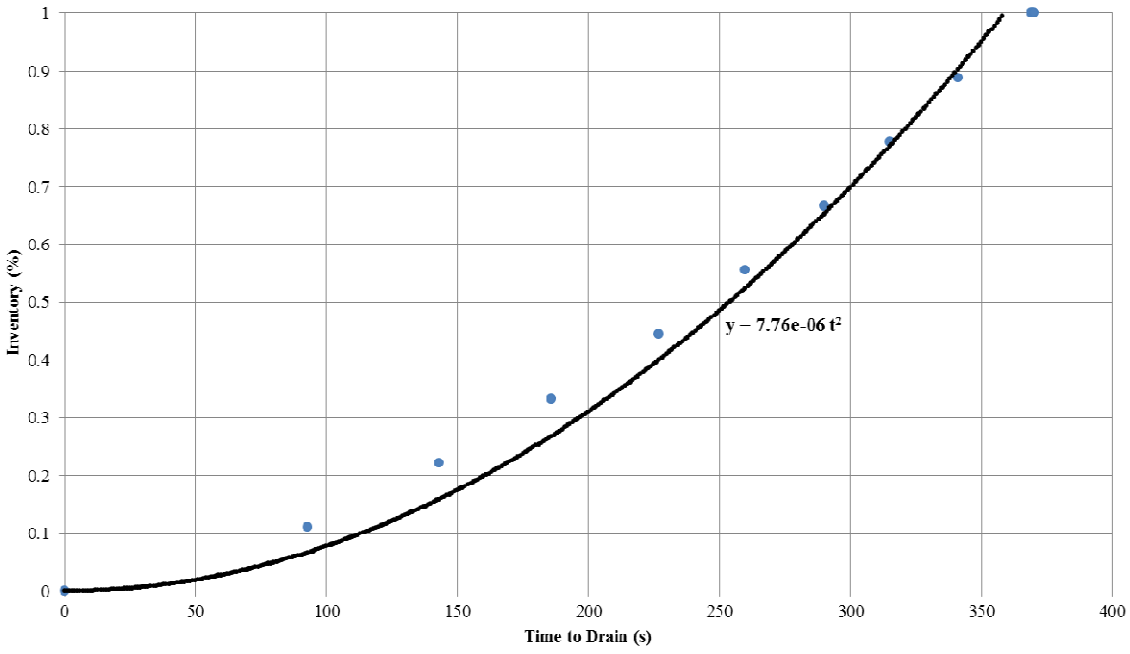

Figure 6. Time to drain MANOTEA pipe for known inventories at room temperature.

Thermocouples

Thirty type-J thermocouples connected to three Pico Technology TC-08 data loggers were used to track temperature as a function of time. Temperature data was then used to close the energy balance. By National Institute of Standards and Technology (NIST) standards, error for "standard" type-J thermocouples should be less than +/- 2.2 ^{o}C. Each TC-08 data logger came with a 12-point calibration for the temperatures ranging from -100 to 1200 ^{o}C. Based on the calibration, for the range of temperatures found in MANOTEA, an additional error of no more than +/- 0.50 ^{o}C can be attributed to the data logger.

Data loggers are extremely sensitive to humidity. Since MANOTEA was built in a laboratory without temperature control near the Severn River, humidity was a concern and ensuring the integrity of the data paramount. Prior to each experiment, the temperature of the lab was compared to the cold junction reading on the three data loggers. After the experiment raw data was downloaded from the loggers and plotted. Knowing the initial temperature was the temperature of the lab and knowing that temperature would level at 100 ^{o}C during the boiling/stripping process, a two point calibration was possible. These two points were plotted and a linear fit was performed with a spreadsheet program in order to obtain a mapping or calibration equation. The raw data from each thermocouple was individually mapped and 'temperature versus time plots' were generated for the respective transient. Figure 7 is a plot of the typical raw temperature as a function of time data for "CC01". The figure shows temperature readings from the moment the boiler was filled through the termination of the experiment, to include all preparation steps. Steps are labeled on

the figure. Figure 8 is a plot showing the calibration curve for the same thermocouple during the same transient. Figure 9 is a plot of the calibrated temperature versus time after transient initiation for the data shown in Figure 7 and the calibration curve shown in Figure 8. Note, due to variations in humidity, this calibration process was performed for every thermocouple and every experiment.

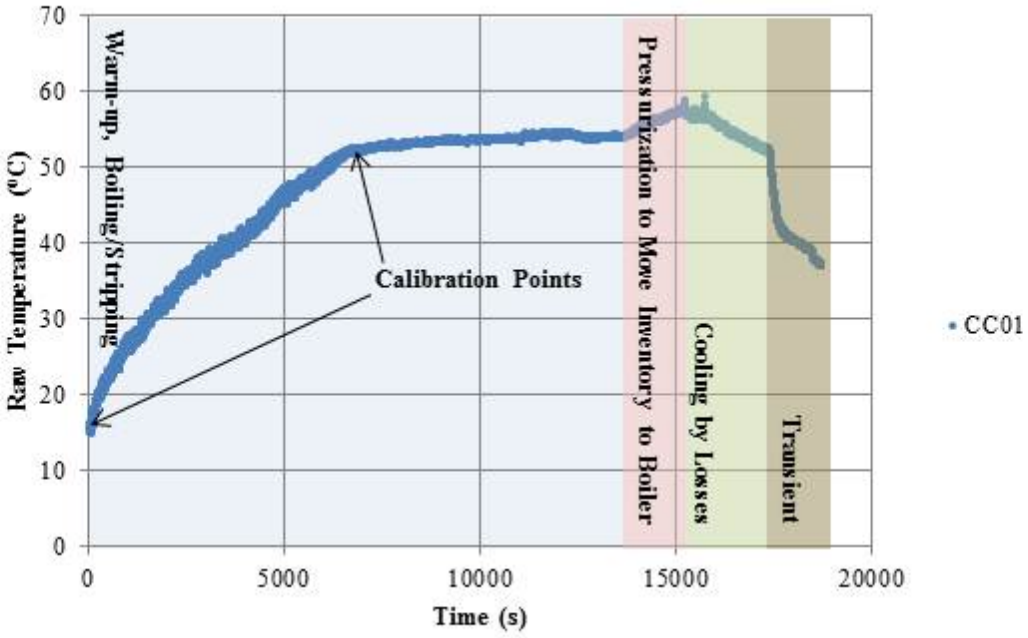

Figure 7. Raw temperature data as a function of time for the CC01 thermocouple during preparation and execution of a typical transient.

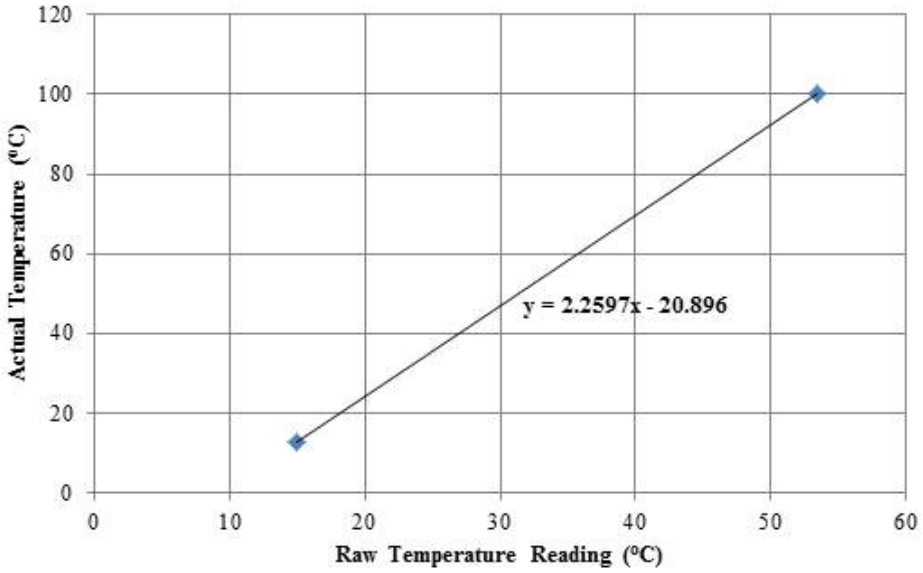

Figure 8. Two-point linear calibration curve for raw CC01 thermocouple data shown in Figure 7.

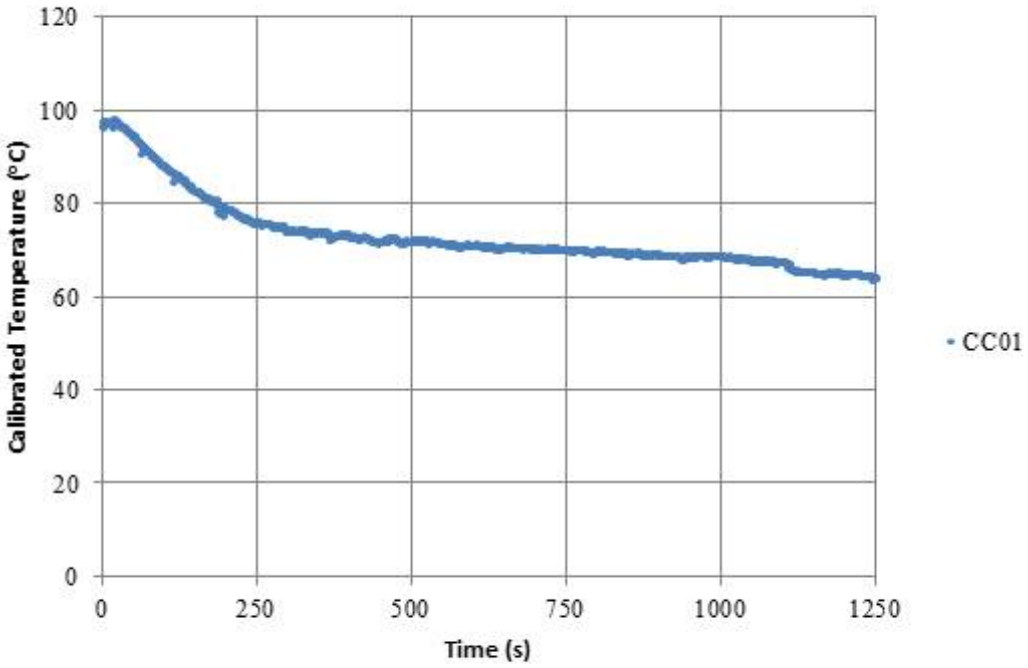

Figure 9. Calibrated temperature data for the CC01 thermocouple over the duration of a typical transient.

Pressure Transducers

The boiler and condenser pipe both have a MicroDAQ LOGiT pressure transducer mounted in their top flange, respectively. The transducers came with a 5-point NIST calibration certificate. Since each transient occurred under saturation conditions, these pressure readings provided a convenient, independent means to verify the bulk temperature profiles in the boiler and condenser. In addition, these devices provide an independent verification of the DP cell readings. Data from these pressure transducers were used to generate pressure as a function of time and pressure as a function of inventory plots. This specific transducer was chosen because the accompanying data logging system was sufficiently robust and easy to install and use. The pressure transducers were "zeroed" before every experiment. Error from the transducer and logging systems was estimated to be no more than 1% of full scale or about +/- 10000 *Pa*.

Nozzles

In order to ensure the accuracy of the mass balance, it was necessary to verify the K-factors (nozzle loss coefficients) advertised for the EZNF series nozzles used in MANOTEA. How the mass balance was closed using a DP cell reading and K-factor will be outlined in detail in Chapter 6.

K-factor verification was performed locally by attaching a "T", with an EZNF nozzle on one opening and a pressure gauge on the other, to the end of a hose. Water exiting the nozzle was directed into a graduated cylinder, and time to transfer a measured volume was tracked with a stop watch. The results of this effort for 3 nozzles are shown in Table 2. The local verification for the 3 nozzles revealed that

the manufacturer's K-factors are acceptably accurate. Since the K-factors for these nozzles were acceptable, verification of all the nozzles used was deemed unnecessary and not performed. Local verification was somewhat crude, but the confidence gained by performing it was invaluable. The largest source of error in the local verification process was the pressure reading, which was taken with a simple analog gauge with 1- *psi* marks. The local verification values were within 10% of the advertised values.

Nozzle	Pressure (bar)	Time (s)	Volume (l)	K Calculated	K Average (~15 C)	K Advertised (@20 C)	K Min	K Min Avg	K Max	K Max Avg
EZNF 01500	3.0	52	0.52	0.35	0.34	0.342	0.34	0.34	0.36	0.35
	3.0	48	0.47	0.34			0.33		0.35	
	3.0	48	0.48	0.35			0.34		0.36	
EZNF 01515	4.1	41	0.51	0.37	0.37	0.342	0.36	0.36	0.38	0.38
	4.1	40	0.51	0.38			0.37		0.39	
	4.1	41	0.51	0.37			0.36		0.38	
EZNF 1500	2.0	10	0.78	3.3	3.6	3.42	3.13	3.39	3.55	3.85
	2.0	9	0.79	3.7			3.51		4.01	
	1.7	11	0.89	3.7			3.53		3.98	

Table 2. Local verification of nozzle manufacturer's advertised K-factors. Highlighted columns show advertised K-factor & minimum and maximum values obtained by local test.

Summary of Estimated Error

Table 3 summarizes the estimated error for each measured or calculated parameter in MANOTEA.

Parameter	**Estimated Maximum Error/Uncertainty**
Raw Temperature	+/- 2.7 ^{o}C
Differential Pressure Gauge	+/- 500 *Pa*
Boiler/Condenser Pressure Transducer	+/- 10000 *Pa*
Inventory/Inventory Transfer	+/- 0.50 *L*

Table 3. Summary of experimental error and estimated measurement uncertainty.

Chapter 5: Test Matrix and Experimental Data

Table 4 is an outline of the experiments performed as part of the present work. All experiments were ran as described in Chapter 3. Each experiment was performed at least twice in order to verify repeatability. Nozzle size and geometry was varied in order to obtain transients of different duration and differing amounts of inventory transfer. All nozzles were purchased from the BETE Spray Nozzle Company and are commercially available. EZNF denotes the nozzle model. The next two digits denote orifice diameter and the last two digits denote spray characteristics.

Bete Nozzle ID	**Spray Characteristic**	**Equivalent Orifice Dia (mm)**	**K-factor**	**Initial Boiler Inv. (L)**	**Initial Cond. Inv. (L)**	**Initial Pressure Differential (kPa)**
EZNF0800	0-deg (Jet)	1.83	1.82	29.2	3.8	21
EZNF0815	15-deg (Fan)	1.83	1.82	29.2	3.8	21
EZNF1500	0-deg (Jet)	2.38	3.42	29.2	3.8	21
EZNF1515	15-deg (Fan)	2.38	3.42	29.2	3.8	21
EZNF3000	0-deg (Jet)	3.57	6.84	29.2	3.8	21

Table 4. Summary of experiments performed.

Results by Nozzle

Data from each of the experiments performed includes boiler pressure, condenser pressure, temperatures (at those locations described in Chapter 3), and differential pressure, all as a function of time. Differential pressure is used to measure primary inventory flow rate and close the mass balance. Temperature data is

used in conjunction with the mass balance to close the energy balance. Mass and energy balances will be presented in Chapter 6.

When plotting variables (pressure and temperature) with respect to time, each of the data sets listed in Table 4 stands alone. Plotting pressure (and therefore bulk temperature, because the systems is at saturation) with respect to the amount of liquid inventory transferred is a useful way to compare datasets from all nozzle sizes and geometries. When this is done for all the data sets and the results plotted on the same axis, all the transients collapse and overlap. This feature will be discussed in more detail in Chapter 7.

EZNF0800 Data

Figure 10 is a plot of the boiler and condenser pressures as a function of time for the EZNF0800 nozzle. Figure 11 and Figure 12 are plots of the condenser centerline (or fluid bulk) and condenser metal surface temperatures, at the 11 elevations outlined in Chapter 3, as a function of time for the same nozzle, respectively. Figure 13 is a plot of boiler surface and centerline temperatures as a function of time at the 3 lateral locations previously described. Legend labels in the temperature plots are of the form CC01 (which would indicate Condenser Centerline temperature at axial location 01 as annotated on Figure 1). Figure 14 is a plot of differential pressure as a function of time of an EZNF0800 transient. Note: throughout this dissertation, timescales were chosen based on transient duration.

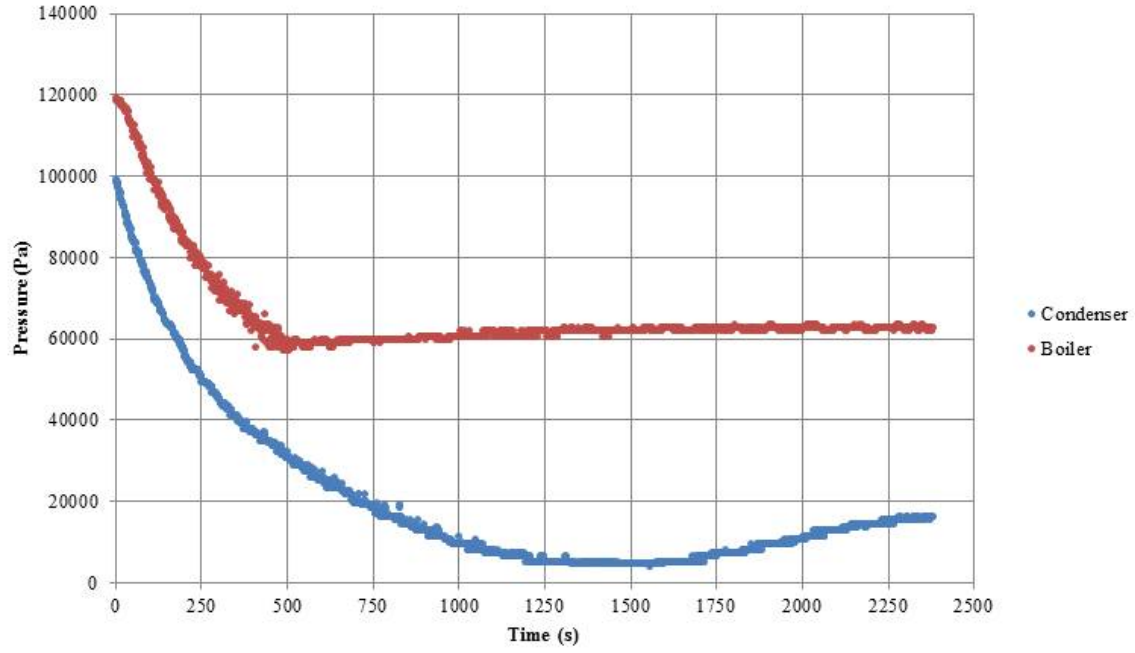

Figure 10. Pressure vs. time after transient initiation for the EZNF0800 nozzle.

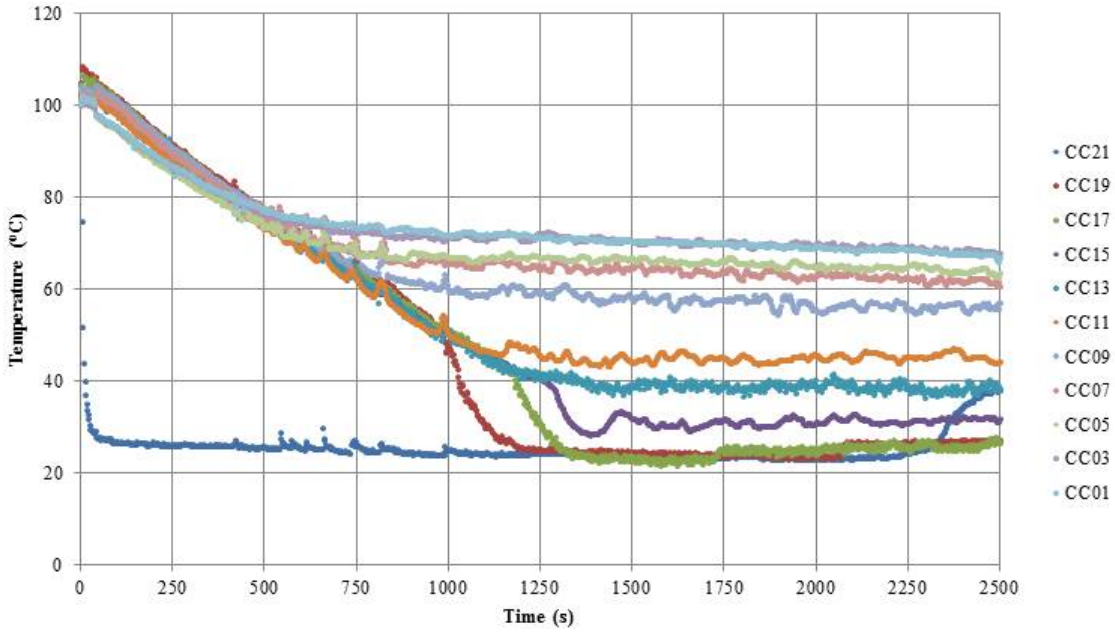

Figure 11. Condenser centerline temperatures vs. time after transient initiation for the EZNF0800 nozzle.

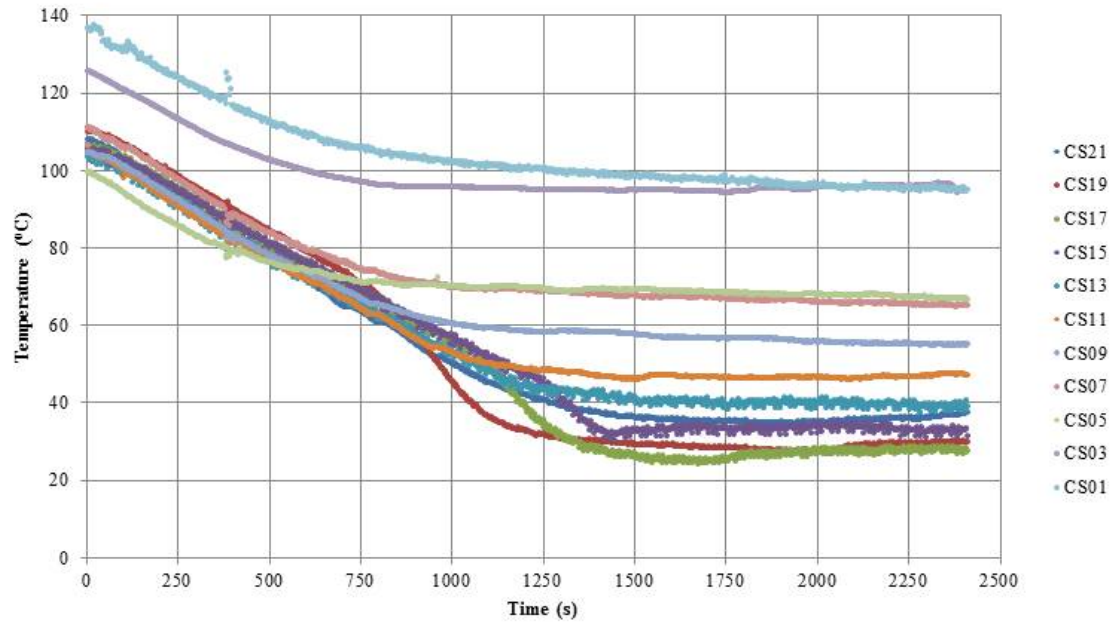

Figure 12. Condenser surface temperatures vs. time after transient initiation for the EZNF0800 nozzle.

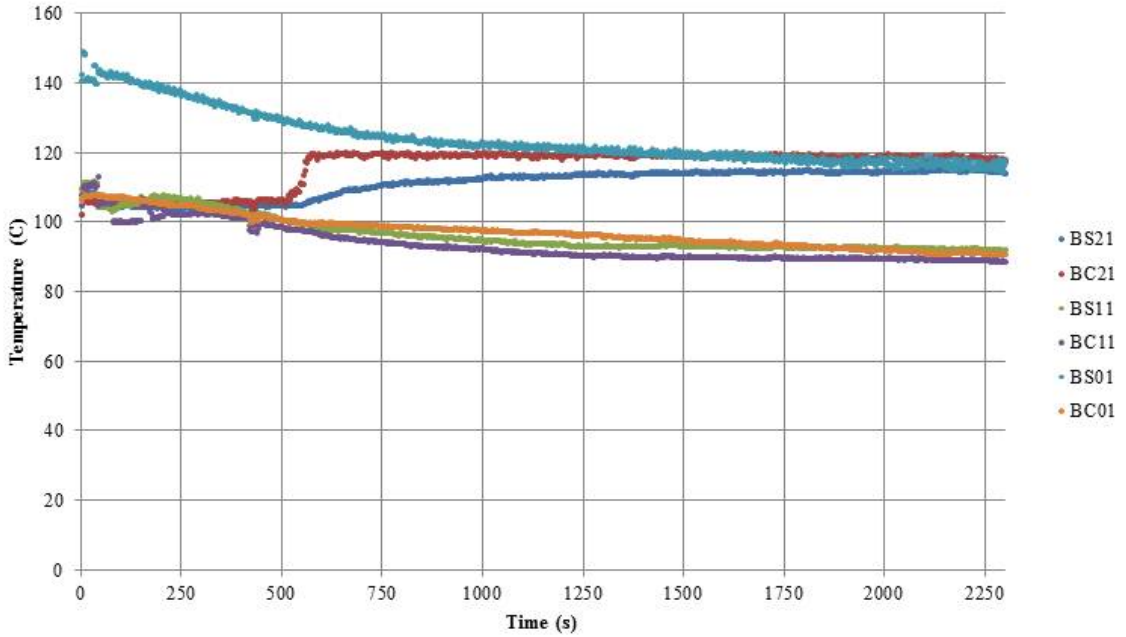

Figure 13. Boiler centerline and surface temperatures vs. time after transient initiation for the EZNF0800 nozzle.

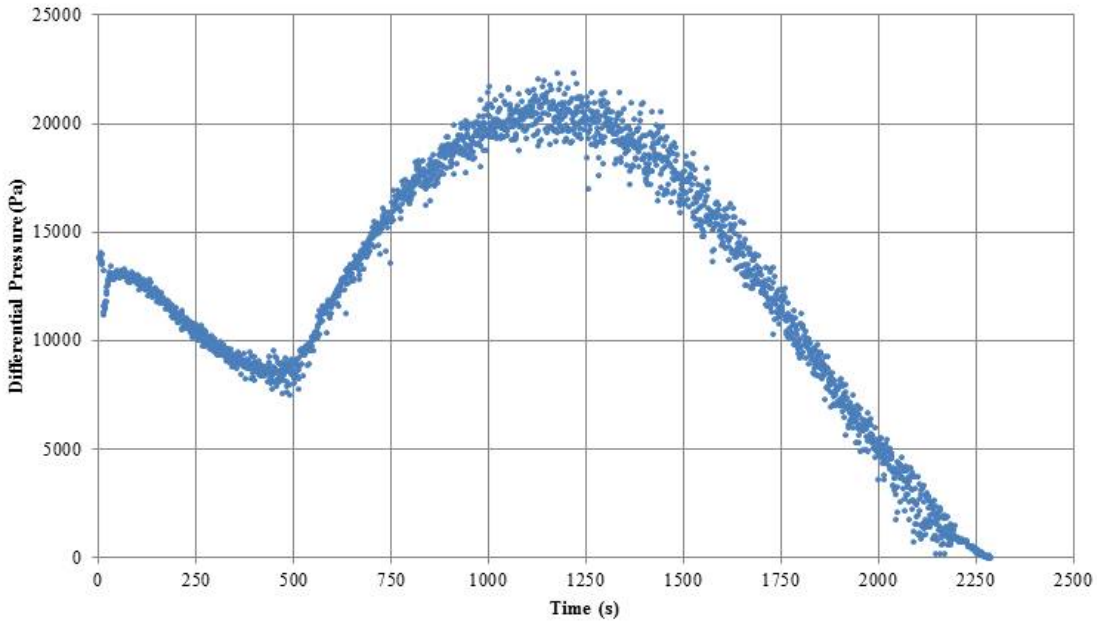

Figure 14. Differential pressure vs. time after transient initiation for the EZNF0800 nozzle.

Note: the behavior observed in Figure 14, which consistently appears in all datasets, will be discussed in Chapter 7.

EZNF0815 Data

Figure 15 is a plot of the boiler and condenser pressures as a function of time for the EZNF0815 nozzle. Figure 16 and Figure 17 are plots of the condenser centerline and condenser surface temperatures as a function of time for the same nozzle, respectively. Figure 18 is a plot of boiler surface and centerline temperatures as a function of time for the EZNF0815 nozzle. Figure 19 is a plot of differential pressure as a function of time of an EZNF0815 transient.

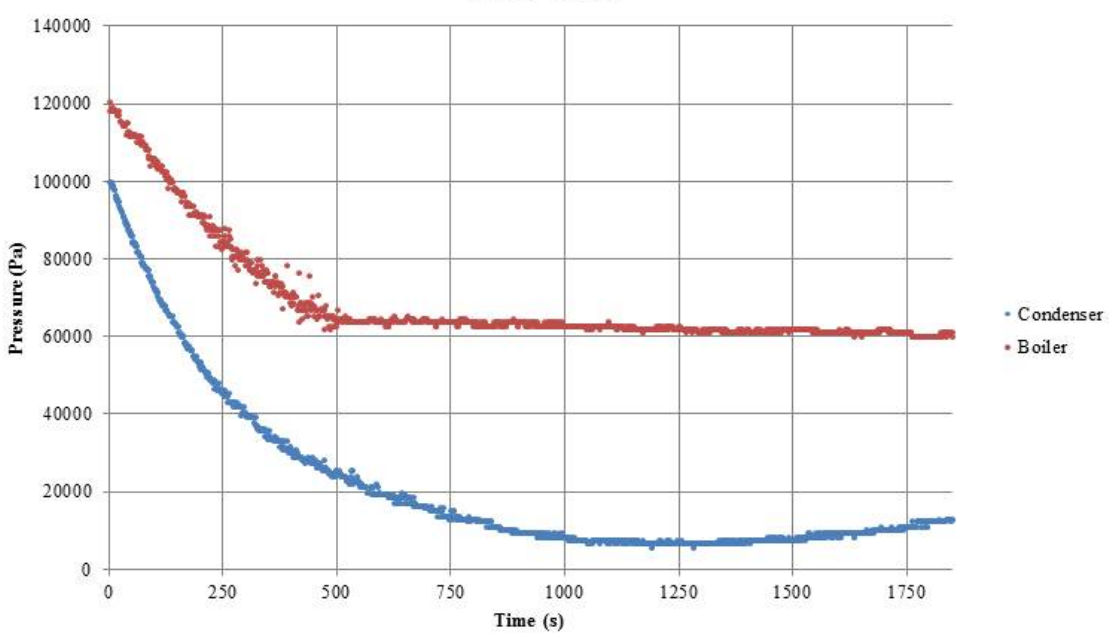

Figure 15. Pressure vs. time after transient initiation for the EZNF0815 nozzle.

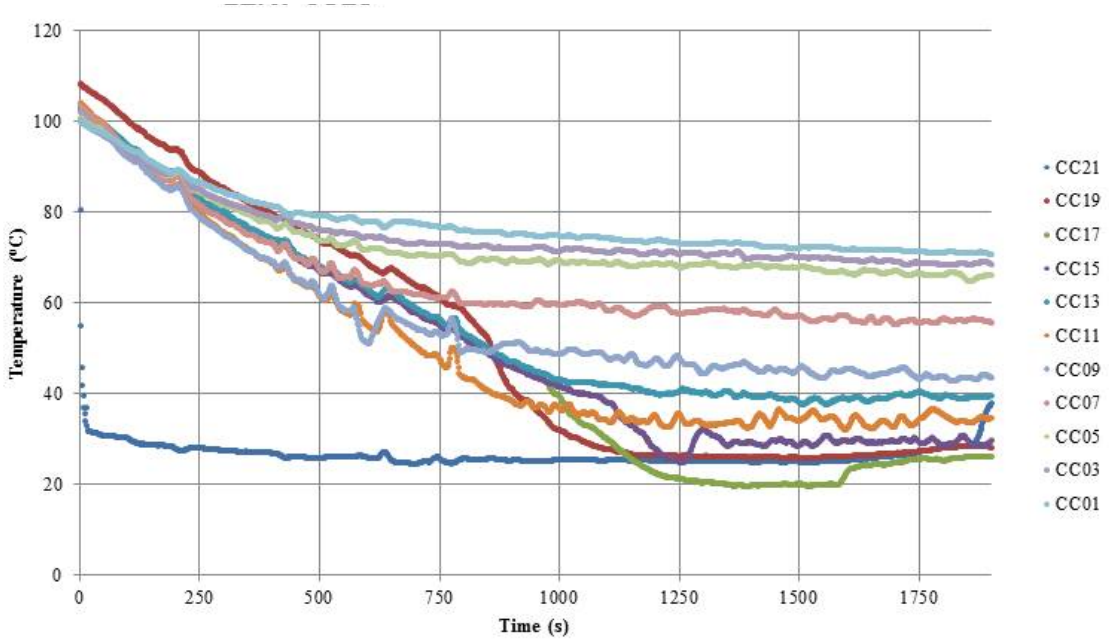

Figure 16. Condenser centerline temperatures vs. time after transient initiation for the EZNF0815 nozzle.

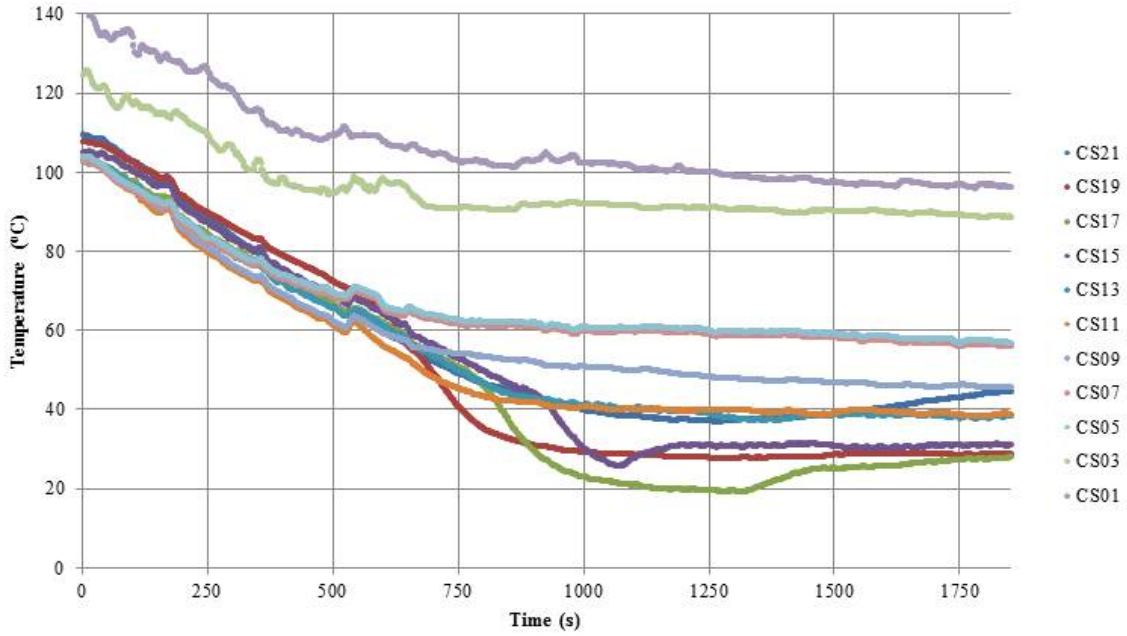

Figure 17. Condenser surface temperatures vs. time after transient initiation for the EZNF0815 nozzle.

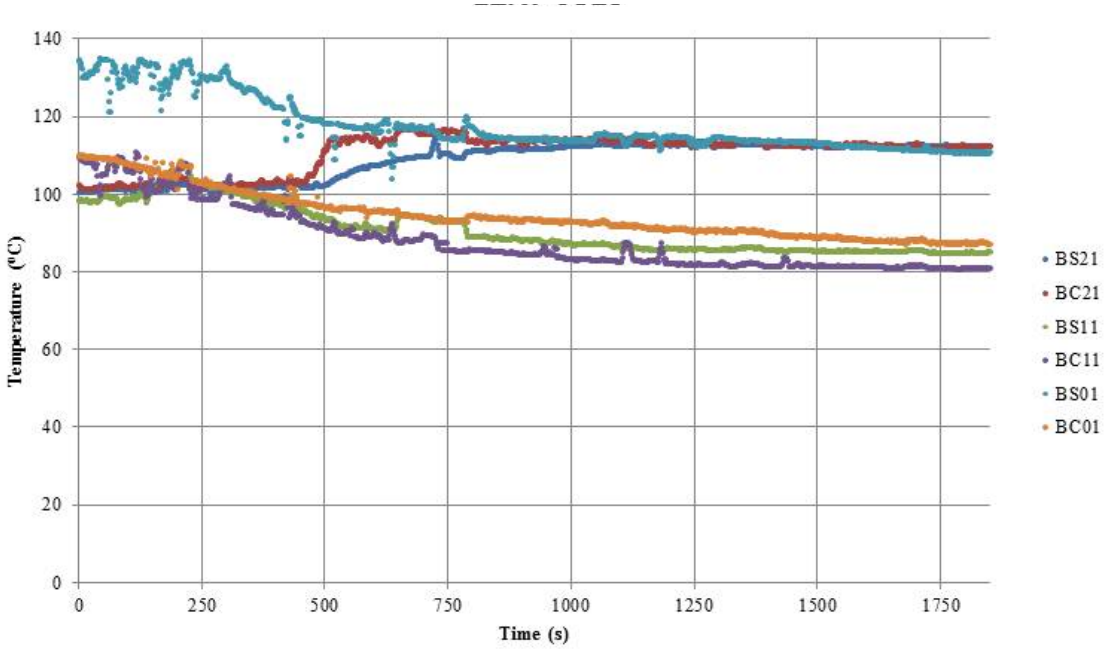

Figure 18. Boiler centerline and surface temperatures vs. time after transient initiation for the EZNF0815 nozzle.

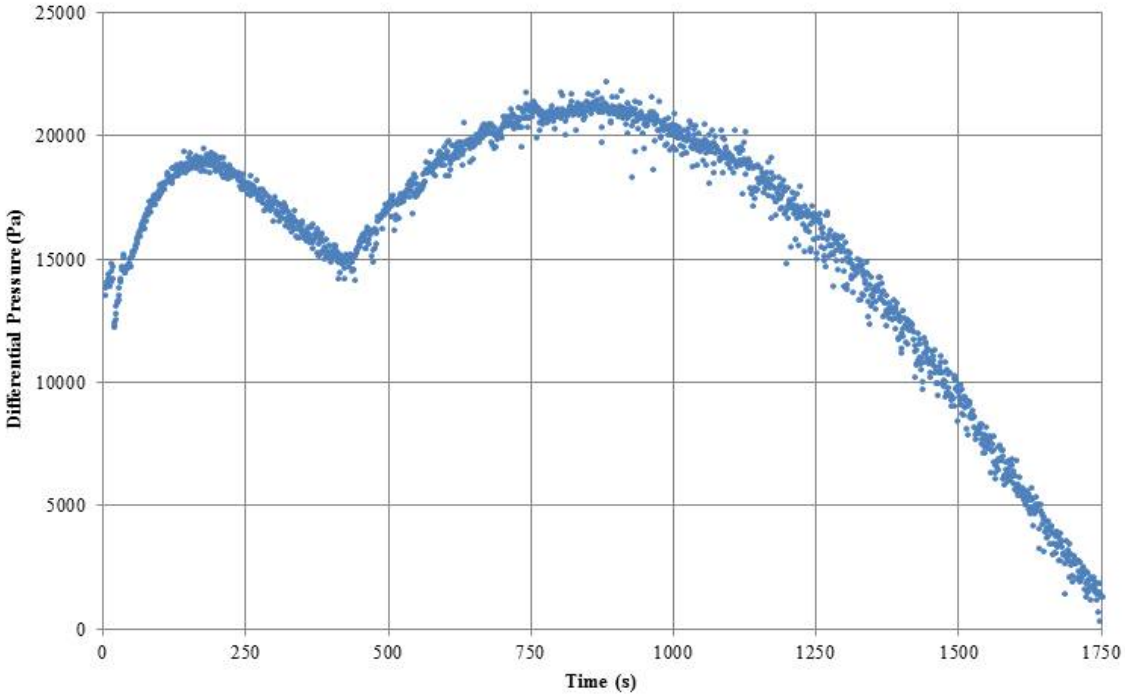

Figure 19. Differential pressure vs. time after transient initiation for the EZNF0815 nozzle.

EZNF1500 Data

Figure 20 is a plot of the boiler and condenser pressures as a function of time for the EZNF1500 nozzle. Figure 21 and Figure 22 are plots of the condenser centerline and condenser surface temperatures as a function of time for the same nozzle, respectively. Figure 23 is a plot of boiler surface and centerline temperatures as a function of time for the EZNF1500 nozzle. Figure 24 is a plot of differential pressure as a function of time of an EZNF1500 transient.

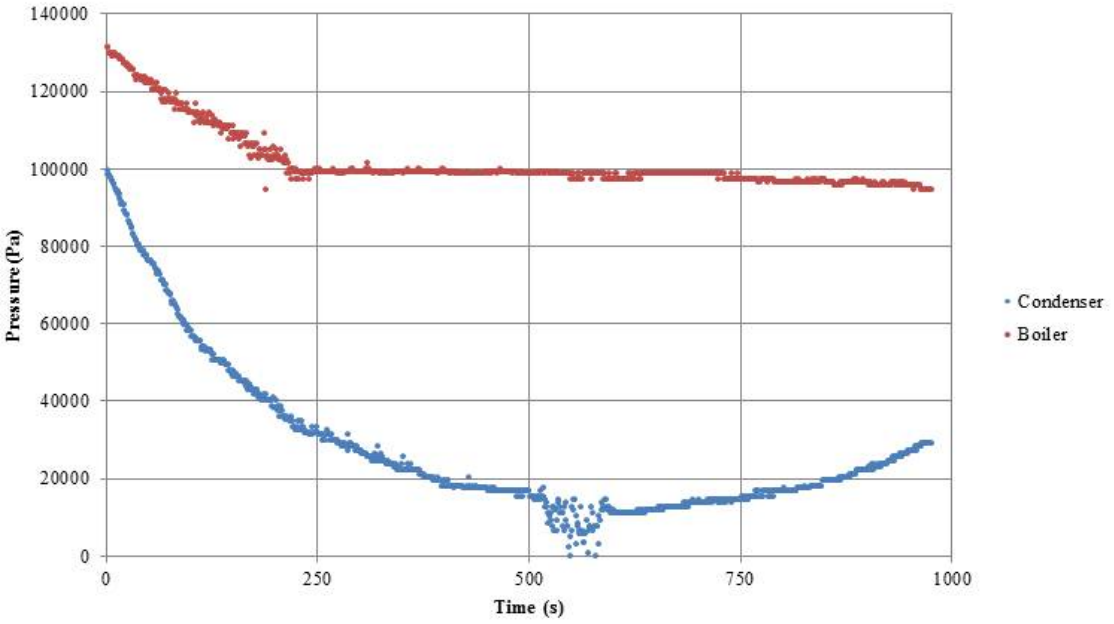

Figure 20. Pressure vs. time after transient initiation for the EZNF1500 nozzle.

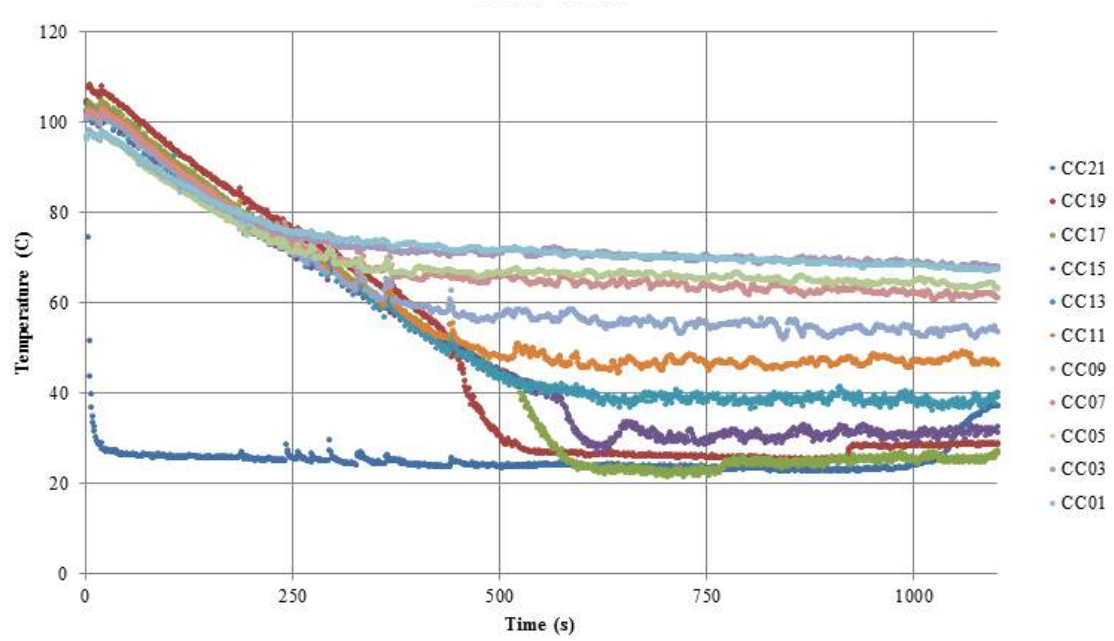

Figure 21. Condenser centerline temperatures vs. time after transient initiation for the EZNF1500 nozzle.

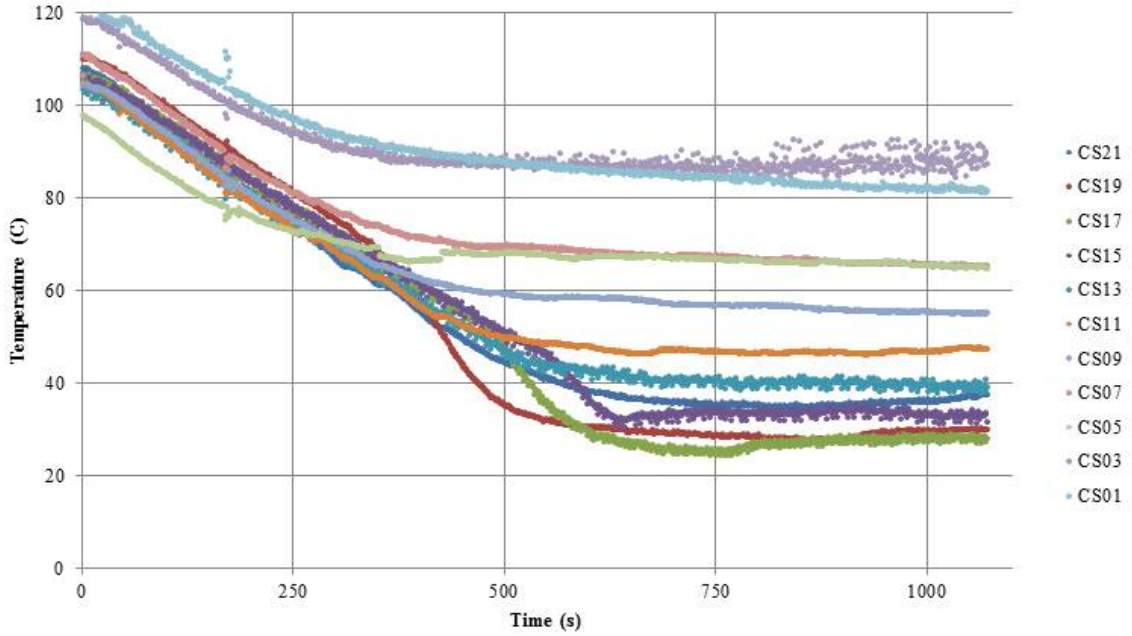

Figure 22. Condenser surface temperatures vs. time after transient initiation for the EZNF1500 nozzle.

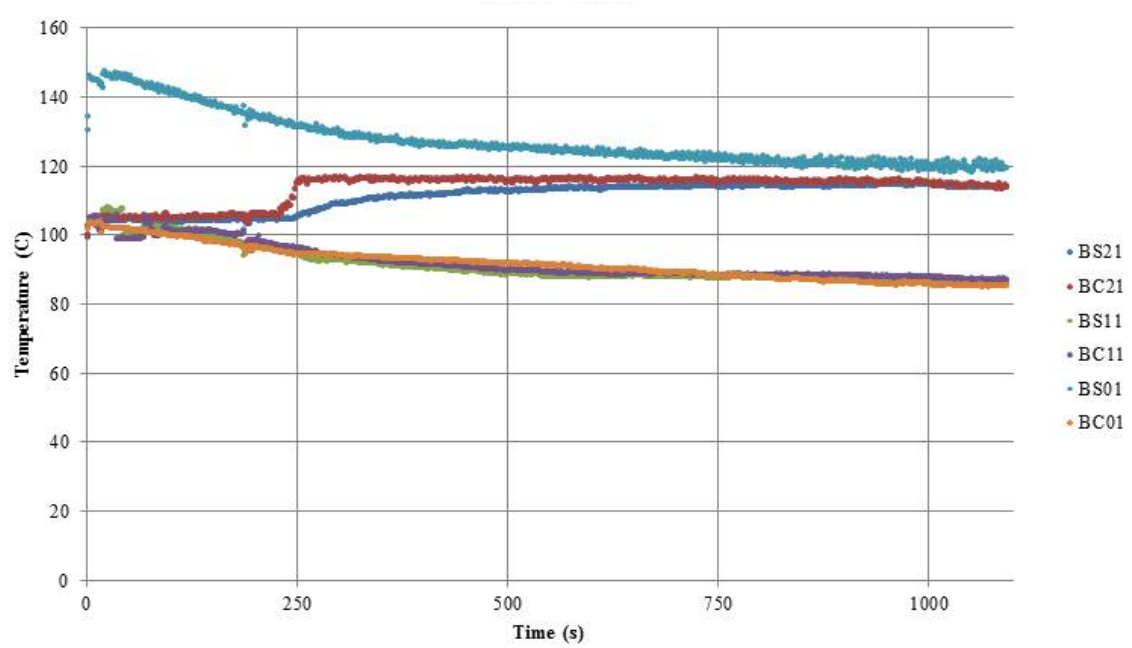

Figure 23. Boiler centerline and surface temperatures vs. time after transient initiation for the EZNF1500 nozzle.

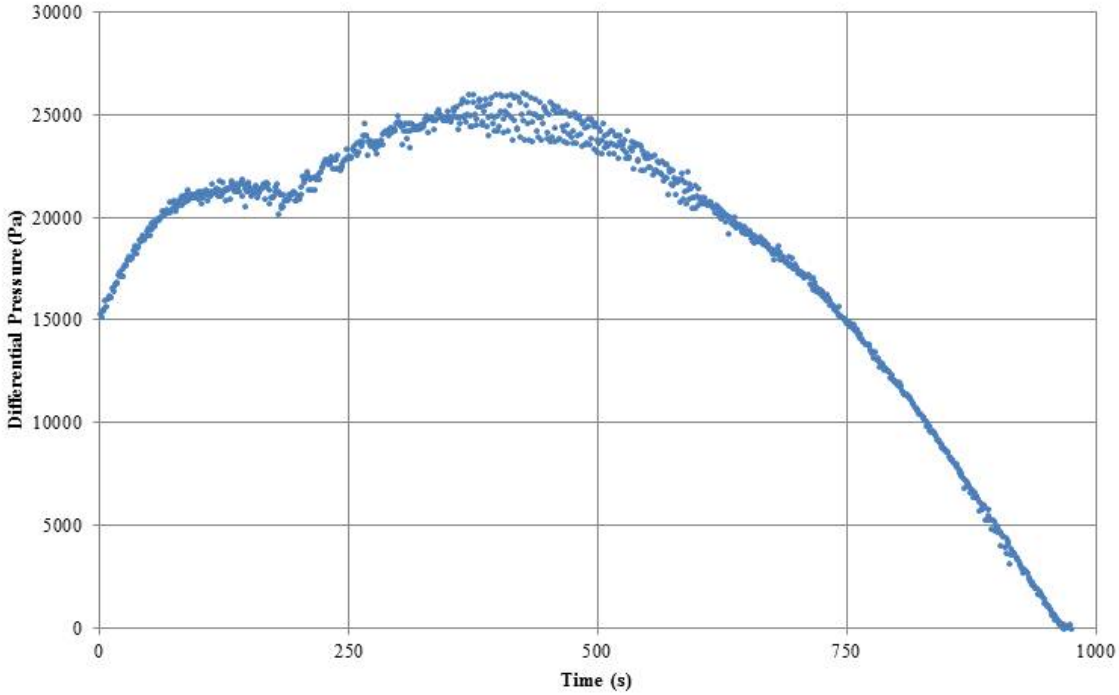

Figure 24. Differential pressure vs. time after transient initiation for the EZNF1500 nozzle.

EZNF1515 Data

Figure 25 is a plot of the boiler and condenser pressures as a function of time for the EZNF1515 nozzle. Figure 26 and Figure 27 are plots of the condenser centerline and condenser surface temperatures as a function of time for the same nozzle, respectively. Figure 28 is a plot of boiler surface and centerline temperatures as a function of time for the EZNF1515 nozzle. Figure 29 is a plot of differential pressure as a function of time of an EZNF1515 transient.

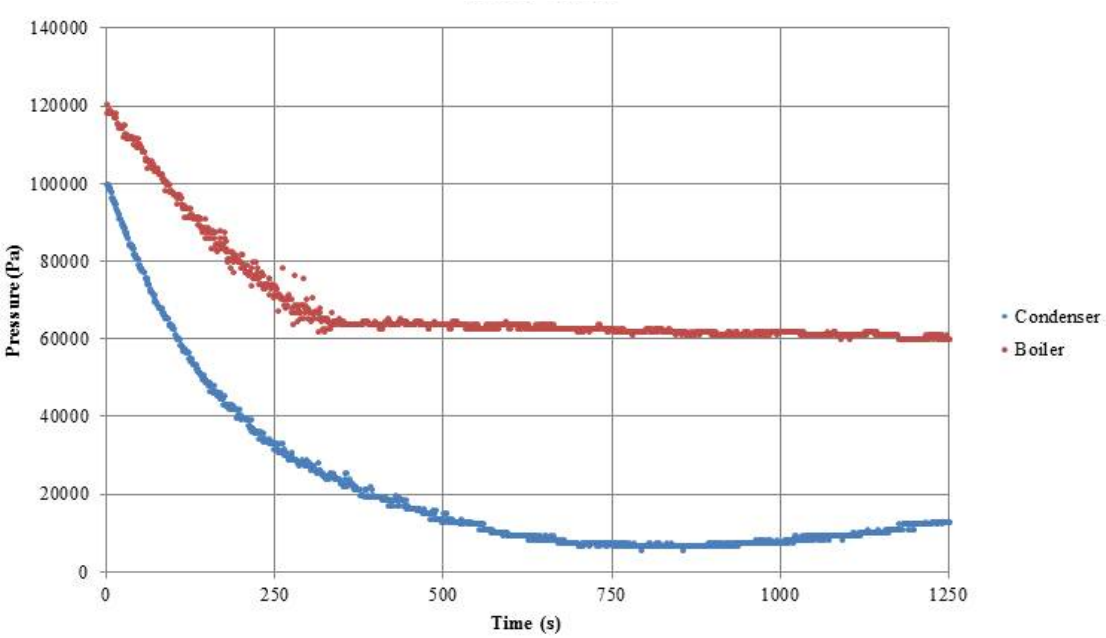

Figure 25. Pressure vs. time after transient initiation for the EZNF1515 nozzle.

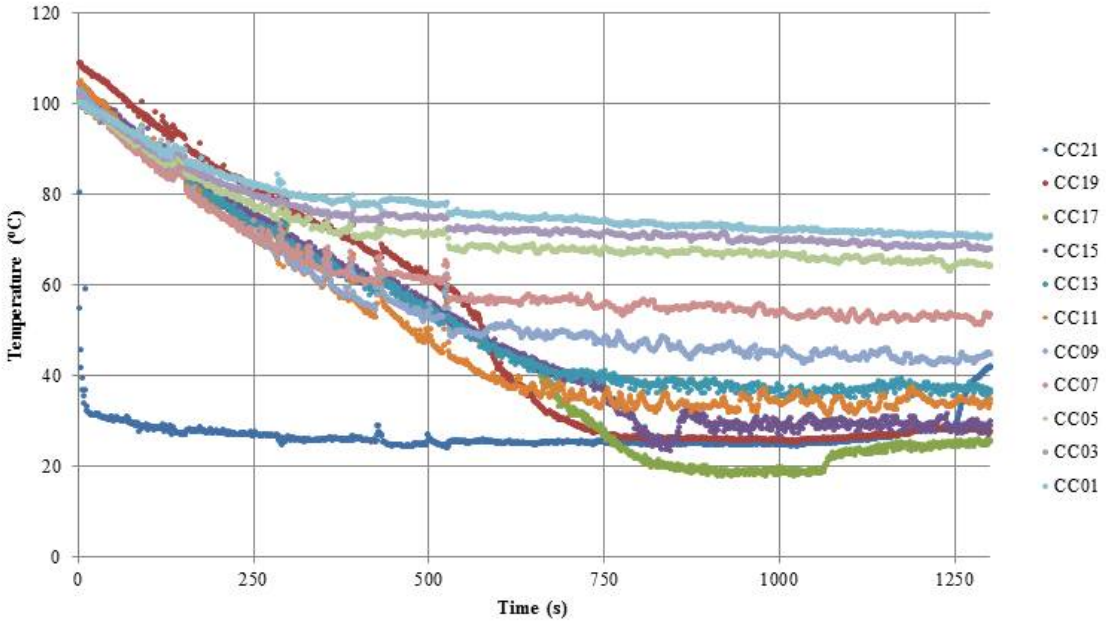

Figure 26. Condenser centerline temperatures vs. time after transient initiation for the EZNF1515 nozzle.

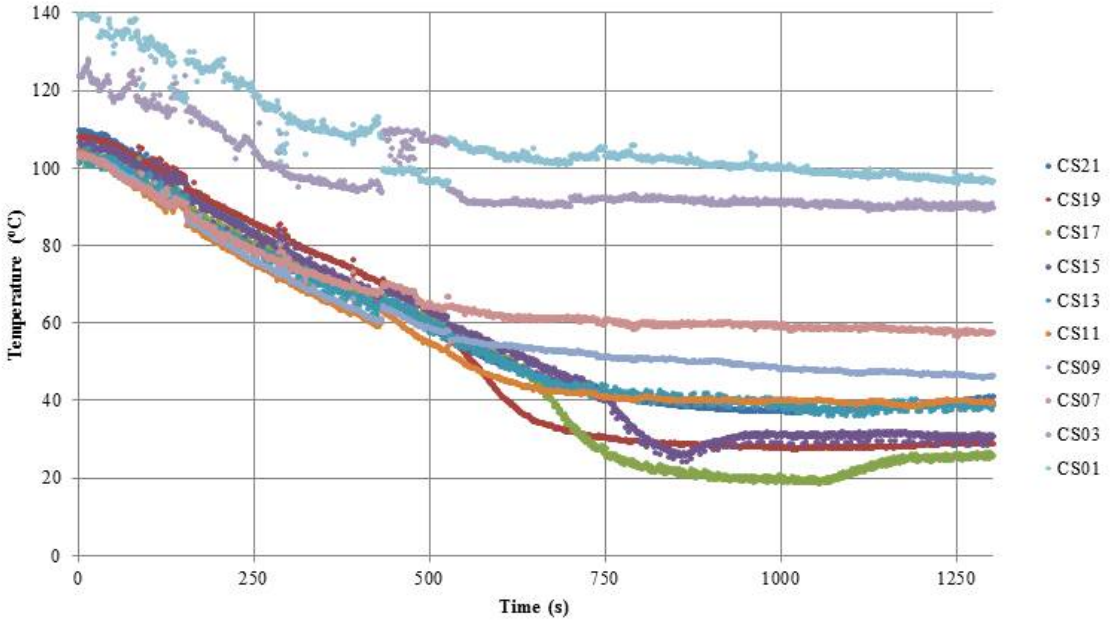

Figure 27. Condenser surface temperatures vs. time after transient initiation for the EZNF1515 nozzle.

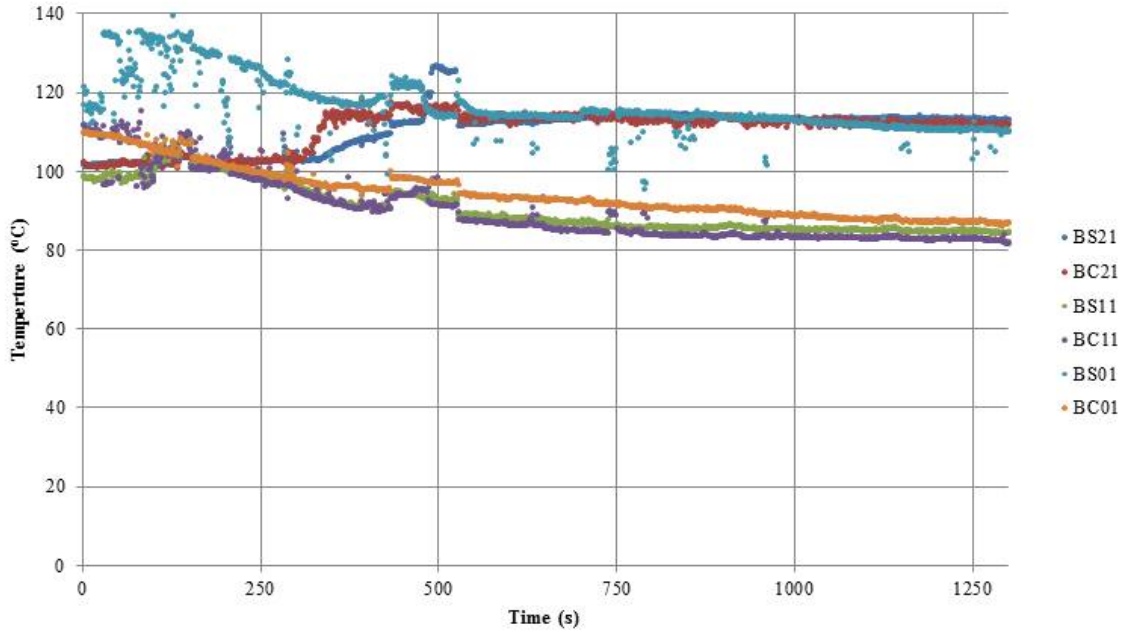

Figure 28. Boiler centerline and surface temperatures vs. time after transient initiation for the EZNF1515 nozzle.

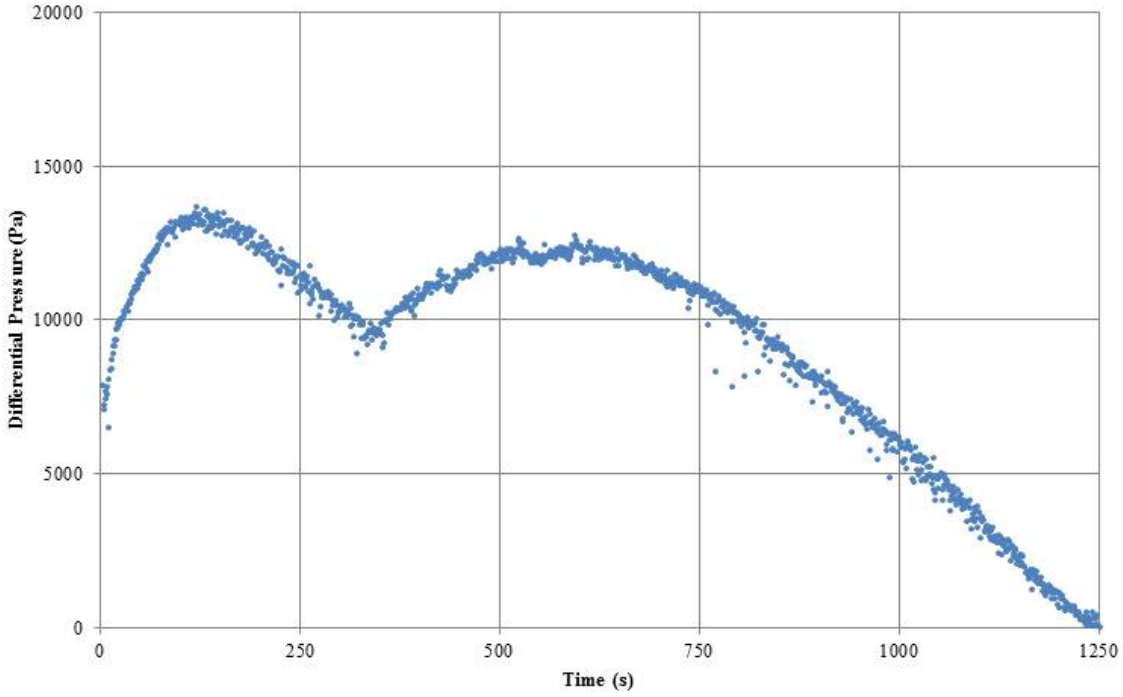

Figure 29. Differential pressure vs. time after transient initiation for the EZNF1515 nozzle.

EZNF3000 Data

Figure 30 is a plot of the boiler and condenser pressures as a function of time for the EZNF3000 nozzle. Figure 31 and Figure 32 are plots of the condenser centerline and condenser surface temperatures as a function of time for the same nozzle, respectively. Figure 33 is a plot of boiler surface and centerline temperatures as a function of time for the EZNF3000 nozzle. Figure 34 is a plot of differential pressure as a function of time of an EZNF3000 transient.

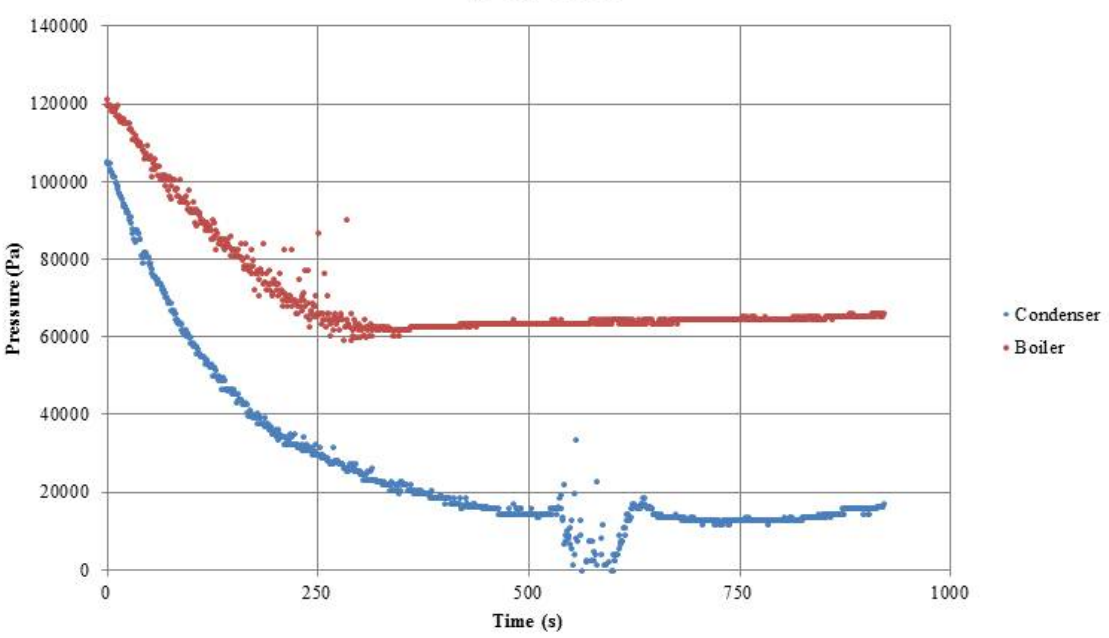

Figure 30. Pressure vs. time after transient initiation for the EZNF3000 nozzle.

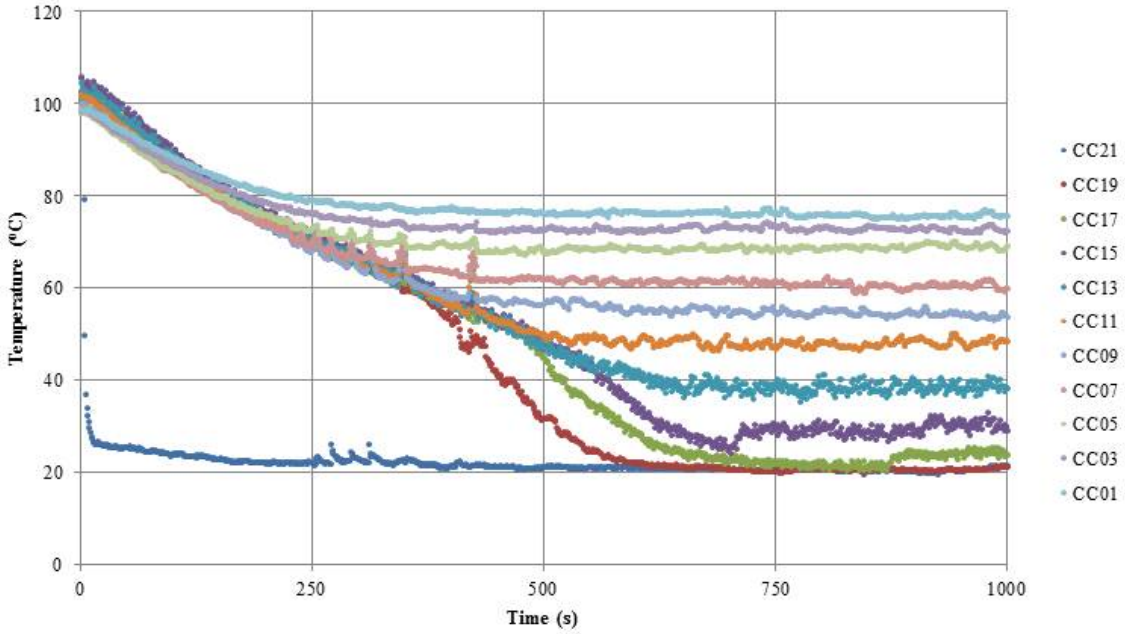

Figure 31. Condenser centerline temperatures vs. time after transient initiation for the EZNF3000 nozzle.

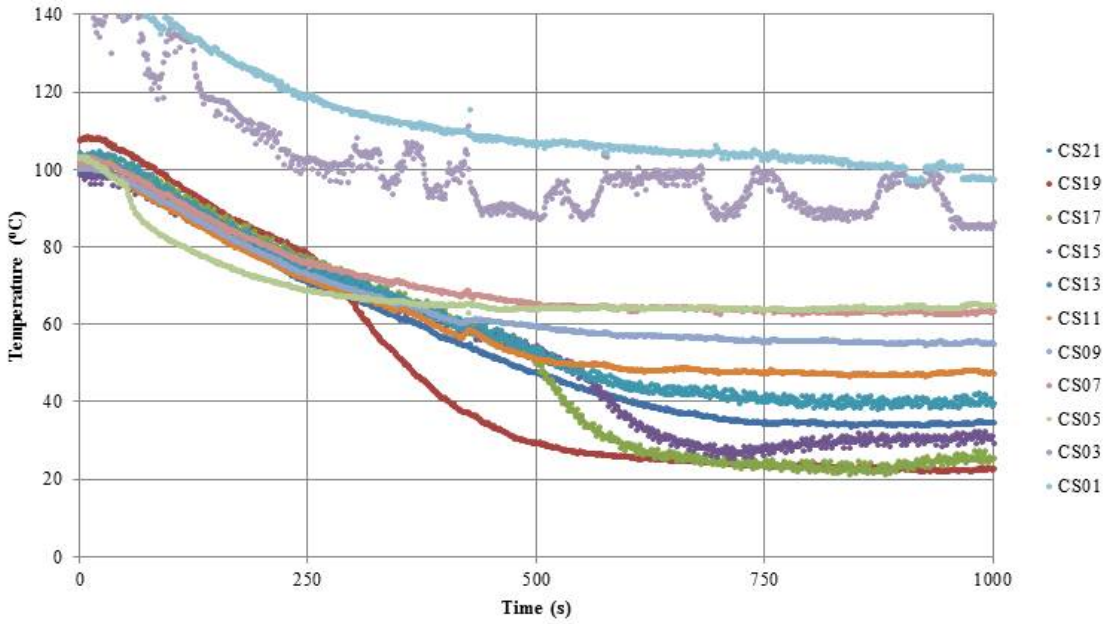

Figure 32. Condenser surface temperatures vs. time after transient initiation for the EZNF3000 nozzle.

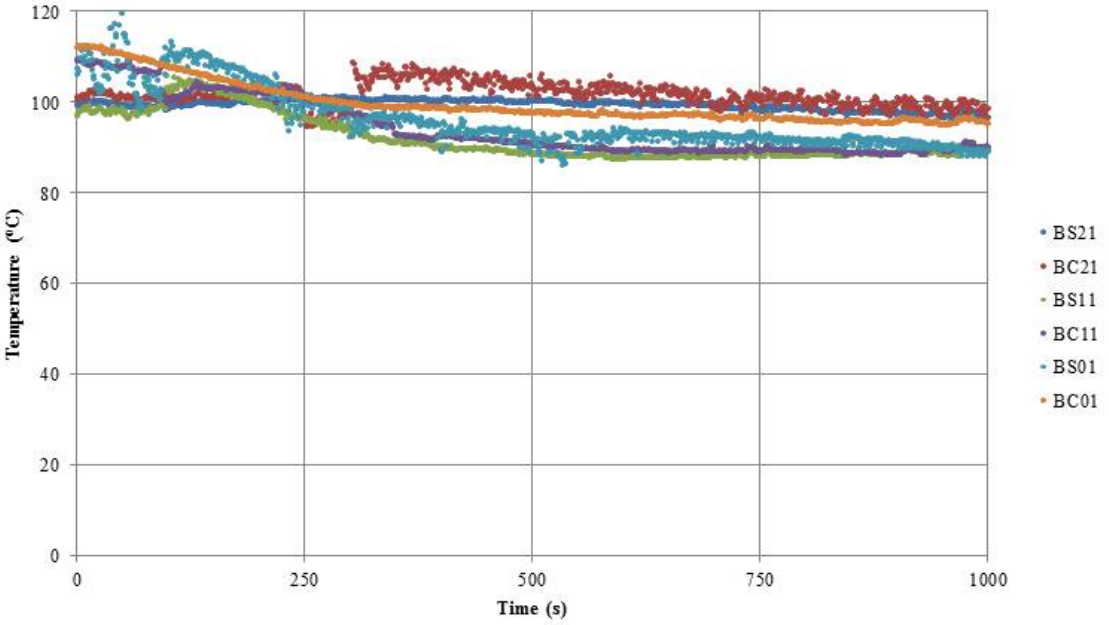

Figure 33. Boiler centerline and surface temperatures vs. time after transient initiation for the EZNF3000 nozzle.

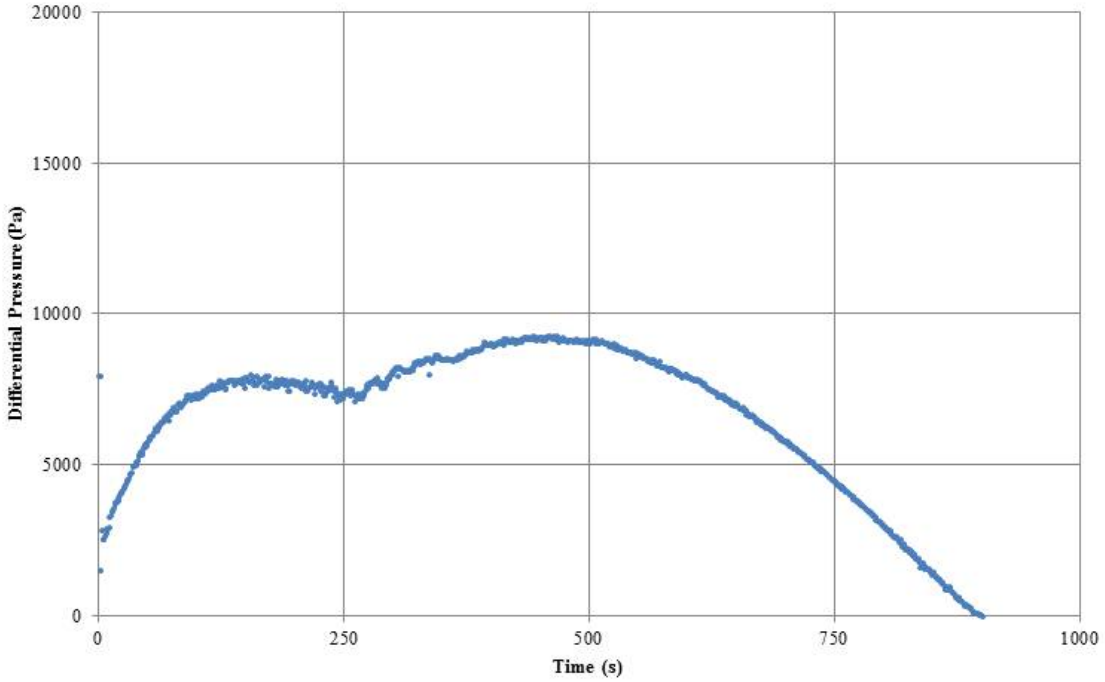

Figure 34. Differential pressure vs. time after transient initiation for the EZNF3000 nozzle.

Chapter 6: Data Analysis

Conservation of Mass

A commercially available Omega PX409-015WDUV differential pressure cell with one tap in the primary stream as it exits the DPHE and one tap in the vapor space of the condenser was used to close the mass balance. The differential pressure gauge was 5-point factory calibrated and local verification of this calibration was conducted with a novel level measuring device based on buoyancy, as outlined in Chapter 4. In addition to this verification, "drain curves" were generated by filling the boiler and condenser pipes to known levels, monitoring the time for each pipe to drain, and then curve fitting the data points. Initial boiler and condenser inventories were known, and the drain curves served as a secondary means to verify the final inventories that were obtained with the differential pressure gauge.

The differential cell measured pressure as a function of time. This data was used to obtain liquid inventory flow rate from the boiler to the condenser pipe using the equation:

$$Flow\ rate = K\sqrt{\Delta p}, \tag{1}$$

where K is the nozzle proportionality constant or loss coefficient provided by the manufacturer (and also verified locally) and Δp is the pressure differential obtained during the experiment and shown in Chapter 5. Using this equation, graphs of liquid inventory vs. time were generated for each transient. Figures 35, 36, 37, 38, and 39 are plots of liquid inventory as a function of time for the EZNF0800, 0815, 1500,

1515, and 3000 transients, respectively. Note that nozzle geometry effects transient duration and amount of liquid inventory transferred during the transient. These differences arise due to differing energy transfer mechanisms and will be discussed in more detail in Chapter 7.

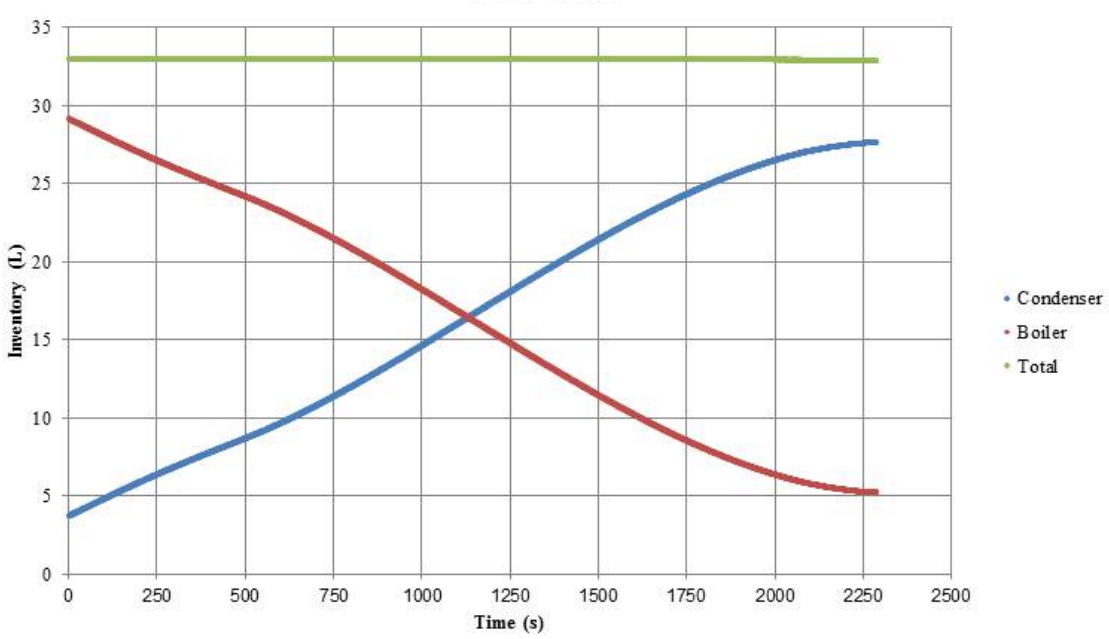

Figure 35. Liquid inventory versus time after transient initiation for the EZNF0800 nozzle.

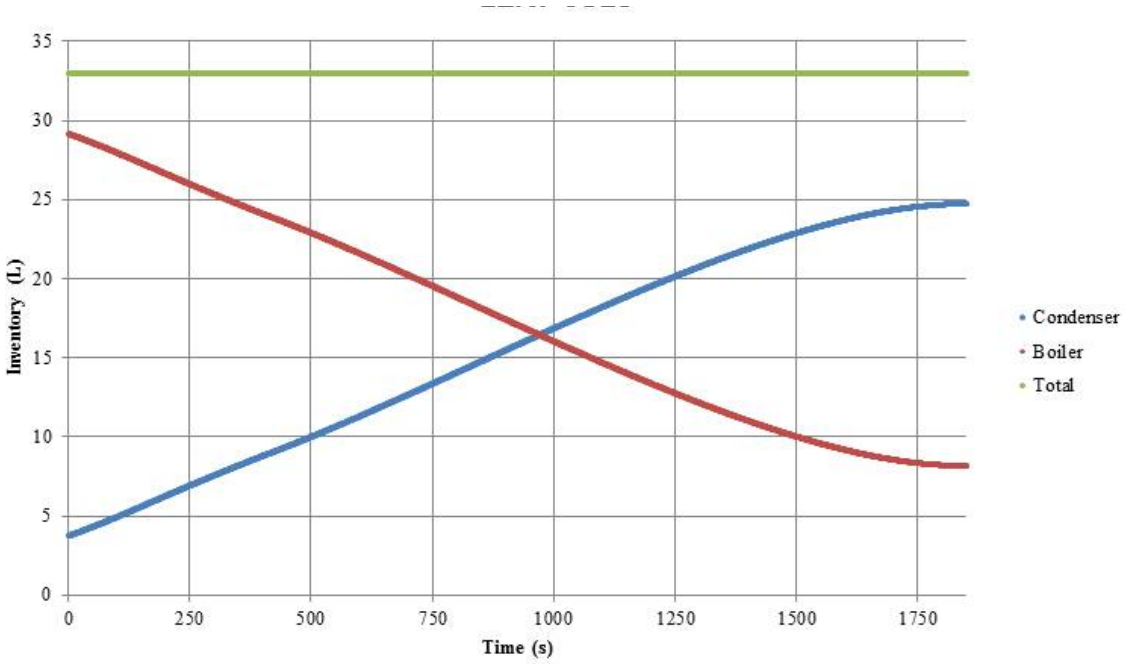

Figure 36. Liquid inventory versus time after transient initiation for the EZNF0815 nozzle.

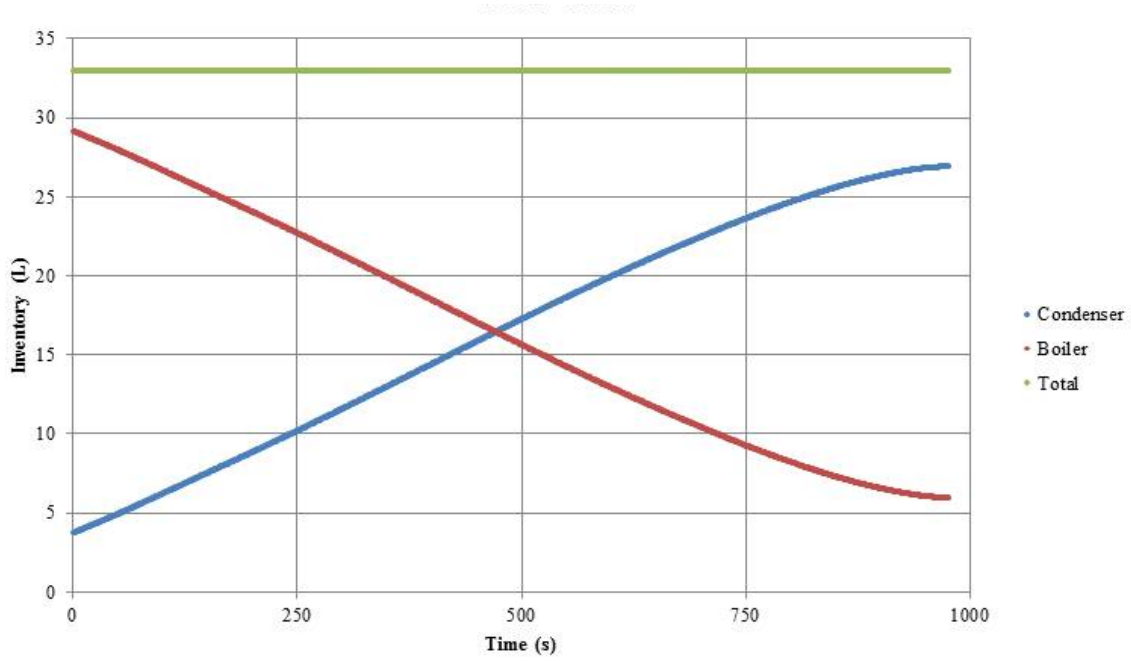

Figure 37. Liquid inventory versus time after transient initiation for the EZNF1500 nozzle.

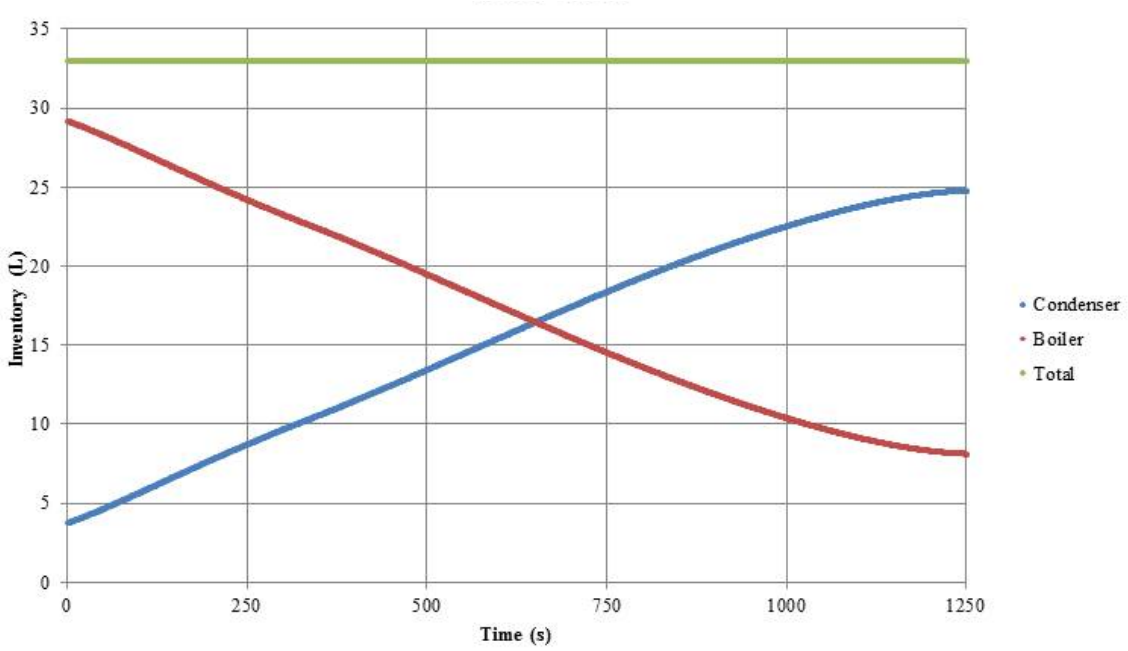

Figure 38. Liquid inventory versus time after transient initiation for the EZNF1515 nozzle.

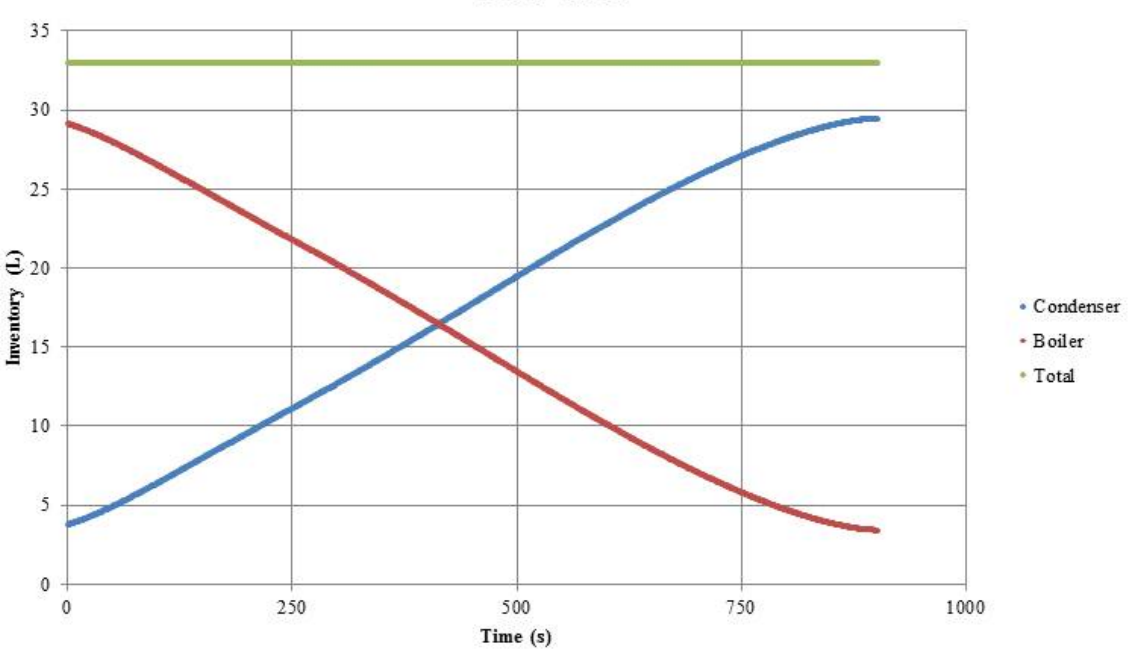

Figure 39. Liquid inventory versus time after transient initiation for the EZNF3000 nozzle.

Conservation of Energy

In order to enable calculation of an energy balance, the condenser pipe was discretized into 12 nodes or cells. The nodes where assigned based on the location of instrumentation, such as thermocouples. Again, scoping experiments revealed that vapor generation in the boiler pipe is sufficient to continuously supply sub-cooled liquid to the condenser. Thus, the boiler does not control the transient and an energy balance for the boiler pipe is not necessary. The total mass (metal & liquid) in each node on the condenser side was calculated. Using the temperature data and the mass balance, initial and final internal energy was calculated for each cell. Heat losses from the header and footer of the condenser pipe were estimated based on transient duration and loss estimates made (during calibration experiments) by filling the condenser, heating to a known temperature, and allowing the pipe to cool while recording how temperature changed with respect to time. Knowing the volume and temperature of the incoming sub-cooled liquid, spray enthalpy was calculated. The energy balance was implemented with the aid of an Excel spreadsheet by plugging these values into the equation 2:

$$\Sigma(U_i)_{cell} + H_{sp} + E_{loss} = \Sigma(U_f)_{cell}$$

$$\Sigma(U_f - U_i)_{cell} = H_{sp} + E_{loss}$$

$$\Sigma[(c_m m_m T_m + c_l m_l T_l)_f - (c_m m_m T_m + c_l m_l T_l)_i]_{cell} = V_l h + E_{loss} \quad (2)$$

where U_i is the initial internal energy for each cell, H_{sp} is the enthalpy of the incoming spray, E_{loss} is the estimated energy loss from the header/footer, U_f is the final internal energy for each cell, c_m is the specific heat of carbon steel (the pipe walls), m_m is the metal mass of each cell, T_m is the surface temperature (i.e.: CS01) of

each cell, c_l is the specific heat of liquid (saturated water), m_l is the mass of the liquid in each cell, T_l is the temperature of the liquid in each cell (i.e.: CC01), V_l is the total of volume of the liquid transferred during the transient, and h is the specific enthalpy of the incoming spray (around 20 ^oC). Equation 2 is essentially a differential energy balance based on the initial and final states. It has been mentioned that MANOTEA transient are integral. Because only initial and final data was used, Equation 2 does not capture the details of our integral transients, and is thereby an approximation. A derivation of an integral energy balance in given in Chapter 7. The integral energy balance is much more complicated to implement, and the complexity does not buy a proportional amount of accuracy. The advantage of the integral energy balance is that it gives insight into the physics behind the transient, whereas Equation 2 is a quick, simple way to verify that the data satisfies conservation of energy.

Table 5 shows the mass associated with each cell and defines cell nomenclature. Tables 6-10 are the energy balance spreadsheets for the EZNF0800, 0815, 1500, 1515, and 3000 transients, respectively. The shaded boxes in Tables 6-10 are the calculated values (in Joules) for the left and right-hand sides of Equation 2. The calculated values differ by less than 5%, as annonated in the figure captions, indicating that the data satisfies the conservation of energy law within reasonable uncertainty limits.

	Metal Mass (kg)	Initial Liquid Mass (kg)	Final Water Mass (kg)
Header	8.99	1.33	1.38
Footer	5.05	Not applicable	Not applicable
“Standard” Cell	7.88	2.66	2.75

Table 5. Table of masses used to perform energy balance.

Location	Initial Temp (C)	Final Temp (C)	Location	Initial Temp (C)	Final Temp (C)	"Cell"	Initial Internal Energy (J)	Final Internal Energy (J)		
CS21	107	36.2	CC21	105	24.2	Header	417478	141240		
CS19	111	29.9	CC19	105	26.6	19	379611	402902		
CS17	106	27.6	CC17	105	25.2	17	362512	379213		
CS15	106	33.6	CC15	102	30.9	15	362512	464157		
CS13	104	38.5	CC13	103	38.9	13	355672	571334		
CS11	105	47	CC11	101	45.4	11	359092	673870		
CS9	105	55.8	CC9	103	55.8	9	359092	821511		
CS7	106	66	CC7	102	62.6	7	362512	933251		
CS5	100	67.6	CC5	101	65.3	5	341992	969240		
CS3	126	96.1	CC3	100	69.1	3	977540	1109657		
CS1	137	95.6	CC1	101	68.7	1	1572722	1103426	Spray	
						Footer	300263	150570	Enthalpy	Losses
						Total (J)	6190672	7720371	1914480	448000
								1529699	1466480	

Table 6. Energy balance spreadsheet for the EZNF0800 transient. Shaded boxes show calculated values for the left and right-hand side of Equation 4. Left and right-hand sides are within ~4%.

Location	Initial Temp (C)	Final Temp (C)	Location	Initial Temp (C)	Final Temp (C)	"Cell"	Initial Internal Energy (J)	Final Internal Energy (J)		
CS21	110	44.3	CC21	109	28.2	Header	429183	172844		
CS19	108	29	CC19	108	28.3	19	369351	259108		
CS17	103	27.7	CC17	103	25.4	17	352252	381815		
CS15	105	31.5	CC15	103	28.8	15	359092	433239		
CS13	103	38.1	CC13	103	39.6	13	352252	577878		
CS11	104	38.6	CC11	104	35.4	11	355672	532117		
CS9	103	45.8	CC9	103	44	9	352252	653942		
CS7	103	56.6	CC7	104	56.6	7	352252	833289		
CS5	102	68.2	CC5	101	66.4	5	348832	983725		
CS3	124	89	CC3	100	68.5	3	970700	1078594		
CS1	140	97.2	CC1	100	71.3	1	1572049	1138284	Spray	
						Footer	306838	156268	Enthalpy	Losses
						Total (J)	6160400	7201104	1506118	414400
								1040704	1091718	

Table 7. Energy balance spreadsheet for the EZNF0815 transient. Left and right-hand sides are within ~5%.

Location	Initial Temp (C)	Final Temp (C)	Location	Initial Temp (C)	Final Temp (C)	"Cell"	Initial Internal Energy (J)	Final Internal Energy (J)		
CS21	107	37.8	CC21	105	35.2	Header	418882	147405		
CS19	111	30.2	CC19	105	29.2	19	380911	268207		
CS17	106	28.1	CC17	103	25.9	17	361588	389037		
CS15	105	31.8	CC15	101	32.8	15	361349	479260		
CS13	104	39.3	CC13	103	38.8	13	354714	572317		
CS11	105	47.5	CC11	102	46.9	11	360220	692883		
CS9	105	55.3	CC9	101	53.1	9	358921	788517		
CS7	106	65.6	CC7	101	61.7	7	365145	921869		
CS5	100	65.1	CC5	96.7	63.7	5	335357	942243		
CS3	119	87.5	CC3	97.2	68.9	3	938117	1078019		
CS1	124	81.7	CC1	96.8	67.7	1	1480752	1044837	Spray	
						Footer	270960	148400	Enthalpy Losses	
						Total (J)	6026593	7472993	1648878	224000
								1446400	1424878	

Table 8. Energy balance spreadsheet for the EZNF1500 transient. Left and right-hand sides are within ~2%.

Location	Initial Temp (C)	Final Temp (C)	Location	Initial Temp (C)	Final Temp (C)	"Cell"	Initial Internal Energy (J)	Final Internal Energy (J)		
CS21	110	39.8	CC21	104	29.9	Header	429183	155286		
CS19	108	29.7	CC19	109	28.9	19	369351	264893		
CS17	102	25.3	CC17	101	24.8	17	348832	366826		
CS15	105	30.5	CC15	103	29.4	15	359092	436601		
CS13	104	39.4	CC13	103	37.7	13	355672	560849		
CS11	104	40.2	CC11	105	34.2	11	355672	524026		
CS9	104	47	CC9	103	43.1	9	355672	647874		
CS7	103	56.7	CC7	101	53.3	7	352252	796333		
CS5	103	65.1	CC5	100	64.6	5	352252	952778		
CS3	124	90.6	CC3	101	69.2	3	976166	1091978		
CS1	139	96.2	CC1	100	71.4	1	1568629	1135995	Spray	
						Footer	304646	156487	Enthalpy Losses	
						Total (J)	6167095	7089926	1246560	280000
								922832	966560	

Table 9. Energy balance spreadsheet for the EZNF1515 transient. Left and right-hand sides are within ~5%.

Location	Initial Temp (C)	Final Temp (C)	Location	Initial Temp (C)	Final Temp (C)	"Cell"	Initial Internal Energy (J)	Final Internal Energy (J)		
CS21	101	34.4	CC21	100	20.5	Header	394068	365918		
CS19	107	22.2	CC19	103	20.6	19	365931	308754		
CS17	103	24.2	CC17	102	24.1	17	352252	355152		
CS15	99.6	30.4	CC15	106	31	15	340624	454343		
CS13	104	39.7	CC13	104	38.1	13	355672	566396		
CS11	101	47.5	CC11	102	48.5	11	345412	710617		
CS9	100	55.2	CC9	100	54.3	9	341992	802505		
CS7	102	63.1	CC7	99.2	60.6	7	348832	900728		
CS5	103	64.2	CC5	98.2	69.1	5	352252	1000562		
CS3	150	91.4	CC3	98.7	72.4	3	1052512	1130882		
CS1	151	99.9	CC1	98.7	75.8	1	1595456	1198380	Spray	
						Footer	330947	166131	Enthalpy	Losses
						Total (J)	6215625	7960368	18059140	212800
								1744743	17846340	

Table 10. Energy balance spreadsheet for the EZNF3000 transient. Left and right-hand sides are within ~3%.

Chapter 7: Discussion

Inverted thermal stratification and circulation cells

Thermal stratification was observed in the condenser pipe for all experiments. Furthermore, this stratification can be described as inverted, because cooler liquid is resting on top of warmer liquid. Thermal inversion layers are common in meteorology, oceanography (Steele, 2009), and, to a lesser extent, nuclear science (Kloppers, 2005). In the MANOTEA experiment, inverted thermal stratification is indicative of an interesting saturation condition in which cooler, denser liquid rests on warmer, less dense liquid. This inverted stratification occurs primarily due to our setup procedures. After venting non-condensable gases, the heater in the condensing pipe is left on and pressure is allowed to build-up in order to fill the boiler pipe. This heat-up phase establishes a temperature gradient over the length of the pipe, with the bottom being much warmer than the top due to its proximity to the heater. Once the transient is initiated and cool spray enters the condenser pipe from the top, the temperature gradient is maintained by lack of fluid circulation. Calculations performed with the aid of Locke (1992), reveal:

$Ra_L^{1/4} = 4.86$ *[dimensionless force]*

$t_D = 0.0662$ *[dimensionless time]*

$2L/D = 186$ *[dimensionless length]*

If $Ra_L^{1/4} << 2L/D$ and $t_D << 2$, the fluid is said to be in the "impeded regime". Thus, MANOTEA transients occur in an impeded regime, meaning: convection is

occurring in small cells (on the order of the diameter of the pipe), at best, capable of communicating only with its nearest neighbors, but vertical or bulk convection is non-existent. Thus, over the relatively short time scale characterized by the duration of a MANTOEA transient, heat transfer within the pooled liquid is occurring primarily by conduction alone. This is a direct consequence of the facility's large aspect ratio. As cooling spray enters, the conduction mechanism cannot transfer energy rapidly enough and little or no mixing occurs. The cooler upper layers end up pressing on the warmer lower layers, providing enough pressure to compensate for temperature-related density differences and maintain equilibrium. Thus, the entire pipe is in equilibrium at a saturation condition with inverted thermal stratification. Inverted thermal stratification was not anticipated, but is an interesting feature of the MANOTEA facility.

Energy Partition

In general it can be said that the size or diameter of the nozzle effects transient duration by allowing more cool spray to enter the condenser pipe during a given time. Thus, for all other things constant, larger diameter nozzles result in faster transients. Unfortunately, this does not give direct insight into how much liquid will be transferred during a transient.

Nozzle geometry effects transient behavior by putting more or less sub-cooled spray on the wall. Subcooled liquid flowing through a fan nozzle hits the pipe wall and cools it, but collapses less vapor. Subcooled liquid flowing through a jet nozzle will fall predominantly into the vapor space, collapsing more vapor and doing more pressure-volume work but not cooling the wall to the same degree as a fan nozzle

with the same diameter. Thus, by doing more pressure-volume work jet nozzles result in more inventory transfer. For a jet nozzle, more of the enthalpy of the incoming subcooled spray goes into collapsing vapor than to cooling the pipe walls.

Figure 40 is a plot of energy transferred from the wall versus volume of liquid transferred from the boiler to the condenser pipe during MANOTEA transients. The figure illustrates how the energy partition, that is what amount of the available, incoming, negative energy (enthalpy) goes into collapsing vapor and what amount goes into cooling the pipe wall, effects inventory transfer. Although not part of the experimental matrix, a transient was ran with an EXNF3015 nozzle in order to determine inventory transferred. For large nozzles, the energy partition has little effect because enough cool spray is entering the condenser to overwhelm the system regardless of nozzle geometry (a rapid condensation transient). As nozzle size decreases, the effects of the energy partition become apparent as an ever increasing difference in the amount of liquid transferred. In the figure, the energy lost by the wall was calculated from the energy balances and liters transferred were taken from the mass balances, both outlined in Chapter 7. The heavy black line suggests the location of a domain delimiter (in the sense described in Chapter 3), but is not based on calculations.

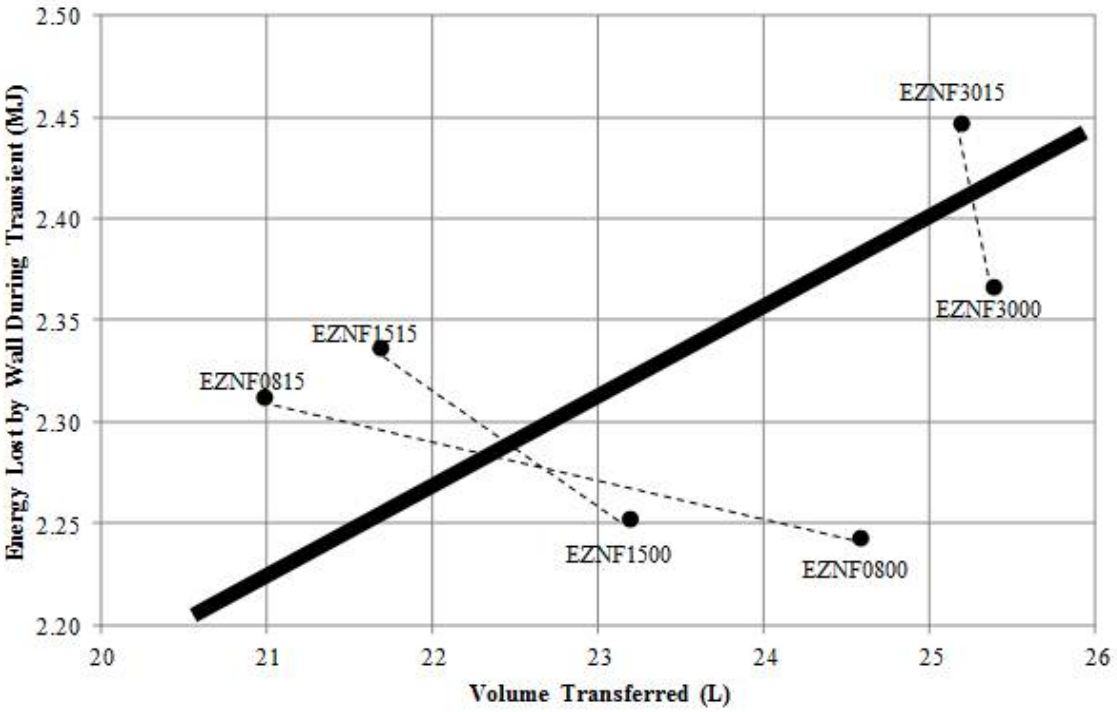

Figure 40. Energy transferred from the wall versus volume transferred from the boiler pipe to the condenser pipe. Plot shows effect of energy partition. Heavy line suggests domain delimiter: somewhere between the two geometries, 15-deg nozzles put more energy into pipe wall and 0-deg nozzles put more energy into vapor.

The energy partition is important for understanding the physics behind the different transients and proves useful when interrogating the TRACE code. It captures the operating domains outlined in Chapter 3. From the data, it can be inferred that nozzle size is mainly responsible for transient duration and nozzle geometry dictates how much inventory will be transferred. However, in reality, duration and inventory transfer is a complex interplay between size and geometry that can be captured only in terms of this energy partition. Yet, it is interesting to note that each of the transients follows the exact same sequence regardless of nozzle size

or geometry. This statement will be justified in the one of the following discussion sections. The importance of the energy partition is the insight it provides into the physics controlling each transient. Although the energy partition is never quantified in the present work because it is difficult to compare directly to TRACE, it is useful and informative to derive an energy balance based on the energy partition.

Derivation of Integral Energy Balance Based on Energy Partition Principle

Liquid mass leaving the boiler is always equal to the liquid mass entering the condenser. Regardless of nozzle, every transient is controlled by a competition between the energy in the metal masses and the energy in the incoming spray. This competition in turn dictates the differential pressure. Coupling these observations with our discovery that a flashing controlled transient is not possible on the MANOTEA allows us to perform an energy balance by investigating the condenser pipe alone. Figure 41 is a schematic of the control volume that will be used to derive an energy balance equation for a MANOTEA transient.

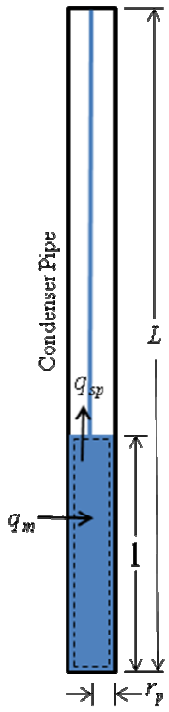

Figure 41. Schematic drawing showing control volume used to derive integral energy balance based on the energy partition.

Treat the spray entering the condenser pipe as a column of liquid that falls into the pool and manages not to hit the wall. Steam is a poor thermal conductor, so little vapor is generated by direct contact at the periphery of the falling liquid column. Nonetheless, a small amount of steam in the vapor space will condense on the surface of the liquid column and warm it during the descent. This mass is negligible. The liquid inventory increases as the spray continues and the amount of wetted metal continues to increase. For now, let's assume that the incoming spray cools and mixes the pooled liquid. Liquid water is a much better thermal conductor than steam, so the majority of the energy stored in the metal mass

is conducted to the water pool, which warms the liquid pool. Justification for these assumptions is given in the Appendix.

Allowing for these assumptions, we draw a deformable control volume (similar the way energy balances are commonly performed for reactor pressurizers) around the pooled liquid in the bottom of the condensing pipe, and write the following differential energy balance equation (note all notation is defined in the list of symbols, abbreviations, and notation at the beginning of this dissertation):

$$dE/dt = c_L(d(m_L T_L)/dt) = c_L m_L(dT_L/dt) + c_L T_L(dm_L/dt) = q_m + q_{sp}$$

Energy/time in metal: $q_m = m_m c_m dT_m/dt$

Energy/time in spray: $q_{sp} = (dm_{sp}/dt)c_{sp}(T_{sp})$

$$c_L m_L(dT_L/dt) + c_L T_L(dm_L/dt) = - m_m c_m dT_m/dt + (dm_{sp}/dt)c_{sp}(T_{sp})$$

Note: $dT_L/dt = (dp/dt)(RT/\Lambda)(T_L/p)$, per Clausius-Clapeyron (see Appendix for a primer on Clausius_Clapeyron) for $T_L = T_{sat}$

$$c_L m_L(dp/dt)(RT/\Lambda)(T_L/p) = - m_m c_m dT_m/dt - (dm_{sp}/dt)c_{sp}(T_L - T_{sp})$$

$$c_L m_L(dp/dt)(RT/\Lambda)(T_L/p) = - [m_m c_m dT_m/dt + (dm_{sp}/dt)c_{sp}(T_L - T_{sp})]$$

$$(1/p)(dp/dt) = - (1/c_L m_L T_L)(\Lambda/RT)[m_m c_m dT_m/dt + (dm_{sp}/dt)c_{sp}(T_L - T_{sp})]$$

Note: $c_{sp} = c_L$

$$(1/p)(dp/dt) = -(\Lambda/RT)[(m_m/m_L)(c_m/c_L T_L)(dT_m/dt)+(1/m_L)(dm_{sp}/dt)(1-T_{sp}/T_L)]$$

$$(1/p)(dp/dt) = (\Lambda/RT)[(m_m c_m/\rho_L c_L T_L)(dT_m/dt) - (dV_L/dt)(1 - T_{sp}/T_L)]/V_L$$

Let $(m_m c_m/\rho_L c_L T_L) = M$ (keeping in mind that $T_L = T_{sat}$ and is basically constant)

$$(1/p)(dp/dt) = (\Lambda/RT)[M(dT_m/dt) - (dV_L/dt)(1 - T_{sp}/T_L)]/V_L$$

From data:

T_{sp} ~= 295 K, $T_L = T_{sat}$ ~= 340 K (an average temp) *and* $(1 - T_{sp}/T_L) = 0.132$

$m_m c_m/\rho_L c_L T_L = M$ ~= (83.0 kg)(0.490 kJ/kgK)/(983 kg/m^3)(4.19 kJ/kgK)

(340 K) = 2.9E-5

$\Lambda/RT = 13.3$

Let $p/p_o = P$, and we can write:

$$P = e^{\int_0^t \{[0.00039(dT_m/dt) - 1.8(dV_L/dt)]/V_L\}\, dt}$$

This equation is true if the metal can be treated as a lumped capacitance. If $Bi > 0.1$, then the metal term would require modification. This modification involves invoking an approximate, truncated infinite series solution (Incropera, 2002; Heisler, 1947). These approximations are tabulated for common geometries and can be implemented in our equation by multiplying the metal term by a constant, χ, where $\chi = 1$ if $Bi < 0.1$:

$$P = e^{\int_0^t \{[0.00039\,\chi\,(dT_m/dt) - 1.8(dV_L/dt)]/V_L\}\, dt} \qquad (3)$$

A closed-form, analytic solution is available for equations of this type. However, leaving it in this form has the advantage of allowing the contribution due to the metal and contribution due to the spray to be plotted separately if desired. Equation 3 is essentially a path or line integral. Thus, it captures the integral nature of the MANOTEA facility and allows this nature to be quantified. The equation tells us that transients are "path dependent" and cannot be properly described or predicted by thermal-dynamic initial and final states (it matters how the facility gets from one state to the next and history will play a role). The effects and phenomena involved in the transients are cumulative. Equation 3 implies that interplay between the metal

contribution and spray contribution to the energy balance will dictate transient nature (duration, liquid transferred from boiler to condenser, etc.).

Contribution from the spray will vary with nozzle geometry. The volume of the metal and initial liquid inventory was fixed for the present work. When metal mass contribution is overwhelmed by the spray contribution, vapor condenses and pressure in the condenser pipe plummets. This happens for all transient outlined in this paper. Differential pressure initially dropped from 21000 *kPa* when the valve was opened to start the transient and then started to increase rapidly. This increase in differential pressure was driven by rapid condensation. When metal mass dominates over spray, pressure in the condenser pipe increased. This happens for the smaller nozzles (EZNF 0400 or smaller) that were used in the scoping experiments performed to write the proposal for the present work. For these smaller nozzles, differential pressure decreased over an extended period of time at transient initiation. This decrease was due to vapor generation in the condensing pipe. A critical amount of inventory must enter the condenser pipe in order for the metal mass to be overwhelmed initially. When vapor generated by the hot metal equals vapor condensed by the incoming spray, pressure will remain constant. In this manner, a transient can be viewed as a competition between the metal and spray contributions to the energy balance. The fundamental consideration at any given time during a transient is how much liquid has been transferred up to and during that instant. Nozzle geometry and the subsequent energy partition is vital to understanding transient behavior.

An explanation of how the parameters in Equation 3 were obtained from the data is presented in the Appendix. Figure 42 is an implementation of Equation 3 for the condenser pipe based on data from an EZNF1500 transient with $\chi = 1$.

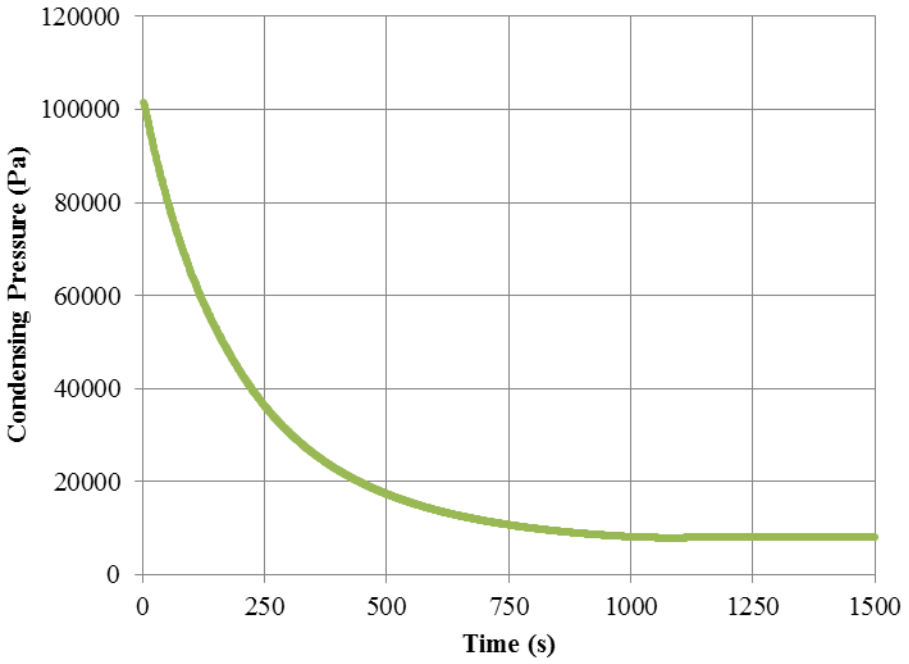

Figure 42. Implementation of Equation 3 with EZNF 1500 experimental data.

As implemented, the model is qualitatively similar for de-pressurization of the condenser pipe, but the re-pressurization effect is not capture. This discrepancy is due to some of the liquid not participating in heat transfer. As previously shown, the pool is not well mixed: it is stratified and sub-cooled liquid is present. Thus, the assumptions that lead to the equation were not met. Nonetheless, it was instructional to derive the equation based on that assumption; it enabled an

equation that is still a good approximation. However, to properly account for the fraction of the pooled water that is actually participating in heat transfer, Equation 3 must be modified:

$$P = e^{\int_0^t \{[0.00039\chi (dT_m/dt) - 1.8(d(fV_L)/dt)] / fV_L\}\, dt} \quad (4)$$

The participating fraction, *f*, ranges from 0 to 1 and delineates how much liquid is participating in energy transfer. At the beginning of the transient, it can be reasoned that all of the liquid will participate and that less liquid will participate as the transient progresses. Analysis of Equation 4 reveals that the participating fraction provides an amplifying mechanism by which re-pressurization can occur. The concept of a participating fraction is reinforced by the presence of inverted thermal stratification in the data. This entire derivation is meant only to show that the physics behind transient behavior is well understood and can be calculated manually, although with some effort. In addition, the derivation re-enforces the integral nature of MANOTEA transients.

Explanation of Differential Pressure Plots

Inspection of the diffential pressure plots Figures 14, 19, 24, 29, and 34, respectively) reveal the presence of two “bumps” or stages. Figure 43 is a reproduction of Figures 10 and 14 side by side for easy comparison. Regardless of transient, condenser pressure drops rapidly, reaches and maintains a minimum value, and finally recovers slightly as the transient terminates. Boiler pressure initially drops rapidly, and then levels off and maintains a constant pressure. Differential pressure is a complex combination of boiler and condenser pressure, respectively.

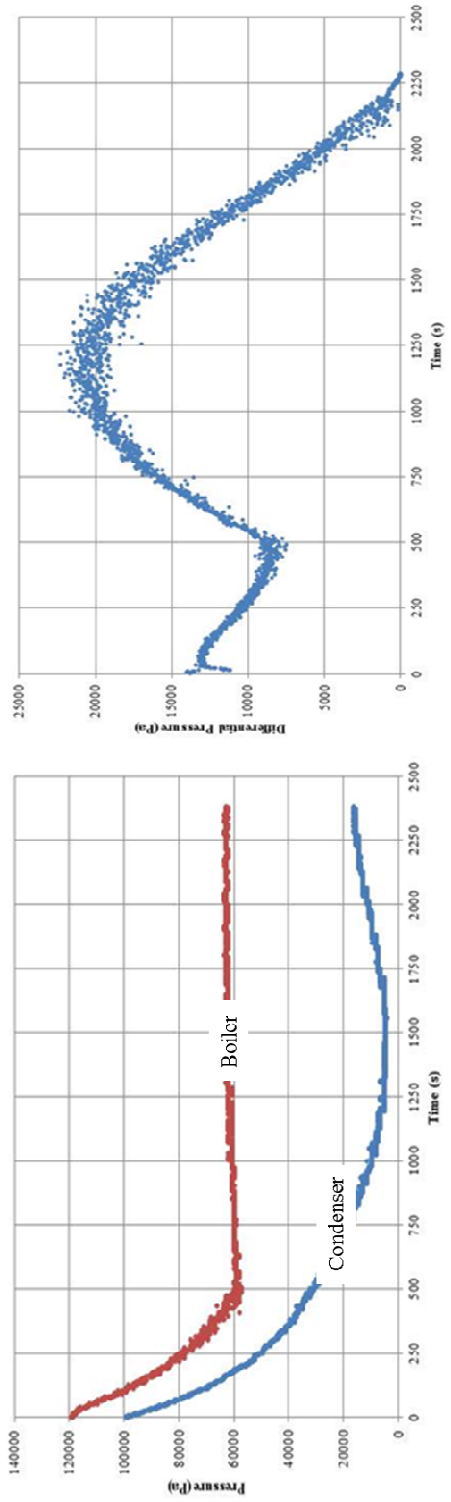

Figure 43. Reproduction of Figures 10 (pressure vs. time) and 14 (differential pressure vs. time), respectively.

The two differential pressure stages are a direct consequence of the two pressure regimes in the boiler pipe. In order to explain the two pressure regimes, the boiler was broken into 10 nodes. Scoping experiments included detailed temperature profiles for the boiler. This data was used to determine the bulk fluid temperature at the center of each node at given times. Boiler pressure data and the mass balance were used to determine the total pressure at the center of each node for the same times. Total pressure in a node is simply the combination of the pressure in the vapor space (available from boiler pressure data) and the pressure due to the volume of liquid above the node (inferred from the mass balance). Pressure and node temperature dictate which nodes are saturated at any given instant. Figure 44 shows the results of this analysis. In the figure, saturated nodes are red and subcooled nodes are blue. Temperature and pressure data on the figure are for the center of each node.

During the stripping process previously described, the boiler is half full of liquid. The liquid is brought to saturation and allowed to boil for several hours in order to strip the non-condensable gases. A great deal of vapor is generated during stripping and the energy from this vapor is deposited, via condensation, into the pipe wall above the water surface. This results in a hot region in the vicinity of axial levels 13-15 (as defined in Figure 1). This warm area persists and is still present at transient initiation.

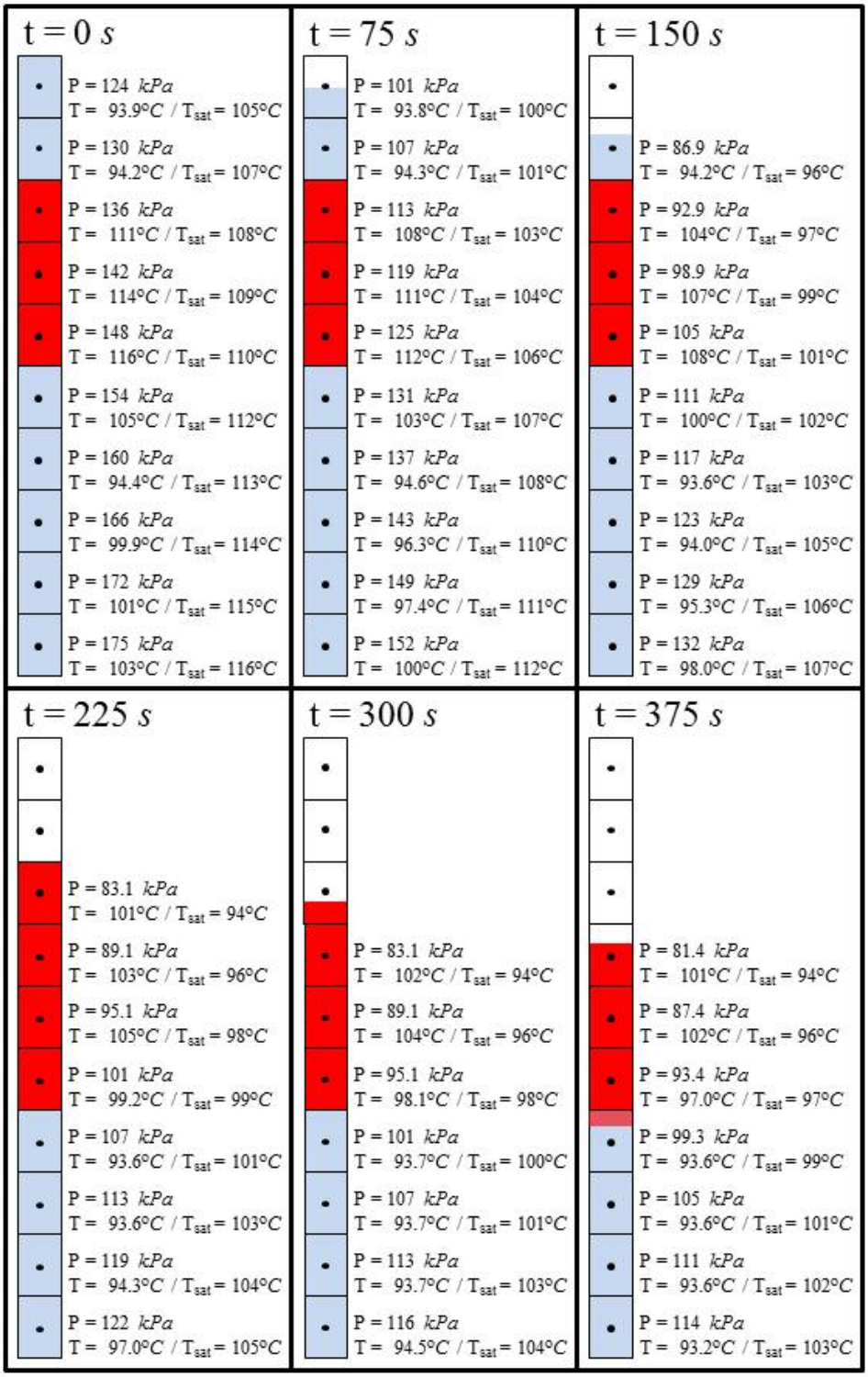

Figure 44. Boiler saturation analysis.

At transient intiation the hot region is saturated and generates vapor. However, a region of subcooled liquid exists above the hot region. In the first boiler pressure regime, pressure decreases because a portion of the vapor generated in the hot region condenses and warms the subcooled liquid above. This pressure decrease is mitigated because some vapor still manages to reach the space above the subcooled liquid. At the same time, liquid inventory in the boiler is decreasing. As inventory decreases, the pressure due to the static head decreases, which results in more liquid reaching saturation and contributing to vapor generation. The net effect is that the pressure in the boiler decreases linearly as it attempts to reach the saturation condition dictated by the wall temperature in the hot region. This phenomenon is known as thermal compliance. Sufficient vapor is always generated and allows the transient to continue unhindered.

Once the subcooled region above the hot region ceases to exist due to inventory depletion, boiler pressure no longer decreases because vapor is continuously generated and all of the vapor is available to hold up the pressure. Boiler pressure stabilizes and assumes a constant, saturated value. In Figure 44, this transition occurs at around 200 seconds. As the transient progresses, inventory continues to be transferred to the condenser reducing the static pressure head and allowing lower nodes to reach saturation and generate vapor in turn. Every transient terminates with boiler pressure still at this saturation pressure. The constant pressure pressure found in the second boiler pressure regime is related to wall temperature and occurs due to the wall's large heat capacity.

Experiment Scope

As mentioned, a difference in liquid transferred exists that is related to nozzle size and geometry and can be captured in terms of an energy partition. This volume difference was used to provide boundaries or scope to the MANOTEA experiments. Figure 45 is a plot of the difference between the volume transferred when using a 0-deg and 15-deg nozzle of the same size versus the nozzle cross-sectional area. The figure shows that large nozzles have a small volume transfer difference as geometry becomes less important because the incoming spray overwhelms the system. The figure also shows that the volume difference is small if the nozzle size becomes small enough, as illustrated with the EZNF04XX series data point. It should be noted that the 04-series was used for original scoping experiments, but that the set is not considered part of the MANOTEA test data because the nozzle size is small enough to delay or prevent transient initiation. This delay or termination is due to insufficient cooling spray entering the condenser. For smaller diameter nozzles of a critical size, a small stream enters the condenser and is immediately vaporized. This vaporization prevents rapid condensation from occurring and provides a lower limit for acceptable nozzle diameter for MANOTEA. Thus, for smaller nozzles, geometry becomes unimportant because the metal masses overwhelm the system. The figure shows that the greatest volume transfer difference occurs for the EZNF08XX series. This large volume difference is interesting, provides insight into the physics at work in the apparatus, and promised to be the most useful data for challenging and interrogating the TRACE code. For this reason, the 08-series data was used for comparison to the TRACE model during the second phase of the present work.

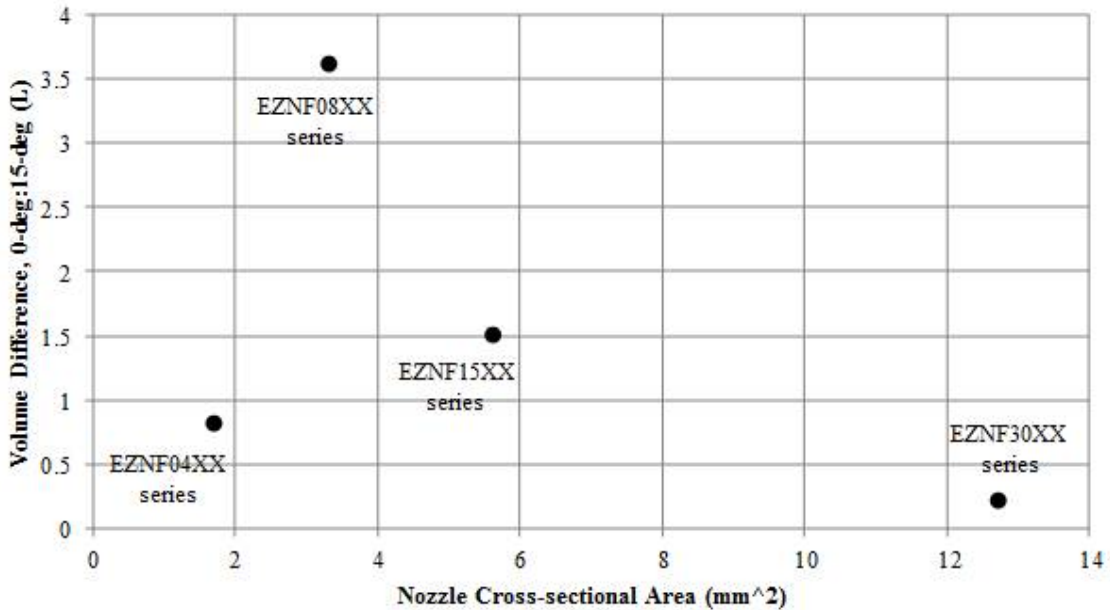

Figure 45. Volume difference between 0 and 15-deg nozzle of fixed cross-sectional area.

Transient Sequence and Integral Nature of Experiment – Summary of All Data Sets

Plotting condenser pressure as a function of inventory instead of time exposes the integral nature of MANOTEA transients, reveals the transient sequence, and allows all the data sets to be summarized on one plot. Figure 46 is a plot of condenser pressure as a function of inventory. The plot shows that regardless of nozzle size or geometry, when time is eliminated, all MANOTEA transients follow the same sequence. For the boiler pipe, pressure first decreases linearly and then levels off. For the condenser side, pressure drops to a minimum value and then recovers slightly. This recovery indicates that flow has stopped and the transient has terminated. Since both sides are at saturation, bulk temperature for the condenser and boiler can be inferred from the pressure data. In this way, all energy and mass information is a subset of the information contained in Figure 46. The figure shows

that the fundamental criterion for determining the state of a MANOTEA transient is the amount of fluid transferred up to and during a given instant in time. This is also a feature in reactor transients, particularly loss of coolant scenarios, and ties the simplified transients produced with MANOTEA to the more complex transients found in actual reactor systems. This link makes the data and finding from this series of experiments relevant and gives meaning to any efforts to test the TRACE code with this data.

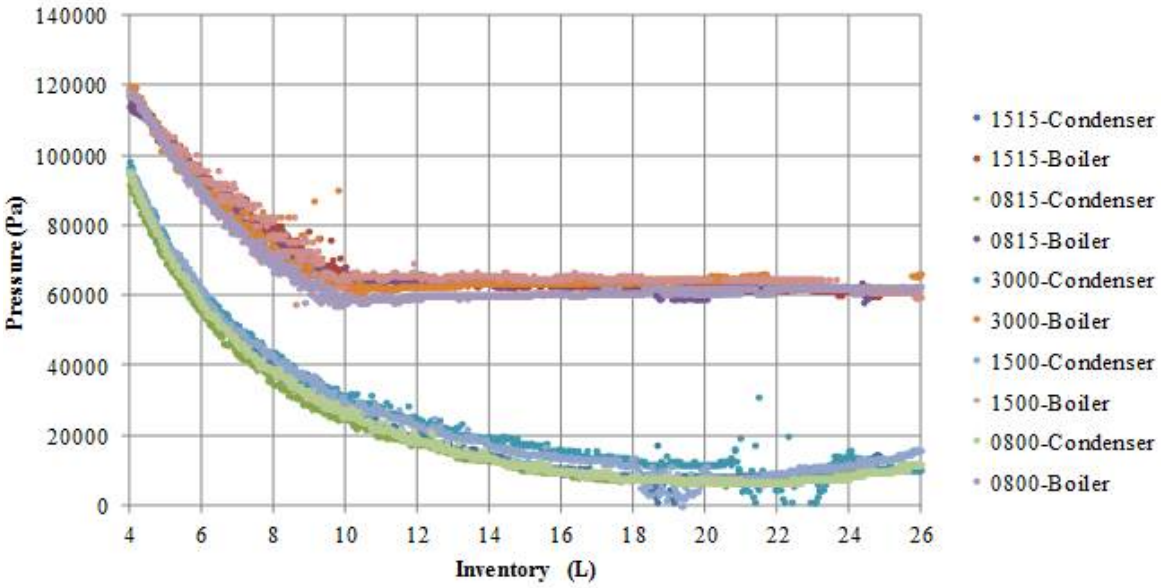

Figure 46. Pressure as a function of condenser inventory for all nozzles.

Effect of Non-condensable Gases

Non-condensable gases are known to significantly degrade the rate of condensation heat transfer in two-phase systems (Hijikata, 1984). These gases tend to migrate and accumulate near the colder surfaces, reducing the partial pressure of the vapor and subsequently the corresponding saturation temperature of the vapor.

Uchida and co-workers (1965) reported that the heat transfer rates depend only on the air-to-steam mass ratio. Air-to-steam ratios less than 0.10 have a small effect on condensation heat transfer. However, for a 0.50 ratio, condensation heat transfer coefficients are cut in half (Uchida, 1965). Non-condensable gases are present in many reactor systems to include, but not limited to, the containment and accumulator. The effects of these gases must be accounted for during reactor transient scenarios. For containment response analysis, safety regulations require the use of the Tagami correlation (1965) for the case of a LOCA and Uchida correlation during a main steam line break scenario (Massoud, 2005).

In MANOTEA, non-condensable gases are purposely stripped because they suppress rapid condensation and could thereby prevent a transient from initiating or slow and prematurely terminate a transient that is already in progress. In spite of efforts to eliminate them from the system, small fractions of non-condensable gases are known to accumulate in the colder spaces in MANOTEA during the stripping process. Namely, some non-condensable gases remain in the primary side of the DPHE. These gases ultimately end up in the condenser. Assuming that all non-condensable gases are removed from the boiler and condenser pipe inventory during the stripping process, and assuming that the primary side of the DPHE is completely full of non-condensable gas (a large over-estimate), the fraction of non-condensable gases in the condenser at transient initiation is estimated to be slightly less than 1%. This estimate is based on the ratio of the volume of the primary side to that of the condenser. Thus, at transient initiation, the partial pressure of the non-condensable gases is around 820 Pa. This value was needed to properly account for non-

condensable gases when modeling MANOTEA with TRACE. Although a small fraction, as the transient progresses and the condenser fills, the fraction becomes larger. Some of the gases are likely absorbed into the pooled water, while some remain in the vapor space. The increasing concentration is eventually a contributing factor to transient termination. It is posited to be one of the reasons for the slight, smooth pressure recovery found in at the end of all MANOTEA transients. This discussion will be revived in Chapter 12 when modeling non-condensable gases will be discussed.

Chapter 8: Experiment Summary

A simplified, integral, condensation-driven transient apparatus named MANOTEA was constructed and calibrated in order to experimentally validate the TRACE plug-in of the NRC's Symbolic Nuclear Analysis Package (SNAP) for rapid condensation transients. The TRACE plug-in is designed to analyze thermal-hydraulic transients. The challenges that integral, condensation-driven transients have posed to thermal-hydraulic codes provided the motivation for the present work. The present work is particularly relevant because many of the proposed passive mechanisms and safety systems found in next generation reactors rely on rapid condensation for normal operation or accident mitigation.

A series of experiments was run on MANOTEA. Raw, standalone data from the facility included: pressure, differential pressure, and temperature profiles, all as a function of time. Using the raw data, a mass and energy balance was closed for each of the transients. Some of the relevant characteristics of the data were discussed and include: inverted thermal stratification in the condenser and nozzle dependent transients that are physically controlled by an energy partition. Plotting pressure as a function of inventory revealed a convenient way to summarize all of the transient datasets and resulted in a transient sequence. This sequence highlights the integral nature of MANOTEA transients and ties the facility to more complex reactor systems. The transient sequence will serve as the fundamental comparison to evaluate TRACE in the next section. Other characteristics will also be compared to

TRACE output. MANOTEA is simple enough that models can be used to perform back-of-the-envelop calculations to predict transient behavior. This was shown by performing an integral energy balance in Chapter 7.

PART 2: TRACE MODELING

Chapter 9: TRACE Introduction

Overview

TRACE is the culmination of over 30 years of development, which began in the wake of Three Mile Island and continues to this day. It is a modernized thermal-hydraulics code designed to combine and extend the capabilities of NRC's 3 legacy safety codes - TRAC-P (PWR), TRAC-B (BWR) and RELAP (NRC Website, 2011). TRACE is currently delivered as a plug-in (loosely: an application) to Symbolic Nucelar Analysis Package (SNAP). SNAP is the NRC's flagship analysis package and is used to certify future reactor designs and improvements. The package incorporates a standard graphical user interface designed to simplify use of the codes, give plug-in users a consistent interface and aid in interoperability between the different plug-ins. The program also fully incorporates a post-processing application used to print results in graphical form (Information Systems Lab., 2010).

The TRACE plug-in is a best-estimate code designed to analyze thermal-hydraulic transients in nuclear and non-nuclear systems. These transients include LOCAs, operational transients, and accidents scenarios in pressurized light-water reactors (PWRs), boiling light-water reactors (BWRs), and experimental facilities designed to simulate reactor transients. In order to analyze these transients, TRACE employs multi-dimensional fluid dynamic, non-equilibrium thermo-dynamic, generalized heat transfer, re-flood, level tracking, and reactor kinetic models (Applied Programming Technology, 2007b).

The code uses either semi-implicit, finite-element or stability enhancing two-step (SETS) techniques to solve 6 field-equations for two-phase flow: conservation of mass for vapor, conservation of mass for liquid, conservation of momentum for vapor, conservation of momentum for liquid, conservation of energy for vapor and conservation of energy for liquid. If needed, additional equations are solved for non-condensable gases and boron concentration. For the interested reader, the semi-implicit, one-dimensional, finite-difference equations used by TRACE to solve the mass, energy, and momentum balances are outlined in the Appendix. Semi-empirical correlations for the equations of state, wall drag, interfacial drag, wall heat transfer, and interfacial heat transfer are used to solve for any remaining variables and close the equations for a solution (Applied Programming Technology, 2007b).

TRACE employs a component-based approach to modeling a system. These components have names that intuitively describe what they are intended to model, for example: PIPE, PUMP, PLENUM, TEE, VALVE, CHAN (BWR fuel channel), JETP (jet pumps), VESSEL, HEATR (feedwater heater), etc. Each physical piece of a system can be represented using these components. In turn, each component can be "nodalized" into some number of volumes or cells over which the fluid, conduction, and kinetics equations are averaged. Node, cell, and volume are all equivalent expressions which mean "finite-element", in the sense of finite-element analysis or numerical methods. A "nodalization" scheme is breaking a larger component, such as PIPE, into smaller cells or nodes in order to allow the code to implement numerical analysis and arrive at a solution (Applied Programming Technology, 2007b).

Advanced computing plays a central role in the design, licensing and operation of nuclear power plants. The modern nuclear reactor system operates at a level of sophistication such simple models are no longer able to predict a system's response to some small change or perturbation. Nonetheless, there is a need to acquire this level of understanding for safe operations. Lessons learned from simulations carried out with thermal-hydraulic codes help form the basis for decisions made concerning plant design, operation, and safety (Applied Programming Technology, 2007b). As part of an ongoing validation process and to ensure the analysis tools may be used with confidence, the NRC asks users to perform assessments and provide feedback on error correction or code improvement (NRC website, 2011). The current work is meant to contribute to this ongoing validation and assessment process. The general flow of the second part of this paper was based on previous works such as the analysis of the PANDA experiments with RELAP5 (Batet, 2001).

The simplicity of MANOTEA means that it is well characterized and easier to model. And yet, as explained in Chapter 7, the facility retains the integral characteristics that are found in more complex reactor systems. If the code properly simulates the behaviors of this simplified system, it lends confidence to its predictive abilities for more complex systems. In this way, the MANOTEA links the code to more complex systems. Due to the simplicity of the MANOTEA facility and its integral characteristics, this effort may prove useful as a benchmark for next generation code development as well. The recent sequence of events at the Fukushima Dai-ichi Power Plant, and the renewed public interest in reactor safety

that it evoked (Jaczko, 2011), serve to highlight the continued relevance of this type of work, the need to bolster confidence, and the merit of remaining vigilant by continuing to challenge and help best estimate codes evolve.

Some TRACE Characteristics

Component and Functional Modularity

TRACE is modularized by component. These components have names that intuitively describe what they are intended to model. Piecing together components, a user can model virtually any system configuration. Components can be modified, improved, or a new one added without disturbing the remainder of the code. The code is also modular by function, meaning: the major aspects of the calculations are performed in separate modules. This feature allows the code to be upgraded with new correlations and information with minimal effort and minimal potential for error (Applied Programming Technology, 2010).

Fluid Dynamics

TRACE is capable of analyzing fluid dynamics in 1-dimensional (1D) and 3-dimensional (3D) space. 1D flows, like those found in a coolant loop, are generally modeled using (1D) components like PIPE and TEE. 3D flows, like those found in a reactor vessel or tank, are modeled using VESSEL. VESSEL is used even if the actual system component is not a reactor pressure vessel – it's the generic TRACE component for capturing 3D geometry. 3D flow calculations can be performed using either Cartesian or cylindrical coordinates. 1D and 3D components can be combined in the same model to simulate complex flow networks or to capture local multidimensional flow. Implemented in a finite element fashion, an upstream

node or donor cell provides boundary conditions for the current node or computational cell. Once flow calculations are complete for the current node, it becomes the new upstream node or donor cell, and so on. A single set of variables (temperature, pressure, etc.) is associated with and characteristic of each node; in this way the node is said to be "homogenized" (Applied Programming Technology, 2007b).

Heat Transfer

TRACE fully integrates heat transfer and fluid dynamic calculations, performing both calculations for a given computational cell or node before moving to the next. TRACE can perform detailed heat-transfer analysis of the VESSEL and standard circulation loop components such as PIPE and TEE. The code tracks energy transferred from the liquid or vapor to the wall, or vice versa. The heat transfer capabilities include 2D conduction calculations within metal structures. Since both fluid dynamic and heat transfer relations cannot be solved simultaneously, TRACE defaults to solving the fluid dynamic equations and then performing heat transfer computations (Applied Programming Technology, 2007b).

Flow-regime-dependent Constitutive Equations

The hydraulic and heat transfer models used during TRACE calculations are selected based on the flow regime present in each hydrodynamic node. The thermal-hydraulic equations describe the transfer of mass, momentum, and energy vapor and liquid phases, and the interaction of these phases with the modeled structure (pipe wall for example). These interactions are highly dependent on flow regime. Thus, in order for TRACE to properly model these interactions, it determines the current regime and then determines the appropriate semi-empirical constitutive models needed (Applied Programming Technology, 2007b; Information Systems Lab., 2010).

Chapter 10: Base Model

Description and Nodalization

A Base TRACE Model of the MANOTEA facility was created using the Symbolic Nuclear Analysis Package (SNAP) interface. Preliminary models were developed by two teams of Naval Academy students during two internships, one internship to the U.S. Nuclear Regulatory Commission and the other to the Nuclear Heat Transfer Lab at Texas A&M University. Characteristics from each of these models were merged to create a Base Model. This model was developed after the MANOTEA facility was built, but before experimental data was available. Since TRACE is used by regulators to make decisions about proposed designs, developing the model prior to obtaining experimental data is a true test of the code and a particularly relevant approach.

Modeling with TRACE is centered on choosing, configuring and connecting components. A subset of this includes determining a nodalization scheme. A diagram of the nodalization scheme serves as a general snapshot of the program or model. Greater detail about initial conditions and other user specified information can be obtained by inspecting TRACE text-based output. These output files are generally very large and thereby not appropriate for the body of a dissertation. With this in mind, a copy of the text-based output for the model used in the present work is available in the Appendix.

Figure 47 shows the nodalization scheme, with heat structures, for the base Model. The nodalization scheme was based on the location of the MANOTEA instrumentation described in Chapter 3. Initial component conditions were based on the initial conditions outlined in Table 1. Choosing a nodalization scheme based on instrument location makes direct comparison between experimental data and TRACE output much easier. Because the condenser and boiler have such a high aspect ratio (84), it was deemed appropriate to treat flow in these sections as near one-dimensional and use the PIPE component. The presence of inverted thermal stratification in the experimental results illustrates the validity of modeling in 1D.

Several experiments were run on the MANOTEA facility as outlined by the test matrix shown in Chapter 5. The EZNF08XX series is of particular interest because it amplifies the effects of the energy partition. Also, if condenser pressure is plotted as a function of inventory, all the experimental data can be summarized on one plot as shown in Chapter 7. Thus, regardless of nozzle size or geometry, all transients follow the same pressure versus inventory trend (all transient sequences are identical). Thus, for the purpose of modeling, it is sufficient to focus on the EZNF08XX series. All TRACE calculations and output discussed throughout the remainder of this dissertation were performed with EZN08XX characteristics.

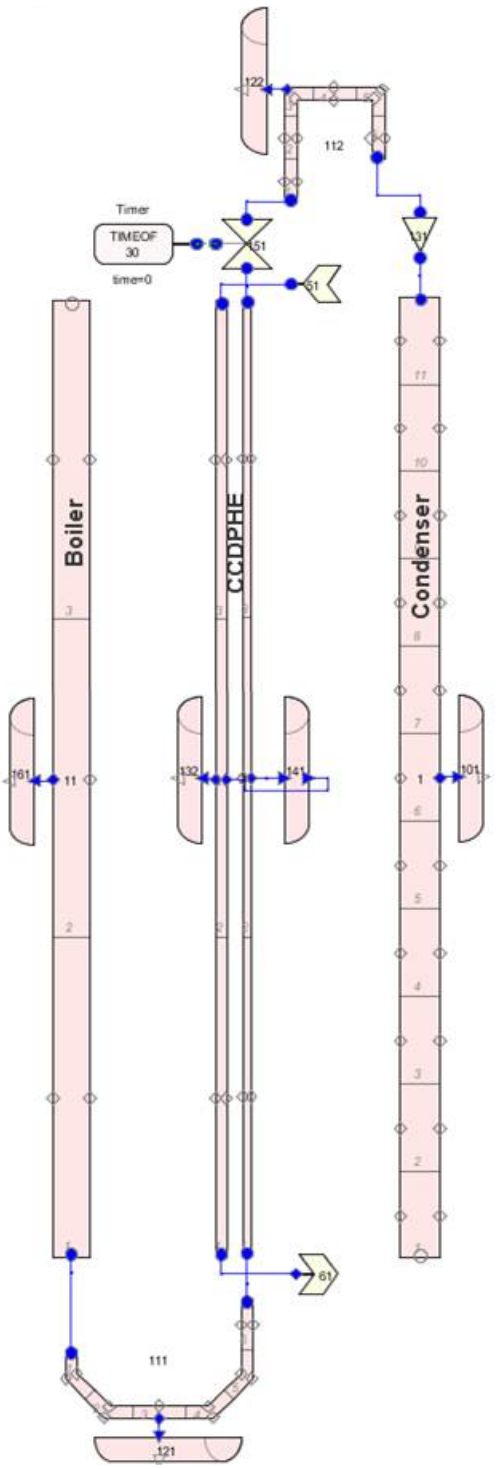

Figure 47. Nodalization and heat structure scheme for the Base TRACE Model of MANOTEA.

Fundamental Comparison

Much like reactor systems, MANOTEA produces integral transients. This renders MANOTEA applicable to real systems and prescribes the fundamental comparison. The fundamental comparison between the code and the data is the liquid transfer up to and during any given point in time. This comparison was made by plotting condenser pressure as a function of condenser inventory. In addition to the fundamental comparison, one-to-one, experiment-to-TRACE output comparisons were made to assess and evaluate the code, as well as provide necessary insight. These comparisons are made in the next chapter along with base model output.

Chapter 11: Base Model Output

The Base Model was created after MANOTEA was constructed but before experimental data was available. Since SNAP is used to make decisions about the safety of *proposed* designs, modeling in this way is particularly relevant because it highlights how some insight is needed about the expected performance in order to ensure that output is real and acceptable. This chapter outlines output from the Base Model. In subsequent Chapters, armed with the results and insight gained from the experiment, modifications are made to the Base Model in order to improve modeling techniques.

TRACE model output outlined in this chapter was primarily generated and formatted with ApPlot. ApPlot is distributed as a plug-in for SNAP. It is a What You See Is What You Get (WYSIWYG) plotting application used for post-processing and creating "publishing-quality" plots (Applied Programming Technology, 2007a). ApPlot pulls information from the TRACE output files, which are text-based. In this chapter, comparisons are made between ApPlot-formatted output and the experimental results presented in Chapter 5. For completeness, the text-based output file is included in the Appendix.

Fundamental Comparison

The fundamental comparison was condenser pressure as a function of condenser inventory. Figure 48 is the model output for condenser pressure versus condenser inventory. The figure was not produced with ApPlot – but rather by

manually eliminating time from the TRACE output for mass and pressure versus time, then plotting with spreadsheet software. Figure 48 is the only comparative figure generated this way.

Comparing Figure 48 to Figure 46 reveals that TRACE slightly over-predicted condenser pressure as a function of condenser inventory. Nonetheless, the fundamental comparison was qualitatively and quantitatively accurate to within estimated experimental uncertainty (+/- 10 *kPa*, +/- 0.5 *L* as outlined in Chapter 4). Although, it is not apparent in Figure 48, TRACE predicted a pressure discontinuity at the termination of the transient. A plot of pressure versus time will be presented in the following section which shows this non-physical situation.

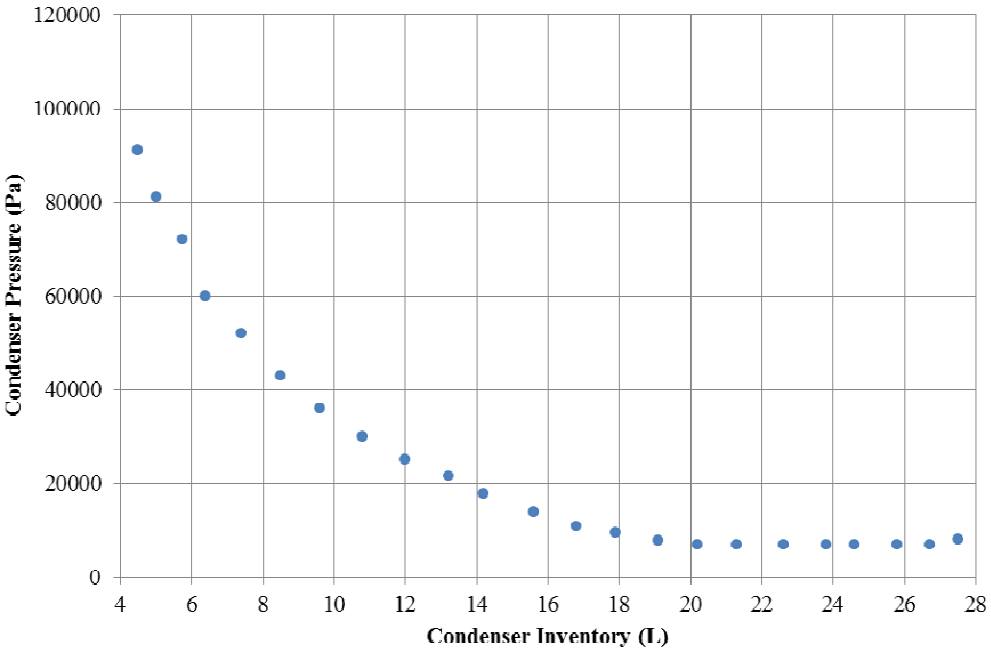

Figure 48. Base Model output for condenser pressure as a function of condenser inventory.

Other One-to-one Comparisons

Pressure

Figure 49 is the model output for boiler and condenser pressure as a function of time. TRACE qualitatively captured the general pressure trends observed in the experiment. The Base Model quantitatively captured condenser pressure, and predicted transient duration well. However, TRACE shows the pressure recovery observed at the termination of all experimental transients as a discontinuity. The discontinuity appears in the final time step and occurs because the code predicts that the condenser pipe fills. Although this effect isn't real and can be ignored it highights another issue. The pressure slope at transient termination does not match the experimental data well. Pressure in the data recovers slightly just before termination. The Base Model does not capture this pressure recovery. TRACE did not quantitatively capture boiler pressure, but does predict two distinct regimes as observed in the experiment. This is not a concern because exact experimental boundary conditions were not used in the model (the initial "hot spot" described in Chapter 7 was not modeled since we simply needed the boiler to generate sufficient vapor). The boiler pressure predicted by TRACE is the pressure for a boiler at a uniform temperature of 105 ^{o}C. In reality, boiler temperature was stratified with a "hot spot". Thus, for the boundary conditions given, TRACE is predicting boiler pressure accurately. Figure 49 can be loosely compared to Figure 10 or 15, respectively. *Time scales for all plots is this dissertation were based on transient duration for the respective situtiation.* Note: transient duration (time) is not the best way to make direct comparisons since it is highly dependent on nozzle geometry.

Direct comparison of Figure 48 to Figure 10 or 15 should be performed with this cautionary note in mind. Condenser pressure as a function of inventory is the only truly valid way to make direct comparisons as explained earlier.

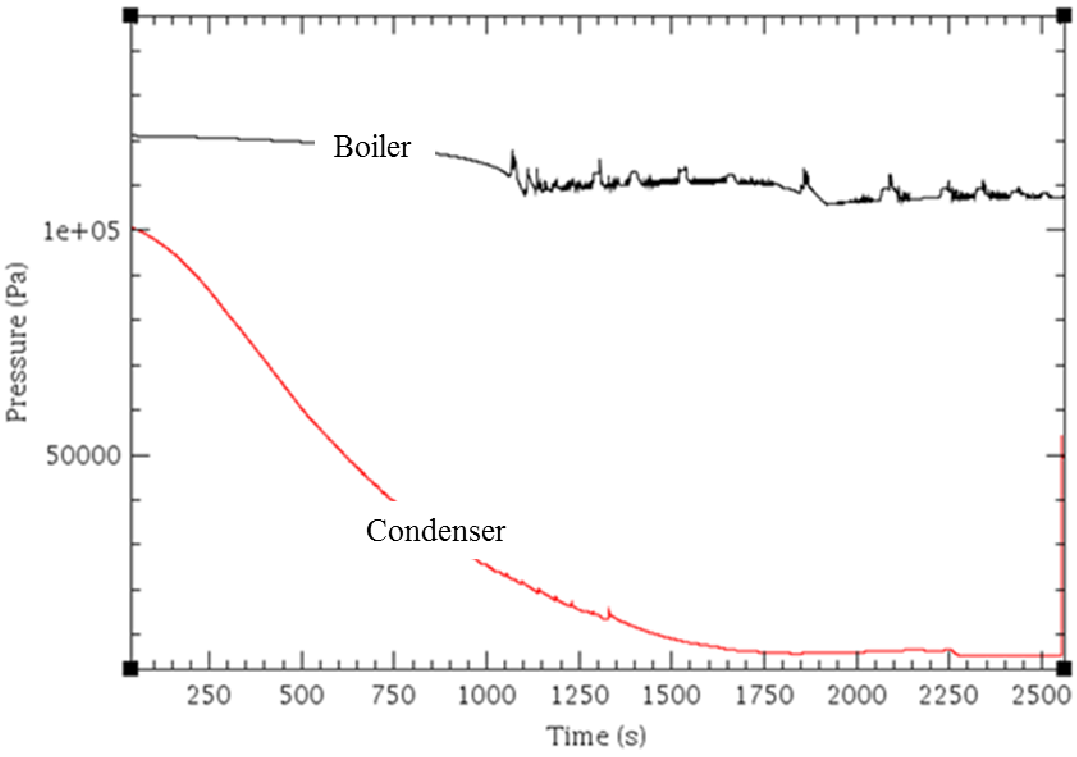

Figure 49. Base Model output for pressure versus time after transient initiation.

Temperature

Figure 50 is the Base Model output for condenser centerline temperature as a function of time. Figure 51 is the output for condenser surface temperature as a function of time.

The Base Model predicted the inverted thermal stratification observed in the MANTOEA condenser. The code also captured the general trends. However,

in general TRACE predicts higher temperatures. This is most evident at the end of the transient. The highest and lowest temperatures found in EZNF08XX data at transient termination were about 70 and 25 ^{o}C, respectively. TRACE predicts a high and low temperature of around 77 and 37 ^{o}C, respectively. This is just outside the estimated uncertainty of the thermocouples; and although a little warm, these values are still a pretty good best-estimate. These warmer values are likely the result of the way TRACE homogenizes nodes in order to make calculations. This homogenization is a relic of the numerical methods used to perform the calculation, is well understood, and of little concern. To further illustrate the effect of this homogenization, examine CC21. In the experiment, CC21 temperature quickly dropped to the temperature of the incoming spray. This occurred because the thermocouple is literally being sprayed by sub-cooled water from the nozzle. However, the Base Model doesn't capture this rapid temperature drop well because CC21 in the model is literally the homogenized, average temperature for the upper 0.30 *m* (1') of condenser vapor space. Figure 50 can be compared to Figure 11 or 16, respectively. Figure 51 can be compared to Figure 12 or 17, respectively. Again, direct comparison should be made with caution and with the understanding that the time scales are intentional plotted differently because the duration of the respective transients are different. Because the transients are integral, time is irrelevant and inventory is the true metric for determining the system's state at any given instant.

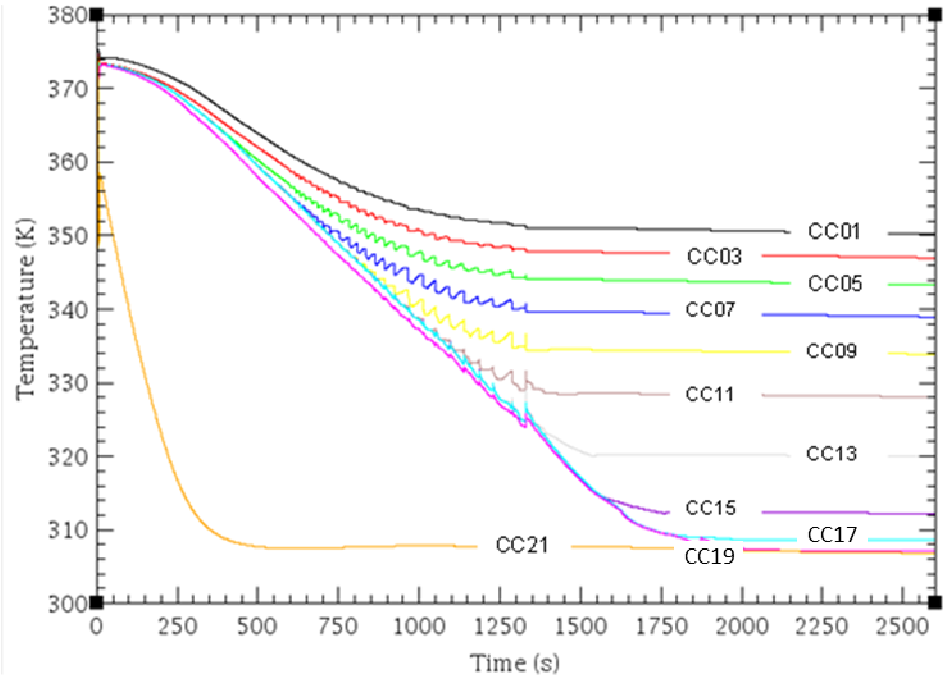

Figure 50. Base Model output for condenser centerline temperature versus time after transient initiation.

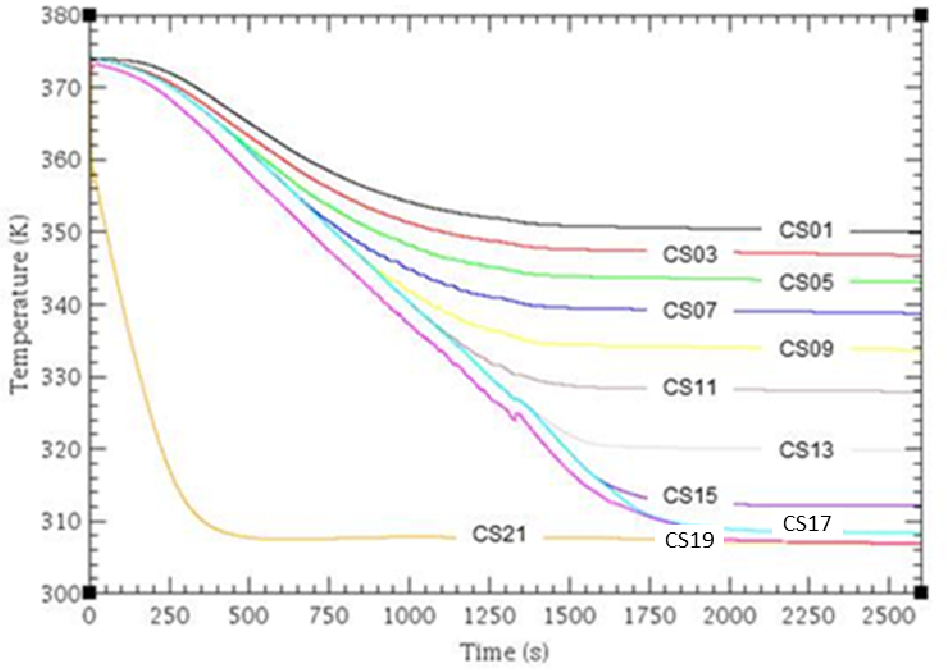

Figure 51. Base Model output for condenser surface temperature versus time after transient initiation.

Figure 52 is a plot of Base Model output for boiler temperatures as a function of time. The boiler centerline temperatures predicted by TRACE are in general agreement with the temperatures observed in the experiment. Boiler surface temperatures are not shown on the figure because they are similar to centerline temperatures and simply clutter the plot. Boiler temperatures and pressures are of little concern to the current work, provided that the boiler condition does not affect or slow the transient. This was confirmed to be the case in both the experimental data and the model output. Figure 52 can be loosely compared to Figure 13 or 18, respectively.

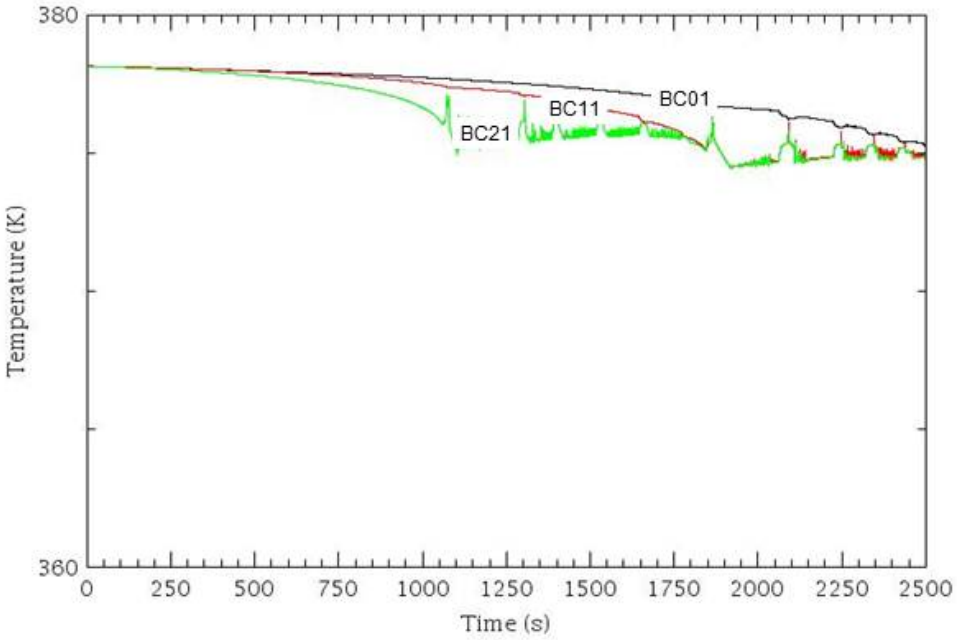

Figure 52. Base Model output for boiler centerline temperature versus time after transient initiation

Inventory

Figure 53 is the Base Model output for mass as a function of time. By outputting mass, TRACE takes into account the mass of the vapor and the liquid. The mass of the vapor is small compared to the mass of the liquid. Mass is the TRACE default output, but liquid volume was measured during the experiment. The figure is presented in the native format, with the understanding that it captures the same information as the inventory plots. Figure 53 can be compared to Figure 14 or 19, respectively.

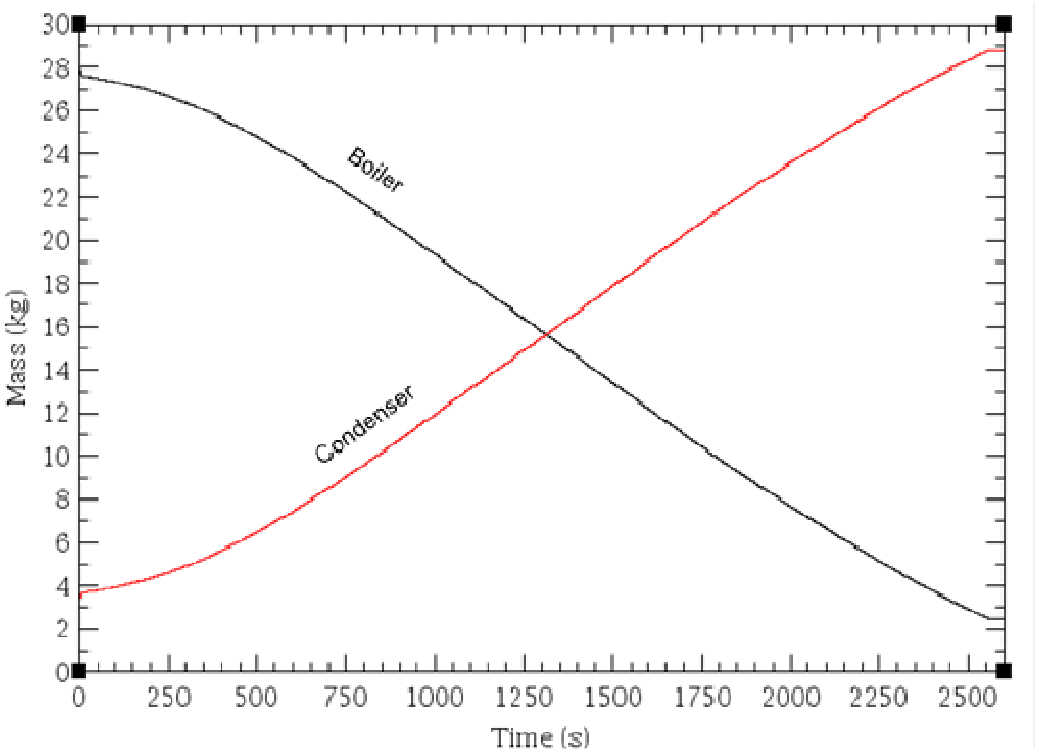

Figure 53. Base Model output for mass (inventory) versus time after transient initiation.

The Base Model showed good qualitative and quantitative agreement with the experimental data. Recall, that the EZNF0815 nozzle (15-*deg* or fan nozzle), transferred approximately 3.5 *L* less than the EZNF0800 nozzle (0-*deg* or jet nozzle) due to the energy partition. The Base Model always predicts that the condenser will fill and terminate with a pressure discontinuity. TRACE does not contain a native utility to model nozzle characteristics in detail (Applied Programming Technology, 2007a & 2007b). Finding a novel way to capture the energy partition in the model should prevent the condenser from filling and provided motivation for the work outlined in the next chapter.

Summary of Relevant Base Model Discrepancies

The fundamental comparison was found to qualitatively and quantitatively agree with the data to within estimated experimental uncertainty. Thus, at the highest level, the Base Model did a good job simulating MANOTEA transients. However, detailed comparison and inspection of Base Model output identified the following relevant discrepancies, which are considered worthy of further investigation:

- Base Model output predicts that transients terminate with a non-physical discontinuity.
- Base Model output predicts that the condenser pipe will always fill.

These discrepancies frame the analysis and provide motivation for the work outlined in Chapter 12, namely: identifying modifications that capture the energy partition (prevent condenser filling) and enable a smooth transient termination - or pinpointing why these discrepancies occurred if no modification fixes them.

Chapter 12: Modifications to Base Model

In an effort to find a way to capture the energy partition (prevent the condenser from filling) and to end the transient smoothly, a list of physical mechanisms observed in the condenser was generated. Events in the condenser alone control MANOTEA transients, so there is no need to analyze the boiler pipe or double-pipe heat exchanger. The list of mechanisms was subsequently mapped to TRACE parameters which might affect calculations of the respective mechanisms. Parameters were modified individually in the Base Model and the resulting condenser final inventory was recorded – in addition to a cursory inspection of relevant output with-respect-to time plots. Subsequently, parameters observed to reduce inventory transfer, and that could be physically justified, were combined to gauge the integral or combined effect and give a lower limit to TRACE output for inventory transfer. Some of the modifications undertaken were based on feedback from the Code Development Branch at the U. S. Nuclear Regulatory Commission. During this effort, over 250 cases were run for single, or combinations of single, modifications. The purpose of these modifications was two-fold. First and foremost, identify proper modeling techniques that prevent the condenser from filling and end the transient gracefully. Second, make sure that due diligence had been paid to developing and modifying the Base Model prior to examining the mechanisms behind the predictions that the code made.

List of Physical Phenomena Present in the Condenser Pipe

Table 11 is a list of phenomena, mechanisms, or time constants observed in the MANOTEA condenser pipe. The table contains a short description of each mechanism and an estimate of the mechanism's ability to affect the duration or amount of liquid transferred during a transient.

Mechanism/Phenomena	Relative Ability to Affect Transient	Description
Axial Conduction (metal)	Small	Conduction along the length of the pipe in the metal wall.
Radial Conduction (metal)	Intermediate	Radial conduction along the thickness of the pipe wall.
Axial Conduction (liquid)	Small	Upward/downward conduction in the pool water of the condenser.
Radial Conduction (liquid)	Small	Outward conduction, toward the pipe wall, in the pooled water of the condenser.
Axial Conduction (vapor)	Small	Upward or downward conduction in the vapor space above the pooled water.
Radial Conduction (vapor)	Small	Outward conduction, toward the pipe wall, in the vapor space above the pooled water.
Liquid Convection	Small	Heat transfer resulting from circulation of the pooled water in the condenser.
Vapor Convection	Small	Heat transfer resulting from circulation of the vapor above the pooled water.
Rapid Condensation	Large	Efficient energy transfer due to latent heat caused by spraying cool water into the vapor space, pressure-volume work associated with the condensation mechanism.
Metal Quenching	Large	Energy transfer resulting from spray cooling of the metal wall.
Nozzle (Liquid) Geometry	Large	Nozzle size and spray character (0-deg, 15- deg), closely related to how much metal quenching or rapid condensation occurs.
Liquid Flow Rate	Large	Rate at which cool spray enters the condenser via the nozzle, related to rapid condensation, metal quenching, and nozzle geometry.

Table 11. List of mechanisms found in the condenser pipe of MANOTEA.

Mapping Phenomena to TRACE Parameters

Table 12 is a summary mapping the phenomena listed in Table 11 to parameters in TRACE that may be modified in order to prevent the condenser pipe from filling or smooth transient termination. It should be noted: many of the TRACE modifications listed will affect more than one of the physical mechanisms or phenomena.

Mechanism/Phenomena	TRACE Parameter	Purpose
Axial Conduction (metal)	User Defined Material: Copper	Enhance heat conduction (preference energy transfer to wall).
	User Defined Material: Insulation	Suppress heat transfer to the wall (preference energy transfer to the vapor space).
Radial Conduction (metal)	User Defined Material: Copper	Enhance heat conduction.
	User Defined Material: Insulation	Suppress heat conduction.
Axial Conduction (liquid)	User Defined Liquid	Not feasible: TRACE is meant for water only.
	Nodalization	Increase axial nodes in order to capture effect(s) better.
Radial Conduction (liquid)	User Defined Liquid	Not feasible.
	Replace Pipe with Vessel	Allows conduction between adjacent cells
Axial Conduction (vapor)	User Defined Liquid	Not feasible.
	Nodalization	Increase axial nodes in order to capture effect better.
Radial Conduction (vapor)	User Defined Liquid	Not feasible.
	Replace Pipe with Vessel	Allows conduction between adjacent cells.
Liquid Convection	Replace Pipe with Vessel	Allows convection between adjacent cells.
Vapor Convection	Replace Pipe with Vessel	Allows convection between adjacent cells.
Rapid Condensation	Add Non-condensable Gases	Suppress/diminish condensation.
	Nodalization or Vessel	Force calculation in smaller cells instead of homogenizing larger cells.
Metal Quenching	N-rods	Enhance effective surface area (preference more energy transfer to the wall)
	Accumulator: Falling Film	Force energy transfer to wall by making spray a film.
	Accumulator: Suppression Pool	Modify energy transfer to wall/vapor.
	Accumulator: Liquid Separator	Modify energy transfer to wall/vapor.
Nozzle (Liquid) Geometry	Accumulator: Falling Film	Force energy transfer to wall.
	Modify K-factor in Nozzle	Modify condensation by manipulating spray characteristic.
	Modify Nozzle (Fill) Size	Modify condensation by manipulating Spray.
Liquid Flow Rate	Modify Losses in Copper Tube	Reduce amount of incoming spray.

Table 12. TRACE modifications that may allow physical mechanisms found in the MANOTEA condenser to be enhanced or suppressed.

Base Model Modification Results and General Observations

Table 13 lists single modifications made to the Base Model. The final mass output is listed next to each modification. Although approximately 250 separate cases were ran, this table does not list them all, only the more relevant cases or cases of interest. For example, more than 44 axial nodes were attempted, but more nodes did not further reduce inventory transfer. The purpose of this table is to illustrate that time and thoughtful analysis have been spent with the model prior to a formal discussion of discrepancies between the code and the experiment. Again, liquid transfer is the fundamental comparison, and related to the energy partition, which is why this effort focuses on modifying this output. These modifications were attempts to capture the energy partition and terminate the transient smoothly. Recall, a 3.00 *L* difference was observed between the final condenser inventory when using the EZNF0800 and EZNF0815 nozzle, respectively. By properly modeling or capturing the energy paritition, it is possible to get the code to predict an inventory difference as well.

Modifications to "Base" Model				Mass (kg)
# of Pipe Nodes			6	28.79
			11	28.79
			44	28.72
Model Pipe as Vessel	Axial Levels	Radial Rings	Azimuthal Sector	
	11	1	1	28.79
	11	2 - fluid in outer	1	28.31
	11	2 - fluid in inner	1	28.86
	6	2	1	28.38
Surface Multiplier (enhance condenser surface area 5X)				28.52
Change Wall Material to Copper (excellent conductor, enhanced heat transfer to wall)				15.77*
Change Wall Material to Insulation (poor conductor, no heat transfer to wall)				28.87
Change Friction Factors in Copper Tubing			Default	28.79
			Realistic Est.	28.73
			Exagerated	28.73
Non-condensable Gases			500 Pa	28.58
			5000 Pa	26.91
			10000 Pa	25.92
Change Accumulator Model			Falling Film	28.73
			Suppress. Pool	28.73
Nozzle Friction Factor			5X	28.79
			10X	28.79

* Calculation terminated prematurely.

Table 13. List of modifications to the Base Model and subsequent final condenser inventory predicted by TRACE.

Modeling the pipe with the VESSEL component and adding non-condensable gases will be discussed in detail later in this Chapter.

Changing the number of axial pipe nodes had little effect on final inventory. For more than 44 nodes, the calculation began to take extremely long. Slightly less final inventory is seen for 44 nodes, and all other parameters (pressure, etc.) remain the same regardless of nodalizaton. Specifically, the discontinuous pressure recovery is still present.

Enhancing the surface area of the pipe wall by using the N-RODS parameter reduced the final inventory by approximately 0.25 kg. By enhancing the

surface area, we have enabled the code to capture a hint of the energy partition and what occurs when a fan nozzle is used. More energy from the incoming spray being transferred to cooling the wall (as opposed to collapsing the vapor space) resulted in less inventory transfer and smaller final condenser inventory. Enhancing the surface area in the model allows TRACE to preference more energy to the wall. No further advantage was noted by enhancing the area more the 5X entry listed in the table.

Changing the wall material to copper (a user defined material with better conduction characteristics than carbon steel) caused the code to progress through approximately half the transient before abruptly terminating with a fatal error.

Changing the wall material to insulation (a user defined material which does not allow conduction) resulted in slightly more inventory transfer. This slight increase is due to a slightly lower temperature profile. Making the wall insulated commits all of the (negative) energy of the incoming spray to collapsing the vapor space. Noting this enhanced inventory transfer and recalling that enhancing the surface area of the metal decreased inventory transfer, lends credence to the idea of the energy partition and the physics upon which it was based.

Changing the frictional losses in the copper tubing resulted in a slight decrease in predicted final inventory. Exaggerating the losses to 5 or 10 times a realistic value had little effect. Changing the friction factors in the tubing caused the transient to last longer, but did little to reduce or prevent inventory transfer.

Changing the accumulator model from “no accumulator” to “falling film” or “suppression pool” cause a slight decrease in predicted final condenser

inventory. "Falling film" forces TRACE to treat the incoming spray as a film falling down the pipe wall, and modifies the way the code homogenizes the calculation node. This modification is not significant enough to cause the large inventory differential noted in the experiment.

Much like changing the losses in the copper, changing the nozzle friction factor simply caused the transient to last longer, but did little to reduce or prevent inventory transfer.

Non-condensable Gas Modifications to Base Model

Non-condensable gases are purged from the system by boiling the inventory for 3 hours. Non-condensable gases are known to hinder condensation (Uchida, 1965) and are stripped to ensure MANOTEA transients start properly and do not terminate prematurely. Because a small amount (approximately 1% or 820 *Pa*, as discussed in Chapter 7) of non-condensable is known to accumulate in DPHE, it was suggested that gases should be added to the code in order to see what happens. When a transient is initiated, these gases lead the sub-cooled water into the condenser. In order to capture the effect of the gases and the appropriate concentration, the primary side of the DPHE was model as being full of air at transient initiation.

As expected, the presence of non-condensable gases caused less liquid inventory to be transferred during the simulated transient. It should be emphasized again that the energy partition is responsible for this bulk effect in the MANOTEA facility, but the presence of non-condensable gases does contribute slightly. Although a small fraction, as the transient progresses and the condenser fills, the non-condensable fraction becomes larger. Some of the gases are likely absorbed into the

relatively cool pooled water, while some remain in the vapor space. The increasing concentration in the vapor space is eventually a contributing factor to transient termination. In addition, the presence of non-condensable gases is posited to be one of the reasons for the slight, smooth pressure recovery found at the end of all MANOTEA transients.

Figure 54 shows an order of magnitude parametric study performed with TRACE. The figure shows three plots: 50, 500, and 5000 *Pa* of non-condensable gas in the condenser at transient initiation, respectively.

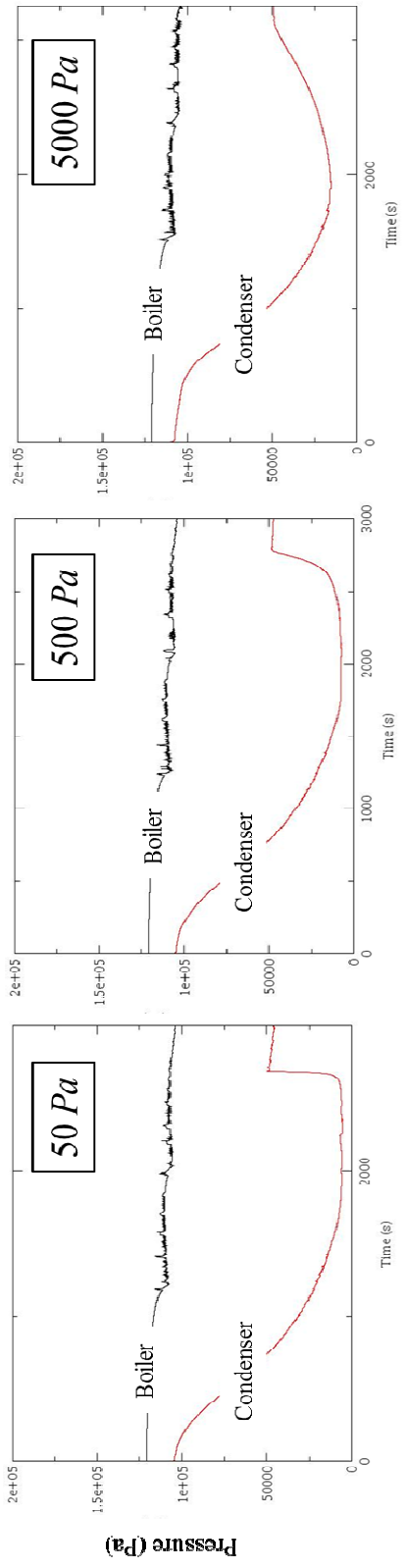

Figure 54. Parametric non-condensable gas study performed with TRACE.

Note that the times scales shown in Figure 54 are not the same, but the pressure scales are the same. The figure illustrates the effects of non-condensable gas in general. For large enough initial concentration, TRACE predicts that condensation will be suppressed and transient initiation delayed. In addition, for larger concentrations, the minimum pressure prediction is greater than for smaller concentrations, again indicating reduced condensation. For a non-condensable concentration on the order of our estimate for the MANOTEA facility, transient termination begins to look like the experimental data (see Figure 10, 15, etc). However, in all cases, pressure (and the shape of the pressure curve) at transient initiation is slightly different from that observed in the data. Modeling the condenser pipe with the VESSEL component eliminated this discrepancy, and will be discussed more later in this Chapter.

VESSEL Modifications to Base Model

When employing finite difference analysis, one set of parameters is associated with or characteristic of each cell or node. This feature has been referred to as homogenization. The motivation for modeling the 1D condenser pipe with the 3D VESSEL component was to try to reduce the node size and force the energy partition to occur.

Using the PIPE component to model the condenser forces the upper portion of the condenser, where the sub-cooled spray enters, to be treat as one node. Thus, the spray comes into the upper node and is homogenized in order to implement finite-difference equations for mass, energy, and momentum. After calculations haves been performed for this initial calculation node, it becomes the donor node for

a series of subsequent calculations, to include wall heat transfer. In this manner, it is truly impossible to capture the effect of a fan nozzle and preference energy transfer (the energy partition) to the wall while employing the PIPE component.

Figure 55 is an overheard view of the VESSEL component configured with 11 axial nodes (not viewable in the figure), 2 radial ring nodes, and 1 azimuthal sector node. Configuring the component in this way allows the energy partition to be simulated. Incoming sub-cooled spray can be directed into the outer ring where it is homogenized and finite-difference and constitutive equations solved. This node then becomes the donor node for a calculation with the carbon-steel pipe wall on the outside and a portion of the vapor space on the inside. In this manner, the spray is allowed only to "communicate" with a smaller portion of the vapor space initially. The subsequent calculations with the wall and the vapor space forces some of the incoming (negative) energy to the wall, much like a fan nozzle exchanges a portion of the energy directly with the wall. The presence of an extra step before the spray can communicate with the wall means that the energy partition effect will be diminished when compared to the effect observed in the experiment.

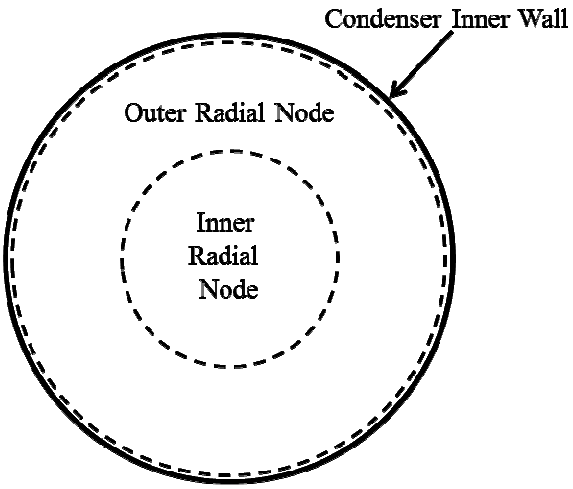

Figure 55. Top view of VESSEL component with 2 radial ring nodes and 1 azimuthal node.

As shown in Table 13, when incoming spray was directed into the inner radial node, the resulting final condenser inventory is 28.86 *kg*. If the incoming spray is directed into the outer radial node, the resulting final condenser inventory is 28.31 *kg*. Also note from Table 13, when the VESSEL is configured to 1 radial ring node and 1 azimuthal node (essentially forcing the VESSEL to behave like a PIPE component), the final condenser inventory matches that predicted with a PIPE component configured with the same scheme and is 28.79 *kg*. Thus, when the spray was forced into the vapor space and not allowed to communicate directly with the wall, more pressure-volume work was done and more liquid inventory was transferred. When the spray was forced to communicate with the wall by directing it into the outer radial ring, less pressure-volume work was done and more quenching, resulting in reduced liquid inventory transfer. This reinforces the validity of framing MANOTEA transients in terms of an energy partition. Furthermore, using the

VESSEL component allows the energy partition to be recreated or captured in an conclusive manner. Unfortunately, the inventory differences observed with TRACE are not of the same magnitude as those observed with the EZNF08XX series experiments. However, it does suggest that the TRACE condensation model is overstated. This observation has been made for TRACE's predecessors RELAP5 and RELAP5 -3D in previous works as well (Woods, 2009; Moon, 2000; Choi, 2002).

Modeling the condenser as a VESSEL also resulted in better agreement in the shape and slope of the pressure versus time plots – particularly at transient initiation. These results are reasoned to be related to the ability of the VESSEL component to better capture the small circulations cells described in Chapter 7.

Chapter 13: Final TRACE Model

A Final Model of MANOTEA was created implementing relevant modifications and lessons learned from the Base Model modifications exercise outlined in Chapter 12. Namely, the Final Model incorporated two important changes: add non-condensable gases in the DPHE at transient initiation and use of the VESSEL component instead of the PIPE component to model the condenser pipe. The adjective "final" is used not in the sense that the model is perfect, but in the sense that enough information has been gathered to make recommendations. Accounting for the small fraction of non-condensable gases eliminated the pressure discontinuity predicted by the Base Model (one of the two fundamental discrepancies outlined Chapter 11). Implementing the VESSEL component prevented the condenser from filling – although not to the extent observed in the experiment - by capturing the energy partition (the second fundamental discrepancy). However, VESSEL also introduces a new discrepancy.

Nodalization Scheme

The Final Model condenser used 11 axial nodes, 1 radial ring node, and 1 azimuthal node. This nodalization scheme is recommended for modeling jet nozzles. In order to capture the energy partition and better predict fan nozzle transients, the condenser should simply be re-nodalized to have 2 or more radial rings as described in Chapter 11. Renodalizing from 1 to 2 radial rings takes less effort than renodalizing from 2 to 1 radial ring. Thus, the Final Model incorporated a VESSEL component with 1 radial ring. Figure 56 shows the nodalization scheme, with heat structures, for the Final Model.

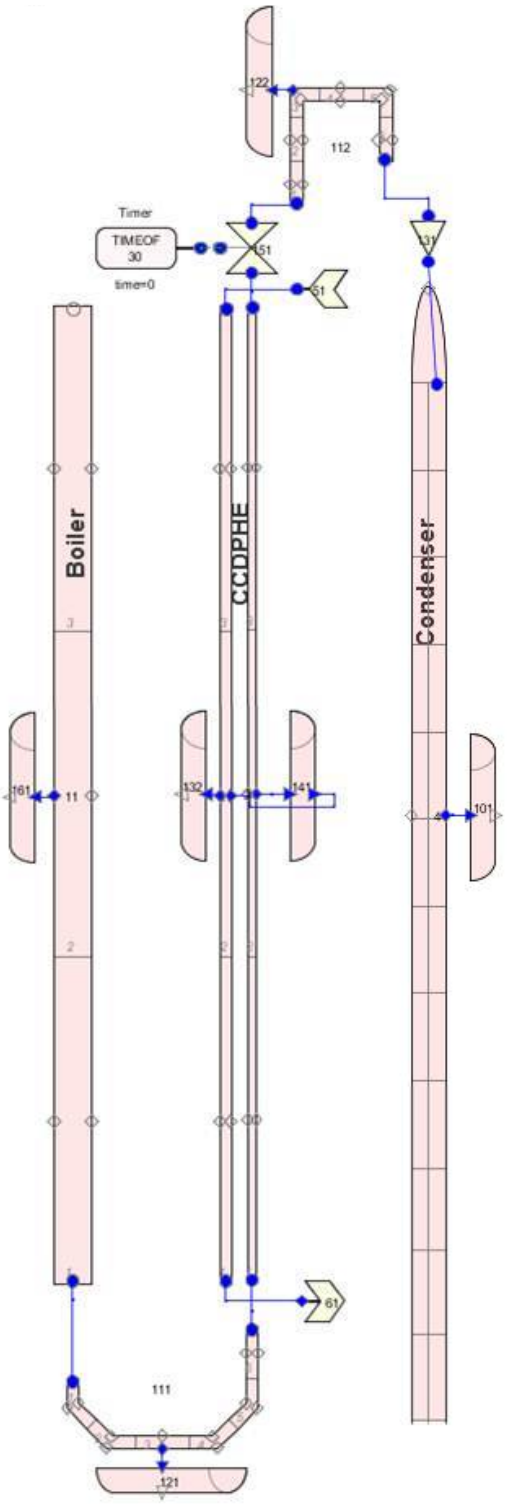

Figure 56. Nodalization and heat structure scheme for the Final TRACE Model of MANOTEA.

Fundamental Comparison

Because MANOTEA is an integral facility, the most important data point is how much inventory has been transferred. Thus, the fundamental comparison between the data and the TRACE models was condenser pressure as a function of condenser inventory.

Figure 57 shows the Base and Final Model outputs for condenser pressure versus condenser inventory. For reference, two sets of experimental data are also plotted on the figure.

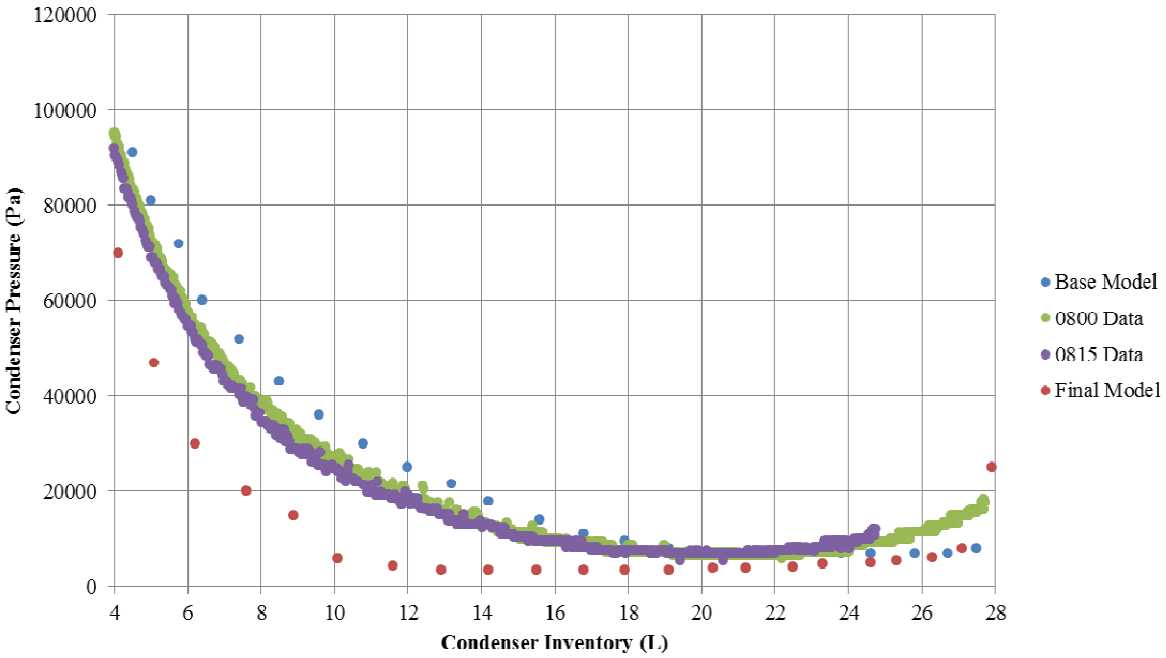

Figure 57. Fundamental comparison between MANOTEA data and TRACE models.

The Base Model slightly over-predicted condenser pressure as a function of condenser inventory. The Base Model was qualitatively and quantitatively accurate to within experimental uncertainty, but failed to capture the pressure recovery during transient termination. By adding non-condensable gas to the model in the appropriate proportion, the Final Model was able to capture the pressure recovery to within experimental uncertainty. However, the Final Model under-predicted condenser pressure versus condenser inventory during the first half of the transient. Certain portions of the early-transient behaviors predicted by the Final Model are outside of experimental uncertainty. The lower-than-observed-pressures in the Final Model are due to the VESSEL component modification. Regardless of nodalization, VESSEL always under-predicted early pressure for all cases attempted. VESSEL allows 3D fluid movement. The under-prediction is attributed to this feature and is likely due to more fluid movement and heat convection than actually occurred in the highly linear, thermally stratified condenser. The advantage to using VESSEL was that it provided a mechanism to capture the energy partition and prevent the condenser from filling. In this manner, using the VESSEL component is a trade-off.

Other One-to-one Comparisons

Pressure

Figure 58 is the Base and Final Model output for boiler and condenser pressure as a function of time, respectively. TRACE qualitatively captured the general pressure trends observed in the experiment. The Base Model quantitatively captured condenser pressure, and predicted transient duration well. However, the pressure slope predicted by the Base Model at transient initiation does not match the experimental data well – the pressure plot seems to lag slightly behind what was observed in the experiment. In addition, the Base Model predicted a non-physical pressure discontinuity at transient termination. Again, by incorporating non-condensable gases into the Final Model, this discontinuity is eliminated via mechanisms explained in Chapter 7. However, as mentioned in the preceding section, the Final Model under-predicted condenser pressure versus condenser inventory during the first half of the transient. Both models predict two distinct pressure regimes in the boiler, which was also noted in the experiment. However, TRACE did not quantitatively capture boiler pressure. Because the present work is focused on rapid condensation transients and MANTOEA transients are not affected by the boiler, this discrepancy is considered minor and is left for future work. Timescales on Figure 58 are tied to the code's prediction for transient termination, and are therefore different.

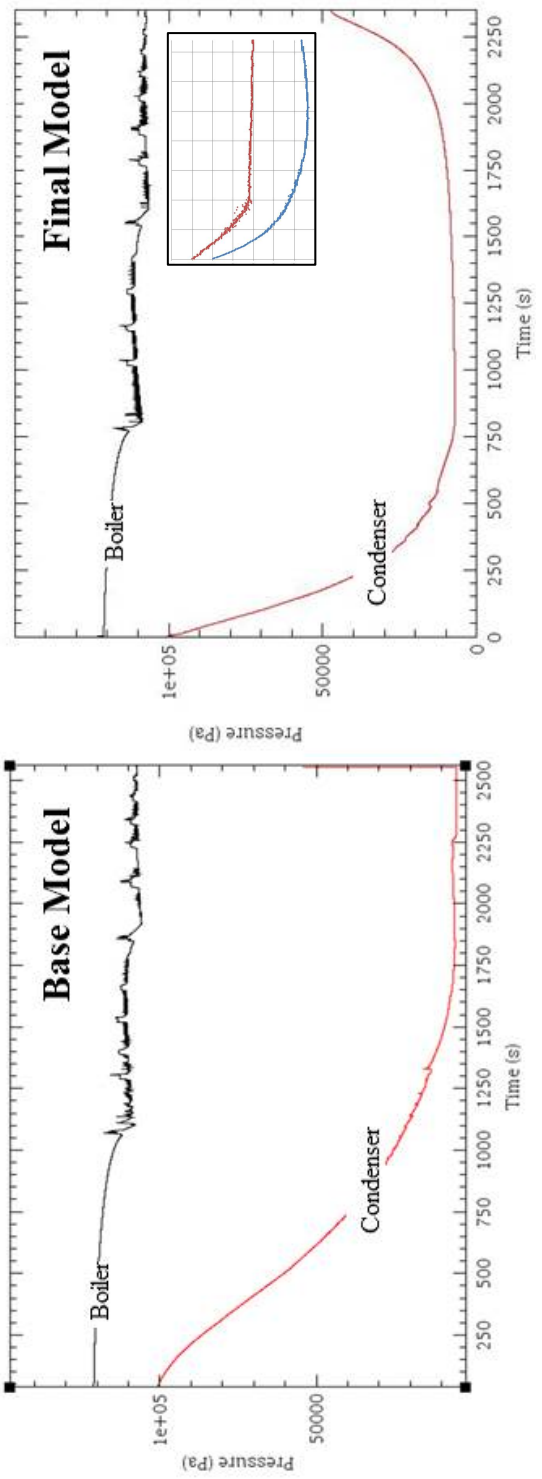

Figure 58. Base and Final Model output for pressure versus time after transient initiation. Inset is qualitative snapshot of experimental data for quick comparison.

Temperature

Figure 59 is the Base and Final Model outputs for condenser centerline temperature as a function of time. Condenser surface temperatures are directly related to condenser centerline temperatures and not shown in this section. Timescales are again tied to transient termination.

Both models predicted the inverted thermal stratification observed in the MANTOEA condenser. In addition, both captured the general trends. However, the Base Model predicted slightly higher than experimentally observed temperatures. The Final Model predicted lower than experimentally observed temperatures and cooled much faster. These results are consistent with the pressure versus time profiles predicted by both models, as well as the pressure versus inventory plots.

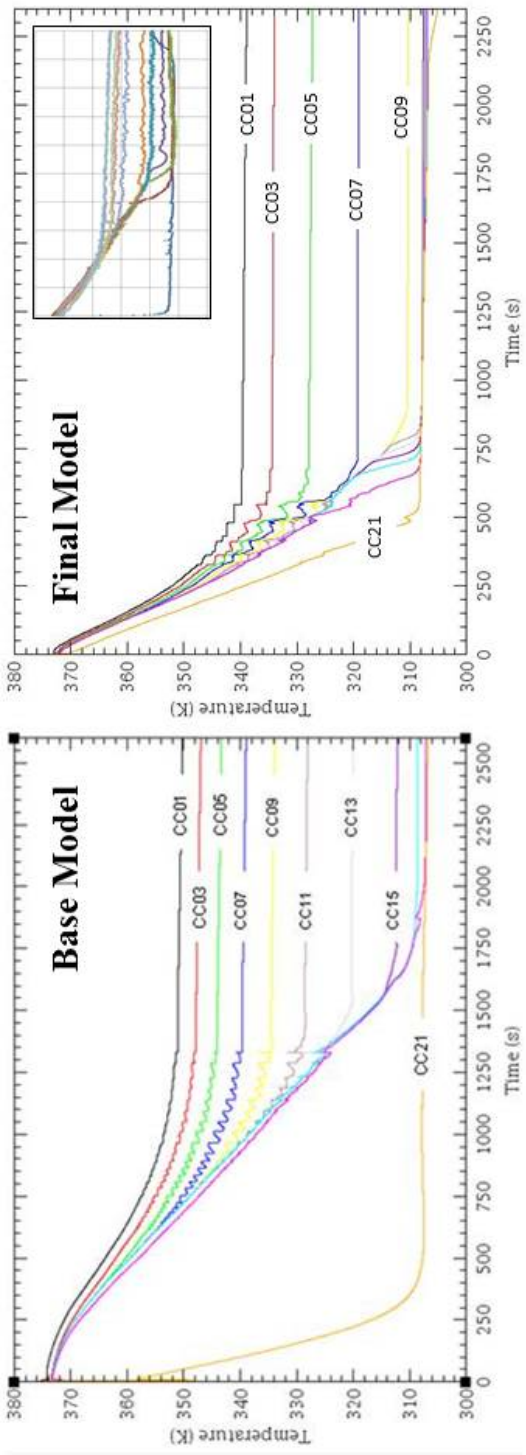

Figure 59. Base and Final Model output for condenser centerline temperature versus time after transient initiation to transient termination. Inset is qualitative snapshot of experimental data for quick comparison.

Inventory

Figure 60 is the Base and Final Model outputs for mass as a function of time. Both models captured the qualitative trends. Inventory is transferred faster in the Final Model prediction as a direct result of the lower temperatures and pressure predicted during the early transient. Thus, these again are consistent with other TRACE outputs for the respective models.

The models also showed quantitative agreement with the experimental data. Recall, that the EZNF0815 nozzle (15-deg or fan nozzle), transferred approximately 3.5 L less than the EZNF0800 nozzle (0-deg or jet nozzle) due to the energy partition. The Base Model always predicted that the condenser will fill and terminate with a pressure discontinuity. The Final Model predicted that the condenser will fill and terminate smoothly when configured with default nodalization. If re-nodalized radially to capture the energy partition, the Final Model will not fill the condenser. Thus, a novel way to capture the energy partition in the model was found. However, the using the VESSEL component introduced some new errors as discussed in the first section of this Chapter. Unfortunately, the inventory differences observed with TRACE are not to the extent as those observed with the EZNF08XX series experiments.

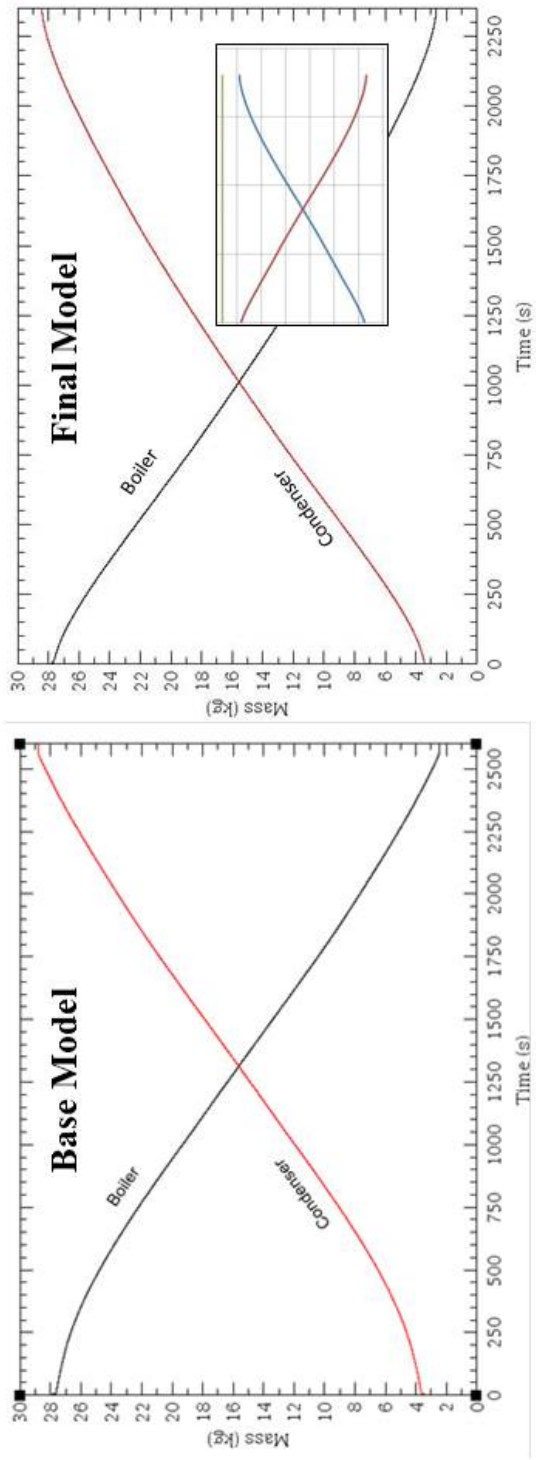

Figure 60. Base and Final Model output for inventory versus time after transient initiation to transient termination. Inset is qualitative snapshot of experimental data for quick comparison.

Chapter 14: Analysis of Main Discrepancies and Anomalies

Before discussing discrepancies, it is fitting to summarize what the code predicted well. The TRACE models predicted the following general trends or phenomena to an acceptable degree:

- The qualitative nature of the fundamental comparison: condenser pressure as a function of condenser inventory,

- The qualitative condenser pressure as a function of time,

- Inverted thermal stratification in the condenser pipe,

- Qualitative temperature as a function of time in the condenser,

- Qualitative boiler and condenser inventory as a function of time,

In addition, by choosing the model appropriate for a given nozzle geometry, TRACE was able to:

- Capture the energy partition,

- Predict whether the transient continued until the condenser filled or terminated before filling.

For the most part, the TRACE models were able to bracket the quantitative nature of the transient variables, with the Base Model providing the upper boundary and the Final Model providing the lower. The condenser always filled when using the PIPE component in the Base Model. By using the VESSEL component in the Final Model, the condenser filling could be prevented but never to the extent observed in the experiment. All other plots (pressure vs. time, temperature vs. time,

etc.) supported these final inventory predictions and presented a consistent story throughout. Although consistent, the TRACE predictions were qualitatively different from the data. All discrepancies between the experiment and model predictions can be summarized as originating in an over-stated condensation model, as discussed in Chapter 12. Due to the consistent nature of the TRACE predictions, discrepancies can be treated as a subset of the fundamental comparison.

Over-stated Condensation Model

Difference between Data and Model

In the Base Model, TRACE always predicted that the condenser would fill and terminate the transient with a pressure discontinuity. The discontinuity was eliminated in the Final Model by adding a small fraction of non-condensable gas, which initially did little to affect rapid condensation but eventually provided an amplifying mechanism to terminate the transient smoothly. The Final Model prevented the condenser from filling by nodalizing a VESSEL component radially to capture the energy partition. In doing so, a transient simulated with the Final Model predicted approximately 0.5 *L* less than a transient simulated with the Base Model. Experimental data showed that transients ran with the EZNF0815 nozzle (15-*deg* or fan nozzle) transferred approximately 3.5 *L* less than the EZNF0800 nozzle (0-*deg* or jet nozzle) due to the energy partition. TRACE consistently transferred more inventory than experimentally observed, suggesting that the code's condensation model is over-stated.

Implications

An over-stated condensation model means that TRACE will amplify or over-predict condensation-induced fluid motion when modeling the following reactor situations/systems:

- Water slug delivery in an annular downcomer,

- Steam discharge into large pools of sub-cooled water like those found in a suppression tank,

- Cold leg oscillations induced by ECC injection,

- Reflux condensation oscillations in U-tube steam generators,

- Oscillations due to combined injection of ECC liquid into both the hot and cold legs,

- Heat and mass transfer due to small pressure and temperature driving forces.

An accurate prediction of the condensation-induced fluid motion in these situations is imperative for the safe regulation and operation of both current and future light-water reactor systems. Over-stated condensation means that TRACE will predict fluid is present in a system or situation when it isn't, or vice versa. The absence of fluid when it was expected to be there is a serious concern.

Possible Source of Discrepancy

TRACE uses models or empirical correlations to solve for heat transfer coefficients and subsequently solve constitutive or balance equations as needed. The code is capable of estimating coefficients for direct contact, drop-wise, and both laminar and turbulent film condensation. TRACE uses typical heat transfer and fluid dynamic qualifiers like void fraction, Reynolds number, and Nusselt

number to determine the appropriate type of condensation correlation to perform the calculation. Film condensation is the default mode (Applied Programming Technology, 2007b).

Each of the empirical correlations has applicable ranges, conditions, and inherent uncertainties. These uncertainties are reasoned to be the primary source of the discrepancies. Recommendations for improvements to the code, such as Batet (2001), Choi (2002), Moon (2000), and Woods (2009), typically focus on adding options to use a different correlation or modifying the code to use improved correlations for a given experiment. For example, TRACE commonly uses the Uchida correlation for condensation in the presence of non-condensable gases.(APT, 2007b; Massoud, 2005). However, to improve the predictive capabilities of the TRACE code for the Passive Containment Cooling System of the proposed ESBWR, the developers modified the code to employ the mass transfer conductance approach developed by Kuhn and co-workers (1994). Once a modification like this is made, the challenge is to ensure that the change is still capable of predicting all the other phenomena correctly – that is: nothing else should be adversely affected by the change. In the case of the Kuhn approach, the NRC subsequently performed analysis and ultimately compared the TRACE output to the Uchida correlation. The modification was able to predict the Uchida data (APT, 2007b). However, if the Uchida correlation over or under-predicts experimental data, TRACE must obviously over or under-predict for the same data. This short discussion also suggests why RELAP5 would over-predict condensation, and its offspring, TRACE, still over-predicts condensation: the evolution process is complex and robust.

Possible Solution

The Base and Final Models bracketed the transient well, and in some cases the predictions were within the uncertainty of the experiment. Thus, the code performed well in predicting MANOTEA transient behaviors. The condensation model is over-stated, but not grossly so.

In the MANOTEA condenser there is a mix of direct condensation with sub-cooled droplets in the vapor space and film condensation on the wall. Because the vapor space and wall are both relatively warm, there is also vaporization in the vapor space and the wall. Rather than choosing a better correlation or modifying the present correlations invoked by the code to better capture MANOTEA behavior, it is suggested that a NOZZLE component could be developed for TRACE.

Currently, nozzles are modeled using the FILL component and assigning a loss coefficient. In some cases, the take-off angle can also be used to help capture some nozzle characteristics. While the FILL component captures the pressure and velocity changes associated with liquid moving through a nozzle, it does not capture the nozzle geometry effects. In a large reactor pressure vessel, these geometry effects could be argued to be negligible. But, in the high aspect ratio pipe like the MANOTEA condenser, these effects become very important. Spray geometry affects the energy partition, which subsequently dictates how much rapid condensation-induced liquid inventory is transferred. A nozzle component could prove useful and greatly simplify modeling of numerous transients.

The TRACE Theory Manual (Applied Programing Technology, 2007b) mentions that developers are working on a droplet field to improve re-flood and spray models. This droplet field could prove useful in improving MANOTEA simulations. The NRC has had an active role in this project, and developers are familiar with the results. As a consequence, the NRC is working on an implicit nozzle model (Staudenmeier, 2011). Merging the spray field and nozzle model work into a single, comprehensive NOZZLE component could greatly improve agreement between TRACE predictions and MANOTEA data by providing an easy means to capture the energy partition and ensure the appropriate mix of film and direct condensation is occurring.

Chapter 15: Modeling Summary

A 1-dimensional Base Model was developed prior to the termination of the experimental phase. Since TRACE is used to make regulatory decisions about the safety of proposed designs, this model was intentionally developed in this manner in order to provide unique insight. Output from the Base Model was eventually compared to experimental data and found to over-estimate the pressures and temperatures observed in the experiment. In addition, this model always predicted that the condenser pipe would fill, and that transients would terminate with a non-physical discontinuity.

A list of the phenomena and their ability to affect the transient was generated, and then mapped to TRACE parameters that could be used to exaggerate or reduce the effect of the relevant phenomena. In general, this exercise was aimed at finding valid ways to capture the energy partition, and in doing so, prevent the condenser from filling. Over 250 TRACE cases were run, and the effective and physically justifiable parameters were incorporated into a 3-dimensional Final TRACE Model. The Final Model incorporated the effects of non-condensable gases, which provided a mechanism by which transients could terminate smoothly and better match the data. Replacing the PIPE component in the Base Model with a radially nodalized VESSEL component in the Final Model, provided an undeniable way to model the energy partition and prevent the condenser from filling.

Whereas the Base Model generally over-predicted parameters, the Final Model generally under-predicted trends observed in the experiments. Thus, the 2 models were able to bracket the fundamental comparison, condenser pressure versus condenser inventory, and other trends observed during the experimental phase. By providing an upper and lower bound, TRACE was deemed capable of effectively modeling integral, rapid-condensation transients.

Thoughtful comparison of the TRACE output to the data led to the conclusion that the condensation model used by the code is over-stated. The code's predecessor's, TRAC and RELAP, where also known to have over-stated condensation models. An over-stated condensation model means that TRACE will amplify or over-predict condensation-induced fluid motion when modeling several common thermal-hydraulic reactor situations important to safe reactor operation.

The TRACE Theory Manual mentions that developers are working a droplet field to improve re-flood and spray models. This droplet field could prove useful in improving simulations of rapid-condensation transients from MANOTEA. The NRC is also working on an implicit nozzle model. Merging the spray field and nozzle model work into a single, comprehensive NOZZLE component could greatly improve agreement between TRACE predictions and MANOTEA data by providing an easy means to capture the energy partition and ensure the appropriate mix of film and direct condensation are occurring.

Chapter 16: Conclusions and Recommendations

Conclusions

The purpose of the present work was to experimentally validate the TRACE (TRAC-RELAP Advanced Computational Engine) plug-in for the Nuclear Regulatory Commission's (NRC's) Symbolic Nuclear Analysis Package (SNAP) for rapid condensation transients. The TRACE plug-in is designed to analyze thermal-hydraulic transients in light water reactors. The challenges that integral, condensation-driven transients have posed to thermal-hydraulic codes provided the motivation for the present work. The present work is particularly relevant because many of the proposed passive mechanisms and safety systems found in next generation reactors rely on rapid condensation for normal operation or accident mitigation.

The present work was undertaken in two phases: an experimental and modeling phase. Data obtained during the experimental phase was subsequently compared to output from a Base TRACE (TRAC-RELAP Advanced Computational Engine) model. Discrepancies between the data and the code output were used to identify potential problem areas in the code, and the improvements where used to generate a Final TRACE model. Comparisons between the models and the data provided a basis for recommendations for potential ways to improve TRACE for condensation-driven transients.

The experimental phase began by constructing and calibrating a simplified, integral, condensation-driven transient apparatus named the UMD-USNA Near One-dimensional Transient Experimental Assembly (MANOTEA). MANOTEA was designed to create rapid condensation transients. The facility is deemed simple enough that human intuition and simple models can still predict transient behavior, yet complex enough to provide a meaningful challenge and validation for the TRACE code.

After calibration, shake-down, and scoping experiments were ran, a series of 5 well-defined transient experiments were ran on MANOTEA and the data analyzed. Each transient was run twice to verify repeatability. Raw, standalone data from the facility included: pressure, differential pressure, and temperature profiles, all as a function of time. Using the raw data, a mass and energy balances were closed for each of the experiments. Some of the relevant characteristics of the data included: inverted thermal stratification in the condenser and nozzle dependent transients that are physically controlled by an energy partition. Plotting pressure as a function of inventory revealed a convenient way to summarize all of the transient datasets and resulted in a transient sequence. This sequence highlighted the integral nature of MANOTEA transients and ties the facility to more complex reactor systems. The transient sequence, which was a plot of condenser pressure versus condenser inventory, served as the fundamental comparison to evaluate TRACE during the second phase of the present work. The first phase terminated with the end of the experiments.

The second phase began by developing a 1-dimensional Base TRACE Model. The Base Model was developed prior to the termination of the experimental phase. Since TRACE is used to make regulatory decisions about the safety of proposed designs, this model was intentional developed in this manner in order to provide unique insight. Output from the Base Model was eventually compared to experimental data and found to over-estimate the pressures and temperatures observed in the experiment. In addition, this model always predicted that the condenser pipe would fill, and that transients would terminate with a non-physical discontinuity.

A list of the phenomena and their ability to affect the transient was generated, and then mapped to TRACE parameters that could be used to exaggerate or reduce the effect of the phenomena. In general, this exercise was aimed at finding unique ways to capture the energy partition, and in doing so, prevent the condenser from filling. Over 250 TRACE cases were run, and the effective and physically justifiable parameters were incorporated into a 3-dimensional Final TRACE Model. The Final Model incorporated the effects of non-condensable gases, which provided a mechanism by which transients could terminate smoothly and better match the data. Replacing the PIPE component in the Base model with a radially nodalized VESSEL component in the Final Model, provided an undeniable way to model the energy partition and prevent the condenser from filling. Whereas the Base model generally over-predicted parameters, the Final Model generally under-predicted trends observed in the experiments. Thus, the 2 models were able to bracket the fundamental comparison, condenser pressure versus condenser inventory.

Thoughtful comparison of the TRACE output to the data led to the conclusion that the condensation model used by the code is over-stated. The code's predecessor's, TRAC and RELAP, where also known to have over-stated condensation models. An over-stated condensation model means that TRACE will amplify or over-predict condensation-induced fluid motion when modeling several common thermal-hydraulic reactor situations important to safe reactor operation.

Recommendations and Future Work

The TRACE Theory Manual mentions that developers are working a droplet field to improve re-flood and spray models. This droplet field could prove useful in improving simulations of rapid-condensation transients from MANOTEA. Throughout the present work, the NRC has had an active role and developers are familiar with the results. As a consequence, the NRC is working on an implicit nozzle model. Merging the spray field and nozzle model work into a single, comprehensive NOZZLE component could greatly improve agreement between TRACE predictions and MANOTEA data by providing an easy means to capture the energy partition and ensure the appropriate mix of film and direct condensation are occurring.

Future work could focus on developing a NOZZLE component and comparing the subsequent TRACE output to MANOTEA data. Should this effort prove successful, other nozzle situations could be modeled for comparison to other datasets. The boiler pipe was of minor concern to the present work, but data from the MANOTEA experiments could be used to draw conclusions about TRACE's flashing models. Further experiments with MANOTEA in the current configuration are of

little use as previously mentioned. However, the facility could be modified to use larger copper tubing in the DPHE. This could create a situation in which the flashing in the boiler and condensation in the condenser pipe are competing to control transient behavior. Data from this modified facility could then be compared to a new TRACE model and may provide some new insight.

APPENDICES

Appendix A: Experimental Procedures Checklist

The following is a detailed, itemized list of steps outlining how to prepare the facility and run a transient:

Procedures to Prepare for Transient

- Reboot computer and verify data acquisition system (DAQ) is functional
- Open tee valves at the top of the boiler and condenser pipe to vent to atmosphere
- Close valve on the bottom of the boiler that allows inventory to flow from the boiler directly to the condenser
- Open valve on the bottom of the boiler that allows inventory to flow from the boiler into the double-pipe heat exchanger (DPHE)
- Install brass cap on the tee in the tubing that connect the boiler directly to the condenser
- Open valve on the bottom of the condenser that allows inventory to flow from the condenser directly to the boiler
- Zero strain gauges and pressure transducers
- Begin temperature, pressure, and strain logging on DAQ
- Open solenoid valve that isolates primary inventory from condenser pipe
- Remove plug from the fill hole at the top of boiler
- Fill boiler with water
- Close solenoid valve

- Close the valve at the bottom of the boiler to isolate the boiler from the DPHE
- Open valve at the bottom of the boiler to allow inventory to flow from the boiler directly to the condenser
- Wait for water to settle to 50/50 (half in the boiler and half in the condenser)
- Add 3.79 *L* (1 U.S. *gallon*) of water to the total inventory via the fill hole
- Install fill hole plug
- Turn boiler and condenser heaters to full power
- Heat inventory in both pipes for about 3 hours in order to de-gas
- Turn off boiler heater
- Close tee valve at the top of condenser isolating it from the atmosphere and opening it to the condenser pressure transducer
- Monitor condensing pressure and continue heating condenser side until water just spills out of the tee valve on the top of the boiler
- Close tee valve at the top of the boiler isolating it from the atmosphere and opening it to the boiler pressure transducer
- Shut off condenser heater and unplug
- Close valves at the bottom of the boiler and condenser to isolate them from each other and prevent inventory from flowing directly between them

- Open valve at the bottom of the boiler to allow inventory to flow through the primary side of the DPHE
- Turn on boiler heater
- Turn on secondary water
- Monitoring boiler and condenser pressure, heat boiler until pressure differential is 21.0 *kPa* with condenser is at 101 *kPa*
- Turn off boiler heater and unplug
- Apparatus is now ready for transient

Transient Initiation and Experimental Procedures

Check initial conditions, and then:

- Open solenoid valve to allow primary inventory to flow from the boiler to the condenser via the DPHE
- Allow transient to proceed to natural termination
- Close solenoid valve
- Turn off secondary water
- Drain boiler and condenser separately and monitor the time to drain
- Terminate logging and save data

Appendix B: Clausius-Clapeyron Primer

The Clausius-Clapeyron equation allows the change in enthalpy during vaporization, sublimation, or melting at a constant temperature to be evaluated from pressure/specific volume/temperature data pertaining to the phase change. In short, it provides a pressure-temperature relationship for saturated states. The equation can be written as:

$$(dp/dT)_{sat} = (h_g - h_f)/(RT^2/p)$$

Letting $\Lambda = (h_g - h_f)$, noting that $\Lambda/RT \sim$ constant (a small change in T results in a large change in p), and separating the variables:

$$(1/p)dp_{\underline{sat}} = (\Lambda/RT)(1/T)dT$$

Integrating both sides, we obtain:

$$\ln(p) = (\Lambda/RT)(\ln(T)) \quad \text{or} \quad p = T^{\Lambda/RT}$$

Note for $p = p_o$ and $T = T_o$, we can write:

$$p_o = T_o^{\Lambda/RT} \quad \text{and} \quad (p/p_o) = (T/T_o)^{\Lambda/RT}$$

Letting $\Pi = p/p_o$, $\Theta = T/T_o$, and $CC = \Lambda/RT$:

$$\Pi = \Theta^{CC}$$

The constant, CC, can be adjusted in order to fit data to pressure-temperature data, such as small portions of the steam tables. Figure A.1 shows a fit for $CC = 13.3$.

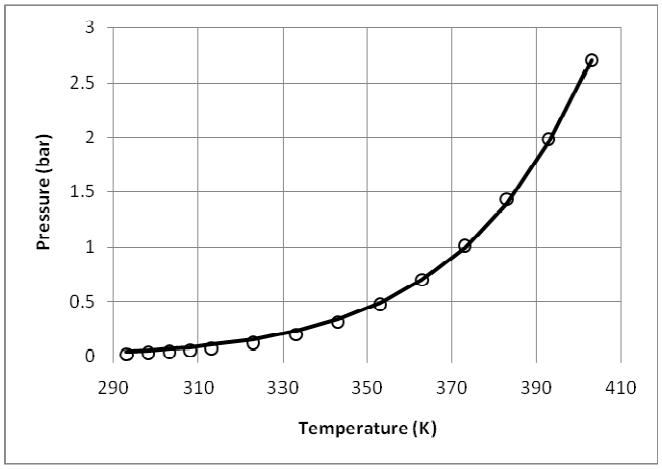

T (K)	P (bar)
293	0.023
298	0.032
303	0.043
308	0.056
313	0.074
323	0.124
333	0.199
343	0.312
353	0.474
363	0.701
373	1.014
383	1.433
393	1.985
403	2.701

Figure A.1. Curve Fit of Clausius-Clapeyron Equation to Steam Table Data (for *CC* = 13.3).

Appendix C: Integral Energy Balance Assumptions

The following assumptions were used to simplify derivation of the integral energy balance. Although many of these assumptions proved false, using them enabled the derivation of an express that captured the energy partition and matched the data fairly well.

Assumption 1: Pool is well mixed.

Combination of momentum from incoming jet, bubble/vapor generation in the pooled liquid by energy transferred from the metal masses (pipe walls), and natural convection currents ensures the pool is well mixed.

Note: MANOTEA data shows that this assumption is invalid. Nonetheless, it is accepted axiomatically in order to ease energy balance derivation and for clarity during early derivation. The energy balance is subsequently modified in order to account for the lack of mixing.

Assumption 2: Vapor contribution to energy balance is small.

Energy in the vapor at transient initiation:

$$E_g = (0.598\ kg/m^3)(0.0274\ m^3)(2510\ kJ/kg)$$

Energy in metal at transient initiation:

$$E_m = (7850\ kg/m^3)(0.0105\ m^3)(0.490\ kJ/kg*K)(100\ K)$$

Energy in pool at transient initiation:

$$E_f = (958\ kg/m^3)(0.00379\ m^3)(419\ kJ/kg)$$

$E_g/(E_g + E_m + E_f) = [41.0/(41.0 + 4040 + 1520)] = 0.00732$ or 0.7% of total energy in the system is in the vapor at transient initiation

A combination of low available energy and poor means to transport it ensures that the vapor contribution is small. As the transient proceeds, vapor volume is reduced. Thus, the contribution starts small and only gets smaller.

Assumption 3: Energy in metal mass is primarily transferred to the pooled liquid.

Energy transferred by 1-D conduction: $Q/A = -k(dT/dx)$ W/m^2

Energy transferred by convection: $Q/A = h(T_m - T_f)$ W/m^2

Initial ratio of energy transferred to the pool to total energy transfer:

$[(0.187\ m^2)(60.0\ W/\ m^2\ K)(5K) + (0.187\ m^2)(51\ W/mK)(5K)/(0.00635\ m)]$ /

$[(1.35\ m^2)(0.00246\ W/mK)(5K)/(0.0381m) + (1.35\ m^2)(1.50\ W/\ m^2\ K)(5K) +$

$(0.187\ m^2)(60.0\ W/\ m^2\ K)(5K) + (0.187\ m^2)(51\ W/mK)(5K)/(0.00635\ m)] =$

7565 W / 7576 W = 0.999 or 99+% of the heat transfer occurs between the metal wall and the pool. As wetted area increases, this percentage increases.

Appendix D: Obtaining Energy Balance Parameters from Data

MANOTEA Integral Energy Balance:

$$P = e^{\int_0^t \{[0.00039\chi\,(dT_m/dt) - 1.8(d(fV_L)/dt)]\,/\,fV_L\}\,dt}$$

dV_L/dt is obtained from a plot of the instantaneous (spray) volumetric flow rate as a function of time. Figure A.2 is an example. This plot is generated by applying the manufacturer's nozzle equation using data gathered by the differential pressure cell. This data is fed directly into the equation above in a spreadsheet.

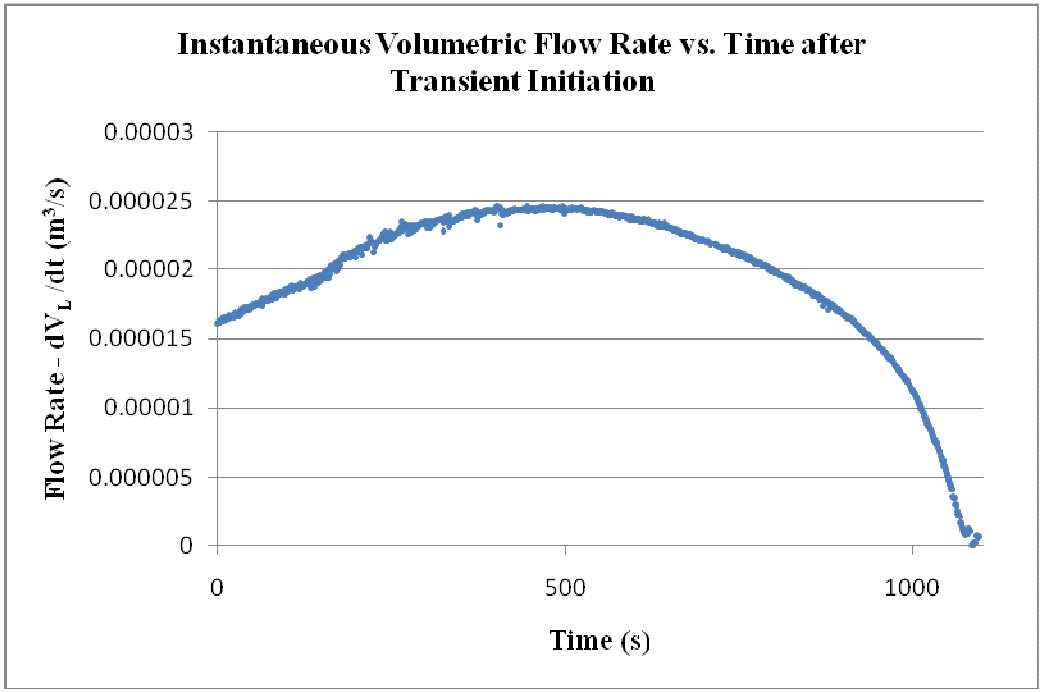

Figure A.2. Instantaneous volumetric flow rate as a function of time.

V_L is obtained by summing the instantaneous volumetric flow rate over time. A result is shown in Figure A.3.

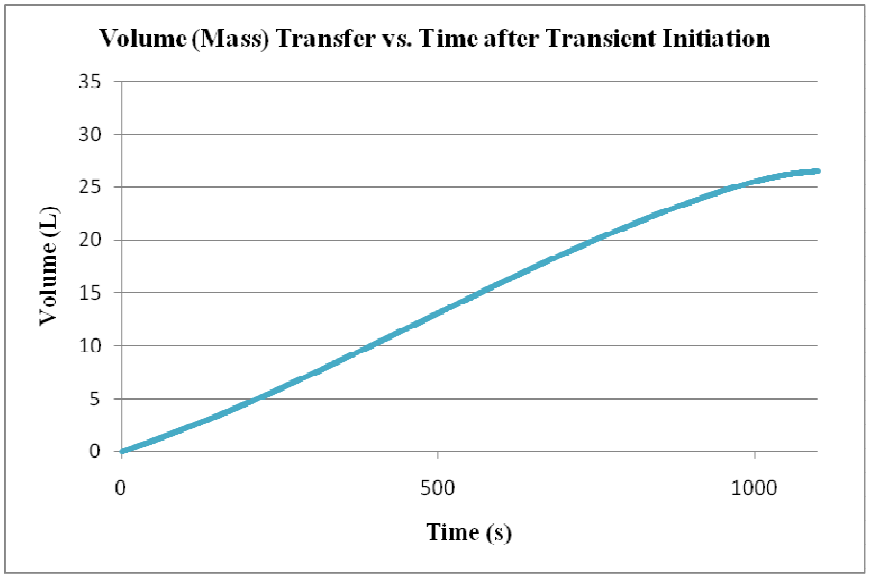

Figure A. 3. Volume as a function of time.

dT_m/dt is obtained by applying a curve fit to condenser pipe temperatures as a function of time. This technique is shown in Figure A.4.

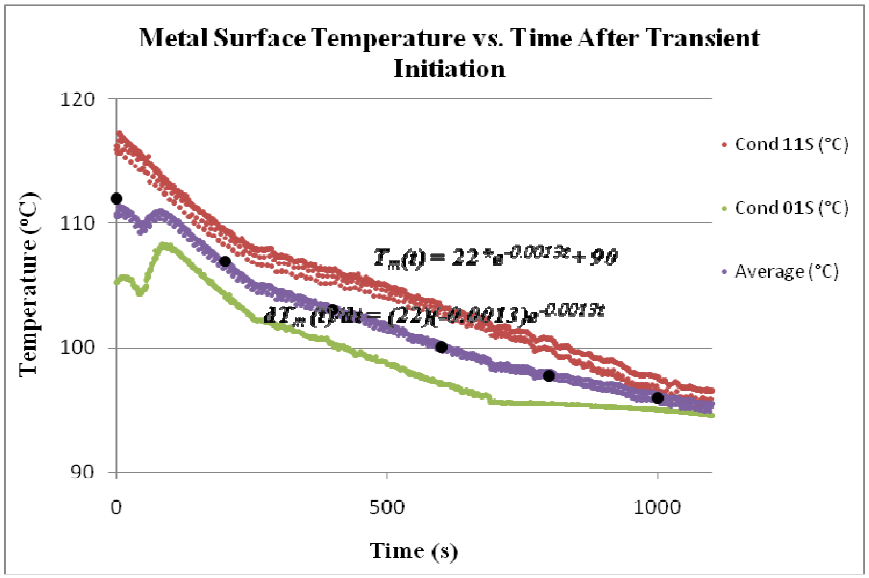

Figure A.4. Change metal temperature as a function of time.

χ and f could theoretically be obtained from the experimental data. However, this is considered tedious and beyond the scope of the present work, since the purpose of the energy balance derivation was simply to prove understanding of the physics involved during transient progression.

Appendix E: TRACE Terminology

The following general, pertinent terms are defined here for clarity:

Mathematical model: refers to the application of the balance equations (and equations of state if needed) to represent a physical phenomena.

Computational cell: a control volume for which the physical phenomena are considered and mathematical models are developed.

Node: is the same as a computational cell. Divide a pipe of length *L* in into *N* pieces, and the pipe would now be said to have *N* nodes of length *L/N*. Each node is associated with a state that describes that node regardless of its size and shape. Thus, each node has only a single temperature (and potentially a single case of other appropriate properties/parameters) associated with it. This temperature is generally taken to be the temperature at the center of the node. If more information about the temperature distribution within an individual node is required, the system would have to be re-nodalized.

Nodalization: in order to determine the state parameters, a system is broken down into several nodes. This process is generally referred to as nodalization.

Control volume: a region of space through which mass/energy flows. A control volume is used to simplify engineering analysis and is usually denoted by a dashed line. Mass/energy is allowed to cross this dashed line which is known as a boundary or system boundary. Control volume pressure and temperature are associated with the center of the volume or node. Control volume velocity (momentum) is associated with the volume's edge or junction.

Junction(s): a flow path that allows separate nodes to communicate. Mass and energy control volumes are connected together by junctions.

Donor cell: the "upstream" node or cell whose properties are used as input for the calculation of the present cell's properties.

Component: a physical piece of equipment represented symbolically in the analysis code. Thermal-hydraulic components include: pipe, tee, valve, pump, etc. Each component can be nodalized or divided into cells. Conservation equations are solved for each cell and passed "downstream". A component is a pre-packaged, but configurable model of common physical structures.

Homogeneous Equilibrium Model (HEM): refers to the treatment of fluid in a computational cell. Assumes liquid and vapor in a given cell are in thermal equilibrium and that both phases flow with the same velocity.

Separated Equilibrium Model (SEM): refers to the treatment of fluid in a computational cell. Assumes liquid and vapor in a given cell are in thermal equilibrium but that each phase travels with a different velocity.

Two-fluid Model: refers to the treatment of fluid in a computational cell. Assuming only liquid and vapor exist in a given computational cell, ten conservation equations (1 conservation of mass for each phase, 1 conservation of energy for each phase, & 3 conservation of momentum equations for each phase) are used to describe the conditions in that cell in terms of 10 unknowns (P, T_l, T_v, v_{xl}, v_{yl}, v_{zl}, v_{xv}, v_{yv}, v_{zv}, & α) . Thus, in this mathematical model, water and steam can be at different temperatures and flowing with different velocities.

Input Deck: a model comprised of all the physical components contained in an apparatus and meant for simulation and analysis of phenomena with a code.

Appendix F: Conservation Equations in Finite Difference Form

The semi-implicit one-dimensional finite-difference equations for the mass, energy, and momentum as implemented in TRACE are shown below. Note, these equations are the same as or similar to those used in legacy codes such as RELAP and TRAC. Some of the terms are intermediate time variables, which are denoted with a tilde (~). Due to the complexity of the equations, they were captured as pictures from the Code Manual (Applied 2007a & 2007b) and directly inserted here. All variables have standard thermal-hydraulic meanings. Three dimensional versions of these equations are available in the reference.

The sum continuity equation:

$$\begin{aligned} V_L[\alpha^n_{g,L}(\tilde{\rho}^{n+1}_{g,L}-\rho^n_{g,L})+\alpha^n_{f,L}(\tilde{\rho}^{n+1}_{f,L}-\rho^n_{f,L})+(\rho^n_{g,L}-\rho^n_{f,L})(\tilde{\alpha}^{n+1}_{g,L}-\alpha^n_{g,L})] \\ +(\dot{\alpha}^n_{g,j+1}\dot{\rho}^n_{g,j+1}v^{n+1}_{g,j+1}A_{j+1}-\dot{\alpha}^n_{g,j}\dot{\rho}^n_{g,j}v^{n+1}_{g,j}A_j)\Delta t \\ +(\dot{\alpha}^n_{f,j+1}\dot{\rho}^n_{f,j+1}v^{n+1}_{f,j+1}A_{j+1}-\dot{\alpha}^n_{f,j}\dot{\rho}^n_{f,j}v^{n+1}_{f,j}A_j)\Delta t = 0 \ . \end{aligned}$$

The difference continuity equation:

$$\begin{aligned} V_L[\alpha^n_{g,L}(\tilde{\rho}^{n+1}_{g,L}-\rho^n_{g,L})-\alpha^n_{f,L}(\tilde{\rho}^{n+1}_{f,L}-\rho^n_{f,L})+(\rho^n_{g,L}+\rho^n_{f,L})(\tilde{\alpha}^{n+1}_{g,L}-\alpha^n_{g,L})] \\ +(\dot{\alpha}^n_{g,j+1}\dot{\rho}^n_{g,j+1}v^{n+1}_{g,j+1}A_{j+1}-\dot{\alpha}^n_{g,j}\dot{\rho}^n_{g,j}v^{n+1}_{g,j}A_j)\Delta t \\ -(\dot{\alpha}^n_{f,j+1}\dot{\rho}^n_{f,j+1}v^{n+1}_{f,j+1}A_{j+1}-\dot{\alpha}^n_{f,j}\dot{\rho}^n_{f,j}v^{n+1}_{f,j}A_j)\Delta t \\ =-\left(\frac{2}{h_g^*-h_f^*}\right)^n_L V_L\Delta t\left[\frac{P^n_{s,L}}{P^n_L}H^n_{ig,L}(\tilde{T}^{s,n+1}_L-\tilde{T}^{n+1}_{g,L})+H^n_{if,L}(\tilde{T}^{s,n+1}_L-\tilde{T}^{n+1}_{f,L})\right]+2V_L\Delta t\Gamma^n_{w,L} \ . \end{aligned}$$

The non-condensable continuity equation:

$$V_L[\rho^n_{g,L}X^n_{n,L}(\tilde{\alpha}^{n+1}_{g,L}-\alpha^n_{g,L})+\alpha^n_{g,L}X^n_{n,L}(\tilde{\rho}^{n+1}_{g,L}-\rho^n_{g,L})+\alpha^n_{g,L}\rho^n_{g,L}(\tilde{X}^{n+1}_{n,L}-X^n_{n,L})]$$
$$+(\dot{\alpha}^n_{g,j+1}\dot{\rho}^n_{g,j+1}\dot{X}^n_{n,j+1}v^{n+1}_{g,j+1}A_{j+1}-\dot{\alpha}^n_{g,j}\dot{\rho}^n_{g,j}\dot{X}^n_{n,j}v^{n+1}_{g,j}A_j)\Delta t = 0 \ .$$

The vapor/gas thermal energy equation:

$$V_L[(\rho^n_{g,L}U^n_{g,L}+P^n_L)(\tilde{\alpha}^{n+1}_{g,L}-\alpha^n_{g,L})+\alpha^n_{g,L}U^n_{g,L}(\tilde{\rho}^{n+1}_{g,L}-\rho^n_{g,L})+\alpha^n_{g,L}\rho^n_{g,L}(\tilde{U}^{n+1}_{g,L}-U^n_{g,L})]$$
$$+[\dot{\alpha}^n_{g,j+1}(\dot{\rho}^n_{g,j+1}\dot{U}^n_{g,j+1}+P^n_L)v^{n+1}_{g,j+1}A_{j+1}-\dot{\alpha}^n_{g,j}(\dot{\rho}^n_{g,j}\dot{U}^n_{g,j}+P^n_L)v^{n+1}_{g,j}A_j]\Delta t$$
$$=\left\{-\left(\frac{h^*_f}{h^*_g-h^*_f}\right)^n_L\frac{P^n_{s,L}}{P^n_L}H^n_{ig,L}(\tilde{T}^{s,n+1}_L-\tilde{T}^{n+1}_{g,L})-\left(\frac{h^*_g}{h^*_g-h^*_f}\right)^n_L H^n_{if,L}(\tilde{T}^{s,n+1}_L-\tilde{T}^{n+1}_{f,L})\right.$$
$$\left.-\left(\frac{P^n_L-P^n_{s,L}}{P^n_L}\right)H^n_{gf,L}(\tilde{T}^{n+1}_{g,L}-\tilde{T}^{n+1}_{f,L})+\left[\left(\frac{1+\varepsilon}{2}\right)h'^{,n}_{g,L}+\left(\frac{1-\varepsilon}{2}\right)h'^{,n}_{f,L}\right]\Gamma^n_{w,L}+Q^n_{wg,L}+DISS^n_{g,L}\right\}V_L\Delta t \ .$$

The liquid thermal energy equation:

$$V_L[-(\rho^n_{f,L}U^n_{f,L}+P^n_L)(\tilde{\alpha}^{n+1}_{g,L}-\alpha^n_{g,L})+\alpha^n_{f,L}U^n_{f,L}(\tilde{\rho}^{n+1}_{f,L}-\rho^n_{f,L})+\alpha^n_{f,L}\rho^n_{f,L}(U^{n+1}_{f,L}-U^n_{f,L})]$$
$$+[\dot{\alpha}^n_{f,j+1}(\dot{\rho}^n_{f,j+1}\dot{U}^n_{f,j+1}+P^n_L)v^{n+1}_{f,j+1}A_{j+1}-\dot{\alpha}^n_{f,j}(\dot{\rho}^n_{f,j}\dot{U}^n_{f,j}+P^n_L)v^{n+1}_{f,j}A_j]\Delta t$$
$$=\left\{\left(\frac{h^*_f}{h^*_g-h^*_f}\right)^n_L\frac{P^n_{s,L}}{P^n_L}H^n_{ig,L}(\tilde{T}^{s,n+1}_L-\tilde{T}^{n+1}_{g,L})+\left(\frac{h^*_g}{h^*_g-h^*_f}\right)^n_L H^n_{if,L}(\tilde{T}^{s,n+1}_L-\tilde{T}^{n+1}_{f,L})\right.$$
$$\left.+\left(\frac{P^n_L-P^n_{s,L}}{P^n_L}\right)H^n_{gf,L}(\tilde{T}^{n+1}_{g,L}-\tilde{T}^{n+1}_{f,L})-\left[\left(\frac{1+\varepsilon}{2}\right)h'^{,n}_{g,L}+\left(\frac{1-\varepsilon}{2}\right)h'^{,n}_{f,L}\right]\Gamma^n_{w,L}+Q^n_{wf,L}+DISS^n_{f,L}\right\}V_L\Delta t$$

The sum momentum equation:

$$(\alpha_g\rho_g)^n_j(v^{n+1}_g-v^n_g)_j\Delta x_j+(\alpha_f\rho_f)^n_j(v^{n+1}_f-v^n_f)_j\Delta x_j+\frac{1}{2}(\dot{\alpha}_g\dot{\rho}_g)^n_j[(v^2_g)^n_L-(v^2_g)^n_K]\Delta t$$
$$+\frac{1}{2}(\dot{\alpha}_f\dot{\rho}_f)^n_j[(v^2_f)^n_L-(v^2_f)^n_K]\Delta t-\frac{1}{2}[(\dot{\alpha}_g\dot{\rho}_g)^n_jVISG^n_j+(\dot{\alpha}_f\dot{\rho}_f)^n_jVISF^n_j]\Delta t$$
$$=-(P_L-P_K)^{n+1}\Delta t+[(\rho_m)^n_jB_x-(\alpha_g\rho_g)^n_jFWG^n_j(v_g)^{n+1}_j-(\alpha_f\rho_f)^n_jFWF^n_j(v_f)^{n+1}_j$$
$$-(\Gamma_g)^n_j(v_g-v_f)^{n+1}_j]\Delta x_j\Delta t-[(\dot{\alpha}_g\dot{\rho}_g)^n_jHLOSSG^n_jv^{n+1}_{g,j}+(\dot{\alpha}_f\dot{\rho}_f)^n_jHLOSSF^n_jv^{n+1}_{f,j}]\Delta t$$

The difference momentum equation:

$$\left(1+\frac{C\rho_m^2}{\rho_g\rho_f}\right)_j^n[(v_g^{n+1}-v_g^n)-(v_f^{n+1}-v_f^n)]_j\Delta x_j$$

$$+\frac{1}{2}\left(\frac{\dot{\alpha}_g\dot{\rho}_g}{\alpha_g\rho_g}\right)_j^n[(v_g^2)_L^n-(v_g^2)_K^n]\Delta t-\frac{1}{2}\left(\frac{\dot{\alpha}_g\dot{\rho}_g}{\alpha_g\rho_g}\right)_j^n VISG_j^n\Delta t$$

$$-\frac{1}{2}\left(\frac{\dot{\alpha}_f\dot{\rho}_f}{\alpha_f\rho_f}\right)_j^n[(v_f^2)_L^n-(v_f^2)_K^n]\Delta t+\frac{1}{2}\left(\frac{\dot{\alpha}_f\dot{\rho}_f}{\alpha_f\rho_f}\right)_j^n VISF_j^n\Delta t=-\left(\frac{\rho_f-\rho_g}{\rho_f\rho_g}\right)_j^n(P_L-P_K)^{n+1}\Delta t$$

$$-\left(FWG_j^n(v_g)_j^{n+1}-FWF_j^n(v_f)_j^{n+1}-\left[\frac{\Gamma_g^n(\rho_m^n v_I^{n+1}-\alpha_f^n\rho_f^n v_g^{n+1}-\alpha_g^n\rho_g^n v_f^{n+1})}{(\alpha_g\rho_g\alpha_f\rho_f)^n}\right]_j\right.$$

$$-(f_x)_j^n\left(\frac{1}{\alpha_g\rho_g}+\frac{1}{\alpha_f\rho_f}\right)_j^n[(f_{wg})_j^n(v_g)_j^{n+1}-(f_{wf})_j^n(v_f)_j^{n+1}]$$

$$\left.+(\rho_m FI)_j^n\{[1+f_x(C_1-1)]_j^n(v_g)_j^{n+1}-[1+f_x(C_0-1)]_j^n(v_f)_j^{n+1}\}\right)\Delta x_j\Delta t$$

$$-\left[\left(\frac{\dot{\alpha}_g\dot{\rho}_g}{\alpha_g\rho_g}\right)_j^n HLOSSG_j^n v_{g,j}^{n+1}-\left(\frac{\dot{\alpha}_f\dot{\rho}_f}{\alpha_f\rho_f}\right)_j^n HLOSSF_j^n v_{f,j}^{n+1}\right]\Delta t$$

$$+\left(\frac{\rho_m}{\rho_g\rho_f}\right)_j^n(\rho_f-\rho_g)_j^n B_y(y_L^n-y_K^n)\Delta t$$

Appendix G: TRACE Input Decks

Note all TRACE modeling/coding was performed using the SNAP GUI. However, for completeness, the input decks were exported to text in order to facilitate those who are used to working with text input.

Base Model Input Deck

```
*
*
*************
* main data *
*************
*
*       numtcr          ieos         inopt          nmat          id2o
            1             0             1             3             0

*
*
*****************
* namelist data *
*****************
*
 &inopts
  dtstrt=1.0,
  ikfac=1,
  ioinp=0,
  noair=0,
  usesjc=3,
  nhtstr=6
 &end
*
***************
* Model Flags *
***************
*
*        dstep         timet
             0           0.0
*       stdyst        transi         ncomp          njun          ipak
             0             1            16             8             1
*         epso          epss
          1.0E-4        1.0E-4
*       oitmax        sitmax        isolut        ncontr         nccfl
            10            10             0             0             0
*         ntsv          ntcb          ntcf          ntrp          ntcp
            23             1             0             0             0
*
************************
* component-number data *
************************
*
*  Component input order (IORDER)
*-- type ---- num ------------ name ----------------  +    jun1   jun2   jun3
* PIPE     *      1 s * Condenser                     +       0     32
* PIPE     *     11 s * Boiler                        +      27      0
* PIPE     *     21 s * CCDPHE Primary                +      28     29
* PIPE     *     31 s * CCDPHE Secondary              +      31      1
* FILL     *     51 s * Hose Inlet                    +       1
* BREAK    *     61 s * Hose Outlet                   +      31
* HTSTR    *    101 s *                               +
* PIPE     *    111 s * Lower BOP                     +      27     28
* PIPE     *    112 s * Upper BOP                     +      26     23
* HTSTR    *    121 s *                               +
```

```
* HTSTR    *    122 s *                                +
* PIPE     *    131 s * Nozzle                         +      23     32
* HTSTR    *    132 s *                                +
* HTSTR    *    141 s *                                +
* VALVE    *    151 s *                                +      29     26
* HTSTR    *    161 e *                                +
*
**********************
* material properties *
**********************
*
*   matb*          50          51          52 e
*  ptbln*           1           1           1 e
*  User Defined Material : 50
*
*n: Copper Alloy
*
*d: Copper Alloy
*  prptb         temp         rho          cp        cond        emis
*  prptb*       293.0      8940.6       385.0       394.0         0.0 e
*
*  User Defined Material : 51
*
*n: PVC
*
*  prptb         temp         rho          cp        cond        emis
*  prptb*       293.0      1390.0       900.0        0.16         0.0 e
*
*  User Defined Material : 52
*
*n: Insulation
*
*  prptb         temp         rho          cp        cond        emis
*  prptb*       293.0    48.05539       670.0 0.033172414         0.0 e
*
*
*
************************************************
* Starting Signal Variable Section of Model      *
************************************************
*n: Boiler Pressure
*
*         idsv          isvn          ilcn          icn1          icn2
             1            21            11             3             0
*n: CC19
*
*         idsv          isvn          ilcn          icn1          icn2
             2            23             1            10             0
*n: CC11
*
*         idsv          isvn          ilcn          icn1          icn2
             3            23             1             6             0
*n: CC15
*
*         idsv          isvn          ilcn          icn1          icn2
             4            23             1             8             0
*n: CC07
*
*         idsv          isvn          ilcn          icn1          icn2
             5            23             1             4             0
*n: CC13
*
*         idsv          isvn          ilcn          icn1          icn2
             6            23             1             7             0
*n: CC09
*
*         idsv          isvn          ilcn          icn1          icn2
             7            23             1             5             0
*n: CC03
*
*         idsv          isvn          ilcn          icn1          icn2
```

```
             8            23             1             2             0
*n: CC21
*
*         idsv          isvn          ilcn          icn1          icn2
             9            23             1            11             0
*n: CC17
*
*         idsv          isvn          ilcn          icn1          icn2
            10            23             1             9             0
*n: CC05
*
*         idsv          isvn          ilcn          icn1          icn2
            11            23             1             3             0
*n: CC01
*
*         idsv          isvn          ilcn          icn1          icn2
            12            23             1             1             0
*n: BC21
*
*         idsv          isvn          ilcn          icn1          icn2
            13            23            11             3             0
*n: BC11
*
*         idsv          isvn          ilcn          icn1          icn2
            14            23            11             2             0
*n: BC01
*
*         idsv          isvn          ilcn          icn1          icn2
            15            23            11             1             0
*n: Primary Inlet
*
*         idsv          isvn          ilcn          icn1          icn2
            16            23            51             1             0
*n: Primary Outlet
*
*         idsv          isvn          ilcn          icn1          icn2
            17            23            61             1             0
*n: Condenser Pressure
*
*         idsv          isvn          ilcn          icn1          icn2
            24            21             1            11             0
*n: Boiler Inventory
*
*d: FlashLevel
*         idsv          isvn          ilcn          icn1          icn2
            25           124            11             0             0
*n: Boiler Initial Inventory
*
*d: FlashIntLevel
*         idsv          isvn          ilcn          icn1          icn2
            26           125            11             0             0
*n: Condenser Initial Inventory
*
*d: CondeIntLevel
*         idsv          isvn          ilcn          icn1          icn2
            27           125             1             0             0
*n: Condenser Inventory
*
*d: CondeLevel
*         idsv          isvn          ilcn          icn1          icn2
            28           124             1             0             0
*n: Timer
*
*         idsv          isvn          ilcn          icn1          icn2
            30             0             0             0             0
************************************************
* Finished Signal Variable Section of Model      *
************************************************
*
*
*
```

```
*
*****************************************
* Starting Control System Section of Model  *
*****************************************
*
****** Control Blocks ******
*n: PressDif
*
*d: PressDif
*         idcb          icbn          icb1          icb2          icb3
             -1            44             1            24             0
*       cbgain        cbxmin         cbmax        cbcon1        cbcon2
            1.0       -1.0E20        1.0E20           0.0           0.0
*
*****************************************
* Finished Control System Section of Model  *
*****************************************
*
*
*
*
*******   type           num        userid                component name
pipe                       1             0                       Condenser
*       ncells         nodes          jun1          jun2          epsw
             11             0             0            32           0.0
*       nsides
                0
*         ichf         iconc      pipetype          ipow        npipes
                1             0             0             0             1
*        radin            th         houtl         houtv         toutl
             0.0           0.0           0.0           0.0           0.0
*        toutv          pwin         pwoff         rpwmx         pwscl
             0.0           0.0           0.0           0.0           0.0
* dx    *   0.58181818  0.58181818  0.58181818  0.58181818s
* dx    *   0.58181818  0.58181818  0.58181818  0.58181818s
* dx    *   0.58181818  0.58181818  0.58181818e
* vol   *    2.6533E-3   2.6533E-3   2.6533E-3   2.6533E-3s
* vol   *    2.6533E-3   2.6533E-3   2.6533E-3   2.6533E-3s
* vol   *    2.6533E-3   2.6533E-3   2.6533E-3e
* fa    *   4.56037E-3  4.56037E-3  4.56037E-3  4.56037E-3s
* fa    *   4.56037E-3  4.56037E-3  4.56037E-3  4.56037E-3s
* fa    *   4.56037E-3  4.56037E-3  4.56037E-3  2.63022E-6e
* kfac  *          0.0         0.0         0.0         0.0s
* kfac  *          0.0         0.0         0.0         0.0s
* kfac  *          0.0         0.0         0.0        3.42e
* grav  *          1.0         1.0         1.0         1.0s
* grav  *          1.0         1.0         1.0         1.0s
* grav  *          1.0         1.0         1.0         1.0e
* hd    *       0.0762      0.0762      0.0762      0.0762s
* hd    *       0.0762      0.0762      0.0762      0.0762s
* hd    *       0.0762      0.0762      0.0762     1.83E-3e
* nff   *            1           1           1           1s
* nff   *            1           1           1           1s
* nff   *            1           1           1           1e
* alp   *          0.0        0.65         1.0         1.0s
* alp   *          1.0         1.0         1.0         1.0s
* alp   *          1.0         1.0         1.0e
* vl    *          0.0         0.0         0.0         0.0s
* vl    *          0.0         0.0         0.0         0.0s
* vl    *          0.0         0.0         0.0         0.0e
* vv    *          0.0         0.0         0.0         0.0s
* vv    *          0.0         0.0         0.0         0.0s
* vv    *          0.0         0.0         0.0         0.0e
* tl    *        378.0       378.0       378.0       378.0s
* tl    *        378.0       378.0       378.0       378.0s
* tl    *        378.0       378.0       378.0e
* tv    *        378.0       378.0       378.0       378.0s
* tv    *        378.0       378.0       378.0       378.0s
* tv    *        378.0       378.0       378.0e
* p     *      1.013E5     1.013E5     1.013E5     1.013E5s
* p     *      1.013E5     1.013E5     1.013E5     1.013E5s
```

```
* p     *      1.013E5     1.013E5     1.013E5e
* pa    *          0.0         0.0         0.0         0.0s
* pa    *          0.0         0.0         0.0         0.0s
* pa    *          0.0         0.0         0.0e
*
*
*******   type           num        userid                component name
pipe                      11             0                         Boiler
*       ncells          nodes          jun1          jun2          epsw
             3              0            27             0           0.0
*       nsides
             0
*         ichf          iconc      pipetype          ipow        npipes
             1              0             0             0             1
*        radin            th         houtl         houtv         toutl
           0.0           0.0           0.0           0.0           0.0
*        toutv          pwin         pwoff         rpwmx         pwscl
           0.0           0.0           0.0           0.0           0.0
* dx    *    2.1333333   2.1333333   2.1333333e
* vol   *   9.72878E-3  9.72878E-3  9.72878E-3e
* fa    *   3.16692E-5  4.56037E-3  4.56037E-3  4.56037E-3e
* kfac  *         0.49         0.0         0.0         0.0e
* grav  *          1.0         1.0         1.0         1.0e
* hd    *      6.35E-3      0.0762      0.0762      0.0762e
* nff   *            1           1           1           1e
* alp   *          0.0         0.0         0.0e
* vl    *          0.0         0.0         0.0         0.0e
* vv    *          0.0         0.0         0.0         0.0e
* tl    *      378.149     378.149     378.149e
* tv    *      378.149     378.149     378.149e
* p     *      1.209E5     1.209E5     1.209E5e
* pa    *          0.0         0.0         0.0e
*
*
*******   type           num        userid                component name
pipe                      21             0                 CCDPHE Primary
*       ncells          nodes          jun1          jun2          epsw
             3              0            28            29           0.0
*       nsides
             0
*         ichf          iconc      pipetype          ipow        npipes
             1              0             0             0             1
*        radin            th         houtl         houtv         toutl
           0.0           0.0           0.0           0.0           0.0
*        toutv          pwin         pwoff         rpwmx         pwscl
           0.0           0.0           0.0           0.0           0.0
* dx    *    2.1333333   2.1333333   2.1333333e
* vol   *    6.7561E-5   6.7561E-5   6.7561E-5e
* fa    *   3.16692E-5  3.16692E-5  3.16692E-5  3.16692E-5e
* kfac  *          0.0         0.0         0.0         0.0e
* grav  *          1.0         1.0         1.0         1.0e
* hd    *      6.35E-3     6.35E-3     6.35E-3     6.35E-3e
* nff   *            1           1           1           1e
* alp   *          0.0         0.0         0.0e
* vl    *          0.0         0.0         0.0         0.0e
* vv    *          0.0         0.0         0.0         0.0e
* tl    *        293.0       293.0       293.0e
* tv    *        293.0       293.0       293.0e
* p     *      1.209E5     1.209E5     1.209E5e
* pa    *          0.0         0.0         0.0e
*
*
*******   type           num        userid                component name
pipe                      31             0              CCDPHE Secondary
*       ncells          nodes          jun1          jun2          epsw
             3              0            31             1           0.0
*       nsides
             0
*         ichf          iconc      pipetype          ipow        npipes
             1              0             0             0             1
*        radin            th         houtl         houtv         toutl
```

```
          0.0           0.0           0.0           0.0           0.0
*        toutv          pwin         pwoff         rpwmx         pwscl
          0.0           0.0           0.0           0.0           0.0
* dx    *    2.1333333   2.1333333   2.1333333e
* vol   *   9.72878E-3  9.72878E-3  9.72878E-3e
* fa    *   5.06451E-4  5.06451E-4  5.06451E-4  5.06451E-4e
* kfac  *          0.0         0.0         0.0         0.0e
* grav  *          1.0         1.0         1.0         1.0e
* hd    *       0.0762      0.0762      0.0762      0.0762e
* nff   *            1           1           1           1e
* alp   *          0.0         0.0         0.0e
* vl    *          0.0         0.0         0.0         0.0e
* vv    *          0.0         0.0         0.0         0.0e
* tl    *        293.0       293.0       293.0e
* tv    *        293.0       293.0       293.0e
* p     *     1.013E5     1.013E5     1.013E5e
* pa    *          0.0         0.0         0.0e
*
*
*d: Hose Inlet
*******   type           num        userid                component name
fill                      51             0                     Hose Inlet
*         jun1          ifty          ioff
            1             2             0
*        twtold          rfmx        concin          felv
          0.0         1.0E20           0.0           0.0
*         dxin          volin         alpin          vlin          tlin
           0.1   5.064506E-4           0.0           0.0         293.0
*          pin          pain        flowin          vvin          tvin
       1.013E5           0.0       0.62957           0.0         293.0
*
*
*d: Hose Outlet
*******   type           num        userid                component name
break                     61             0                    Hose Outlet
*         jun1          ibty          isat          ioff      adjpress
            31             0             0             1             0
*         dxin          volin         alpin           tin           pin
           0.1   5.064506E-4           0.0         293.0       1.013E5
*         pain         concin          rbmx          poff          belv
           0.0           0.0       1.0E20           0.0           0.0
*
*
*******   type           num        userid                component name
pipe                     111             0                      Lower BOP
*        ncells         nodes          jun1          jun2          epsw
             6             0            27            28           0.0
*        nsides
             0
*          ichf         iconc      pipetype          ipow        npipes
             1             0             0             0             1
*         radin            th         houtl         houtv         toutl
           0.0           0.0           0.0           0.0           0.0
*         toutv          pwin         pwoff         rpwmx         pwscl
           0.0           0.0           0.0           0.0           0.0
* dx    *      0.10525     0.10525     0.10525     0.10525s
* dx    *      0.10525     0.10525e
* vol   *   3.33319E-6  3.33319E-6  3.33319E-6  3.33319E-6s
* vol   *   3.33319E-6  3.33319E-6e
* fa    *   3.16692E-5  3.16692E-5  3.16692E-5  3.16692E-5s
* fa    *   3.16692E-5  3.16692E-5  3.16692E-5e
* kfac  *         0.49         0.0         0.0         0.0s
* kfac  *          0.0         0.0         0.0e
* grav  *         -1.0 -0.70682518         0.0         0.0s
* grav  *   0.70710678         1.0         1.0e
* hd    *      6.35E-3     6.35E-3     6.35E-3     6.35E-3s
* hd    *      6.35E-3     6.35E-3     6.35E-3e
* nff   *            1           1           1           1s
* nff   *            1           1           1e
* alp   *          0.0         0.0         0.0         0.0s
* alp   *          0.0         0.0e
```

```
* vl    *          0.0         0.0         0.0         0.0s
* vl    *          0.0         0.0         0.0e
* vv    *          0.0         0.0         0.0         0.0s
* vv    *          0.0         0.0         0.0e
* tl    *        378.0       378.0       378.0       378.0s
* tl    *        378.0       378.0e
* tv    *      378.149     378.149     378.149     378.149s
* tv    *      378.149     378.149e
* p     *      1.209E5     1.209E5     1.209E5     1.209E5s
* p     *      1.209E5     1.209E5e
* pa    *          0.0         0.0         0.0         0.0s
* pa    *          0.0         0.0e
*
*
*******   type           num        userid                component name
pipe                     112             0                      Upper BOP
*       ncells          nodes           jun1          jun2          epsw
             6              0             26            23           0.0
*       nsides
             0
*         ichf          iconc      pipetype          ipow        npipes
             1              0             0             0             1
*        radin            th         houtl         houtv         toutl
           0.0           0.0           0.0           0.0           0.0
*        toutv          pwin         pwoff         rpwmx         pwscl
           0.0           0.0           0.0           0.0           0.0
* dx    *    0.0894667   0.0894667   0.0894667   0.0894667s
* dx    *    0.0894667   0.0894667e
* vol   *   2.83334E-6  2.83334E-6  2.83334E-6  2.83334E-6s
* vol   *   2.83334E-6  2.83334E-6e
* fa    *   3.16692E-5  3.16692E-5  3.16692E-5  3.16692E-5s
* fa    *   3.16692E-5  3.16692E-5  2.63022E-6e
* kfac  *          0.0         0.0         0.0         0.0s
* kfac  *          0.0         0.0        3.42e
* grav  *          1.0         1.0         1.0         0.0s
* grav  *          0.0        -1.0        -1.0e
* hd    *      6.35E-3     6.35E-3     6.35E-3     6.35E-3s
* hd    *      6.35E-3     6.35E-3     1.83E-3e
* nff   *            1           1           1           1s
* nff   *            1           1           1e
* alp   *          1.0         1.0         1.0         1.0s
* alp   *          1.0         1.0e
* vl    *          0.0         0.0         0.0         0.0s
* vl    *          0.0         0.0         0.0e
* vv    *          0.0         0.0         0.0         0.0s
* vv    *          0.0         0.0         0.0e
* tl    *        293.0       293.0       293.0       293.0s
* tl    *        293.0       293.0e
* tv    *        293.0       293.0       293.0       293.0s
* tv    *        293.0       293.0e
* p     *      1.013E5     1.013E5     1.013E5     1.013E5s
* p     *      1.013E5     1.013E5e
* pa    *          0.0         0.0         0.0         0.0s
* pa    *          0.0         0.0e
*
*
*d: Nozzle
* single junction
*******   type           num        userid                component name
pipe                     131             0                         Nozzle
*       ncells          nodes           jun1          jun2          epsw
             0              0             23            32           0.0
*         ichf          iconc      pipetype          ipow        npipes
             1              0             0             0             1
*        radin            th         houtl         houtv         toutl
           0.0           0.0           0.0           0.0           0.0
*        toutv          pwin         pwoff         rpwmx         pwscl
           0.0           0.0           0.0           0.0           0.0
* dx    *    f 0.0000e+00
* vol   *    f 0.0000e+00
* fa    *  f   2.63022E-6e
```

```
* kfac  *  f         3.42e
* grav  *  f         -1.0e
* hd    *  f      1.83E-3e
* nff   *  f            1e
* alp   *    f 0.0000e+00e
* vl    *  f          0.0e
* vv    *  f          0.0e
* tl    *    f 0.0000e+00e
* tv    *    f 0.0000e+00e
* p     *    f 0.0000e+00e
* pa    *    f 0.0000e+00e
*
*
*******   type           num        userid                component name
valve                    151             0                       unnamed
*       ncells         nodes         jun1         jun2         epsw
             0             0           29           26          0.0
*         ichf         iconc          ivty          ivps         nvtb2
             1             0            1             1             0
*         ivtr          ivsv         nvtb1         nvsv          nvrf
             0            30            6             0             0
*       ivtrov        ivtyov        ivtrlo    intlossoff        nkopen
             0             0             0             0             2
*         rvmx          rvov        fminov        fmaxov
         100.0           0.0           0.0           1.0
*        radin            th         houtl         houtv         toutl
           0.0           0.0           0.0           0.0           0.0
*        toutv         avlve         hvlve        favlve          xpos
           0.0   3.166922E-5       6.35E-3           0.0           0.0
* dx    *    f 0.0000e+00e
* vol   *    f 0.0000e+00e
* fa    *  f   3.16692E-5e
* kfac  *  f          0.0e
* grav  *  f          1.0e
* hd    *  f      6.35E-3e
* nff   *  f            1e
* alp   *    f 0.0000e+00e
* vl    *  f          0.0e
* vv    *  f          0.0e
* tl    *    f 0.0000e+00e
* tv    *    f 0.0000e+00e
* p     *    f 0.0000e+00e
* pa    *    f 0.0000e+00e
* vtb1  *         0.0         0.0s
* vtb1  *         1.0         0.0s
* vtb1  *         2.0         0.0s
* vtb1  *         3.0         0.0s
* vtb1  *         4.0         0.0s
* vtb1  *         5.0         1.0e
*
*
****************************************
* Starting Heat Structure Section of Model *
****************************************
*
*******   type           num        userid                component name
htstr                    101             1                       unnamed
*       nzhstr         ittc         hscyl          ichf
            11            0             1             1
*    nofuelrod        plane        liqlev        iaxcnd         pdrat
             1            3             1             0           0.0
*        nmwrx         nfci         nfcil         hdri          hdro
             0            0             1           0.0           0.0
*         nhot        nodes          fmon        nzmax       reflood
             0           11             0           100             0
*     dtxht(1)      dtxht(2)        dznht        hgapo
           0.0           0.0       1.0E-3       6300.0
*
*  idbcin *           2           2           2           2s
*  idbcin *           2           2           2           2s
*  idbcin *           2           2           2e
```

```
*  idbcon *           5           5           5           5s
*  idbcon *           5           5           5           5s
*  idbcon *           5           5           5e
* hcomon1 *           1           1           0           0e
* hcomon1 *           1           2           0           0e
* hcomon1 *           1           3           0           0e
* hcomon1 *           1           4           0           0e
* hcomon1 *           1           5           0           0e
* hcomon1 *           1           6           0           0e
* hcomon1 *           1           7           0           0e
* hcomon1 *           1           8           0           0e
* hcomon1 *           1           9           0           0e
* hcomon1 *           1          10           0           0e
* hcomon1 *           1          11           0           0e
* tsurfo2 *       293.0e
* tsurfo2 *       293.0e
* tsurfo2 *       293.0e
* tsurfo2 *       293.0e
* tsurfo2 *       293.0e
* tsurfo2 *       293.0e
* tsurfo2 *       293.0e
* tsurfo2 *       293.0e
* tsurfo2 *       293.0e
* tsurfo2 *       293.0e
* tsurfo2 *       293.0e
* dhtstrz *  0.58709091  0.58709091  0.58709091  0.58709091s
* dhtstrz *  0.58709091  0.58709091  0.58709091  0.58709091s
* dhtstrz *  0.58709091  0.58709091  0.58709091e
*   rdx   *          1.0e
*  radrd  *    0.038965    0.043325      0.0445    0.052045    0.056405s
*  radrd  *    0.060765    0.065125    0.069485    0.073845    0.078205s
*  radrd  *    0.082565e
*  matrd  *           9           9          52          52 s
*  matrd  *          52          52          52          52 s
*  matrd  *          52          52 e
*    nfax *           1           1           1           1s
*    nfax *           1           1           1           1s
*    nfax *           1           1           1e
*    rftn *       373.0       373.0       373.0       373.0s
*    rftn *       363.0       353.0       343.0       333.0s
*    rftn *       323.0       313.0       303.0       373.0s
*    rftn *       373.0       373.0       373.0       363.0s
*    rftn *       353.0       343.0       333.0       323.0s
*    rftn *       313.0       303.0       373.0       373.0s
*    rftn *       373.0       373.0       363.0       353.0s
*    rftn *       343.0       333.0       323.0       313.0s
*    rftn *       303.0       373.0       373.0       373.0s
*    rftn *       373.0       363.0       353.0       343.0s
*    rftn *       333.0       323.0       313.0       303.0s
*    rftn *       373.0       373.0       373.0       373.0s
*    rftn *       363.0       353.0       343.0       333.0s
*    rftn *       323.0       313.0       303.0       373.0s
*    rftn *       373.0       373.0       373.0       363.0s
*    rftn *       353.0       343.0       333.0       323.0s
*    rftn *       313.0       303.0       373.0       373.0s
*    rftn *       373.0       373.0       363.0       353.0s
*    rftn *       343.0       333.0       323.0       313.0s
*    rftn *       303.0       373.0       373.0       373.0s
*    rftn *       373.0       363.0       353.0       343.0s
*    rftn *       333.0       323.0       313.0       303.0s
*    rftn *       373.0       373.0       373.0       373.0s
*    rftn *       363.0       353.0       343.0       333.0s
*    rftn *       323.0       313.0       303.0       373.0s
*    rftn *       373.0       373.0       373.0       363.0s
*    rftn *       353.0       343.0       333.0       323.0s
*    rftn *       313.0       303.0       373.0       373.0s
*    rftn *       373.0       373.0       363.0       353.0s
*    rftn *       343.0       333.0       323.0       313.0s
*    rftn *       303.0e
*
*******   type           num        userid                component name
```

```
htstr                   121            1                        unnamed
*       nzhstr          ittc         hscyl          ichf
              6             0             1             1
*    nofuelrod         plane        liqlev        iaxcnd         pdrat
              1             3             1             0           0.0
*        nmwrx          nfci         nfcil          hdri          hdro
              0             0             1           0.0           0.0
*         nhot         nodes          fmon         nzmax       reflood
              0             6             0           100             0
*     dtxht(1)      dtxht(2)         dznht         hgapo
            0.0           0.0        1.0E-3        6300.0
*
*  idbcin *           2           2           2           2s
*  idbcin *           2           2e
*  idbcon *           5           5           5           5s
*  idbcon *           5           5e
* hcomon1 *         111           1           0           0e
* hcomon1 *         111           2           0           0e
* hcomon1 *         111           3           0           0e
* hcomon1 *         111           4           0           0e
* hcomon1 *         111           5           0           0e
* hcomon1 *         111           6           0           0e
* tsurfo2 *       293.0e
* tsurfo2 *       293.0e
* tsurfo2 *       293.0e
* tsurfo2 *       293.0e
* tsurfo2 *       293.0e
* tsurfo2 *       293.0e
* dhtstrz *     0.10525     0.10525     0.10525     0.10525s
* dhtstrz *     0.10525     0.10525e
*   rdx   *          1.0e
*  radrd  *    3.175E-3   3.5052E-3   3.8354E-3   4.1656E-3   4.4958E-3s
*  radrd  *    4.826E-3e
*  matrd  *          50          50          50          50 s
*  matrd  *          50 e
*    nfax *           1           1           1           1s
*    nfax *           1           1e
*    rftn *       378.0       378.0       378.0       378.0s
*    rftn *       378.0       378.0       378.0       378.0s
*    rftn *       378.0       378.0       378.0       378.0s
*    rftn *       378.0       378.0       378.0       378.0s
*    rftn *       378.0       378.0       378.0       378.0s
*    rftn *       378.0       378.0       378.0       378.0s
*    rftn *       378.0       378.0       378.0       378.0s
*    rftn *       378.0       378.0       378.0       378.0s
*
*******   type           num        userid                component name
htstr                   122            1                        unnamed
*       nzhstr          ittc         hscyl          ichf
              6             0             1             1
*    nofuelrod         plane        liqlev        iaxcnd         pdrat
              1             3             1             0           0.0
*        nmwrx          nfci         nfcil          hdri          hdro
              0             0             1           0.0           0.0
*         nhot         nodes          fmon         nzmax       reflood
              0             6             0           100             0
*     dtxht(1)      dtxht(2)         dznht         hgapo
            0.0           0.0        1.0E-3        6300.0
*
*  idbcin *           2           2           2           2s
*  idbcin *           2           2e
*  idbcon *           5           5           5           5s
*  idbcon *           5           5e
* hcomon1 *         112           1           0           0e
* hcomon1 *         112           2           0           0e
* hcomon1 *         112           3           0           0e
* hcomon1 *         112           4           0           0e
* hcomon1 *         112           5           0           0e
* hcomon1 *         112           6           0           0e
* tsurfo2 *       293.0e
```

```
* tsurfo2 *       293.0e
* tsurfo2 *       293.0e
* tsurfo2 *       293.0e
* tsurfo2 *       293.0e
* tsurfo2 *       293.0e
* dhtstrz *   0.0894667   0.0894667   0.0894667   0.0894667s
* dhtstrz *   0.0894667   0.0894667e
*   rdx   *         1.0e
*  radrd  *    3.175E-3   3.5052E-3   3.8354E-3   4.1656E-3   4.4958E-3s
*  radrd  *    4.826E-3e
*  matrd  *          50          50          50          50 s
*  matrd  *          50 e
*    nfax *           1           1           1           1s
*    nfax *           1           1e
*    rftn *       373.0       373.0       373.0       373.0s
*    rftn *       373.0       373.0       373.0       373.0s
*    rftn *       373.0       373.0       373.0       373.0s
*    rftn *       373.0       373.0       373.0       373.0s
*    rftn *       373.0       373.0       373.0       373.0s
*    rftn *       373.0       373.0       373.0       373.0s
*    rftn *       373.0       373.0       373.0       373.0s
*    rftn *       373.0       373.0       373.0       373.0e
*
*******   type           num        userid                component name
htstr                    132             1                        unnamed
*       nzhstr          ittc         hscyl          ichf
              3             0             1             1
*    nofuelrod         plane        liqlev        iaxcnd         pdrat
              1             3             1             0           0.0
*        nmwrx          nfci         nfcil          hdri          hdro
              0             0             1           0.0           0.0
*         nhot         nodes          fmon         nzmax       reflood
              0            10             0           100             0
*     dtxht(1)      dtxht(2)         dznht         hgapo
            0.0           0.0        1.0E-3        6300.0
*
*  idbcin *           2           2           2e
*  idbcon *           5           5           5e
* hcomon1 *          31           1           0           0e
* hcomon1 *          31           2           0           0e
* hcomon1 *          31           3           0           0e
* tsurfo2 *       293.0e
* tsurfo2 *       293.0e
* tsurfo2 *       293.0e
* dhtstrz *      0.6196      0.6196      0.6196e
*   rdx   *         1.0e
*  radrd  *      0.0127 0.013205178 0.013710356 0.014215533 0.014720711s
*  radrd  * 0.015225889 0.015731067 0.016236244 0.016741422   0.0172466e
*  matrd  *          51          51          51          51 s
*  matrd  *          51          51          51          51 s
*  matrd  *          51 e
*    nfax *           1           1           1e
*    rftn *       293.0       293.0       293.0       293.0s
*    rftn *       293.0       293.0       293.0       293.0s
*    rftn *       293.0       293.0       293.0       293.0s
*    rftn *       293.0       293.0       293.0       293.0s
*    rftn *       293.0       293.0       293.0       293.0s
*    rftn *       293.0       293.0       293.0       293.0s
*    rftn *       293.0       293.0       293.0       293.0s
*    rftn *       293.0       293.0e
*
*******   type           num        userid                component name
htstr                    141             1                        unnamed
*       nzhstr          ittc         hscyl          ichf
              3             0             1             1
*    nofuelrod         plane        liqlev        iaxcnd         pdrat
              1             3             1             0           0.0
*        nmwrx          nfci         nfcil          hdri          hdro
              0             0             1           0.0           0.0
*         nhot         nodes          fmon         nzmax       reflood
```

```
            0            10             0           100             0
*     dtxht(1)      dtxht(2)         dznht         hgapo
          0.0           0.0        1.0E-3        6300.0
*
*  idbcin *           2           2           2e
*  idbcon *           2           2           2e
* hcomon1 *          21           1           0           0e
* hcomon1 *          21           2           0           0e
* hcomon1 *          21           3           0           0e
* hcomon2 *          31           1           0           0e
* hcomon2 *          31           2           0           0e
* hcomon2 *          31           3           0           0e
* dhtstrz *      0.6196      0.6196      0.6196e
*   rdx   *          1.0e
*  radrd  *    3.175E-3  3.35844E-3  3.54189E-3  3.72533E-3  3.90878E-3s
*  radrd  *  4.09222E-3  4.27567E-3  4.45911E-3  4.64256E-3    4.826E-3e
*  matrd  *          50          50          50          50 s
*  matrd  *          50          50          50          50 s
*  matrd  *          50 e
*    nfax *           1           1           1e
*    rftn *       293.0       293.0       293.0       293.0s
*    rftn *       293.0       293.0       293.0       293.0s
*    rftn *       293.0       293.0       293.0       293.0s
*    rftn *       293.0       293.0       293.0       293.0s
*    rftn *       293.0       293.0       293.0       293.0s
*    rftn *       293.0       293.0       293.0       293.0s
*    rftn *       293.0       293.0       293.0       293.0s
*    rftn *       293.0       293.0e
*
*******   type          num        userid                component name
htstr                   161             1                         unnamed
*       nzhstr          ittc         hscyl          ichf
              3             0             1             1
*    nofuelrod         plane        liqlev        iaxcnd         pdrat
              1             3             1             0           0.0
*        nmwrx          nfci         nfcil          hdri          hdro
              0             0             1           0.0           0.0
*         nhot         nodes          fmon         nzmax       reflood
              0            11             0           100             0
*     dtxht(1)      dtxht(2)         dznht         hgapo
          0.0           0.0        1.0E-3        6300.0
*
*  idbcin *           2           2           2e
*  idbcon *           5           5           5e
* hcomon1 *          11           1           0           0e
* hcomon1 *          11           2           0           0e
* hcomon1 *          11           3           0           0e
* tsurfo2 *       293.0e
* tsurfo2 *       293.0e
* tsurfo2 *       293.0e
* dhtstrz *  0.58709091  0.58709091  0.58709091e
*   rdx   *          1.0e
*  radrd  *    0.038965    0.043325      0.0445    0.052045    0.056405s
*  radrd  *    0.060765    0.065125    0.069485    0.073845    0.078205s
*  radrd  *    0.082565e
*  matrd  *           9           9          52          52 s
*  matrd  *          52          52          52          52 s
*  matrd  *          52          52 e
*    nfax *           1           1           1e
*    rftn *       378.0       378.0       378.0       368.0s
*    rftn *       358.0       348.0       338.0       328.0s
*    rftn *       318.0       308.0       298.0       378.0s
*    rftn *       378.0       378.0       368.0       358.0s
*    rftn *       348.0       338.0       328.0       318.0s
*    rftn *       308.0       298.0       378.0       378.0s
*    rftn *       378.0       368.0       358.0       348.0s
*    rftn *       338.0       328.0       318.0       308.0s
*    rftn *       298.0e
****************************************
* Finished Heat Structure Section of Model *
****************************************
```

```
*
*
*
end
*
*****************
* Timestep Data *
*****************
*        dtmin         dtmax          tend         rtwfp
        1.0E-6           1.0        7000.0          10.0
*        edint         gfint        dmpint        sedint
         100.0           1.0         100.0           1.0
*
*      endflag
          -1.0
```

Final Model Input Deck – Axial Nodes Only

```
*
*
*************
* main data *
*************
*
*       numtcr          ieos         inopt          nmat          id2o
            1             0             1             3             0

*
*
*****************
* namelist data *
*****************
*
 &inopts
  dtstrt=1.0,
  ikfac=1,
  ioinp=0,
  noair=0,
  usesjc=3,
  nhtstr=9
 &end
*
***************
* Model Flags *
***************
*
*        dstep         timet
            0           0.0
*       stdyst        transi         ncomp          njun          ipak
            0             1            19             8             1
*         epso          epss
          1.0E-4        1.0E-4
*       oitmax        sitmax        isolut        ncontr         nccfl
           10            10             0             0             0
*         ntsv          ntcb          ntcf          ntrp          ntcp
           12             1             0             0             0
*
************************
* component-number data *
************************
*
*  Component input order (IORDER)
*-- type ---- num ------------ name ----------------  +    jun1   jun2   jun3
* PIPE     *     11 s * Boiler                         +      27      0
* PIPE     *     21 s * CCDPHE Primary                 +      28     29
* PIPE     *     31 s * CCDPHE Secondary               +      31      1
* VESSEL   *     41 s *                                +
* FILL     *     51 s * Hose Inlet                     +       1
* BREAK    *     61 s * Hose Outlet                    +      31
* HTSTR    *    101 s *                                +
* PIPE     *    111 s * Lower BOP                      +      27     28
* PIPE     *    112 s * Upper BOP                      +      26     23
* HTSTR    *    121 s *                                +
* HTSTR    *    122 s *                                +
* PIPE     *    131 s * Nozzle                         +      23     32
* HTSTR    *    132 s *                                +
* HTSTR    *    141 s *                                +
* VALVE    *    151 s *                                +      29     26
* HTSTR    *    161 s *                                +
* HTSTR    *    171 s *                                +
* HTSTR    *    181 s *                                +
* HTSTR    *    191 e *                                +
*
**********************
* material properties *
**********************
```

```
*
*   matb*          50          51          52 e
*  ptbln*           1           1           1 e
*  User Defined Material : 50
*
*n: Copper Alloy
*
*d: Copper Alloy
*  prptb         temp         rho          cp        cond        emis
*  prptb*       293.0      8940.6       385.0       394.0         0.0 e
*
*  User Defined Material : 51
*
*n: PVC
*
*  prptb         temp         rho          cp        cond        emis
*  prptb*       293.0      1390.0       900.0        0.16         0.0 e
*
*  User Defined Material : 52
*
*n: Insulation
*
*  prptb         temp         rho          cp        cond        emis
*  prptb*       293.0    48.05539       670.0 0.033172414         0.0 e
*
*
*
************************************************
* Starting Signal Variable Section of Model      *
************************************************
*n: Boiler Pressure
*
*         idsv          isvn          ilcn          icn1          icn2
             1            21            11             3             0
*n: BC21
*
*         idsv          isvn          ilcn          icn1          icn2
            13            23            11             3             0
*n: BC11
*
*         idsv          isvn          ilcn          icn1          icn2
            14            23            11             2             0
*n: BC01
*
*         idsv          isvn          ilcn          icn1          icn2
            15            23            11             1             0
*n: Primary Inlet
*
*         idsv          isvn          ilcn          icn1          icn2
            16            23            51             1             0
*n: Primary Outlet
*
*         idsv          isvn          ilcn          icn1          icn2
            17            23            61             1             0
*n: Condenser Pressure
*
*         idsv          isvn          ilcn          icn1          icn2
            24            21            41          1011             0
*n: Boiler Inventory
*
*d: FlashLevel
*         idsv          isvn          ilcn          icn1          icn2
            25           124            11             0             0
*n: Boiler Initial Inventory
*
*d: FlashIntLevel
*         idsv          isvn          ilcn          icn1          icn2
            26           125            11             0             0
*n: Condenser Initial Inventory
*
*d: CondeIntLevel
```

```
*         idsv          isvn          ilcn          icn1          icn2
            27           125             0             0             0
*n: Condenser Inventory
*
*d: CondeLevel
*         idsv          isvn          ilcn          icn1          icn2
            28           124             0             0             0
*n: Timer
*
*         idsv          isvn          ilcn          icn1          icn2
            30             0             0             0             0
************************************************
* Finished Signal Variable Section of Model      *
************************************************
*
*
*
*
*****************************************
* Starting Control System Section of Model  *
*****************************************
*
****** Control Blocks ******
*n: PressDif
*
*d: PressDif
*         idcb          icbn          icb1          icb2          icb3
            -1            44             1            24             0
*       cbgain        cbxmin         cbmax        cbcon1        cbcon2
           1.0       -1.0E20        1.0E20           0.0           0.0
*
*****************************************
* Finished Control System Section of Model  *
*****************************************
*
*
*
*
*******   type           num        userid                component name
pipe                      11             0                        Boiler
*       ncells         nodes          jun1          jun2          epsw
             3             0            27             0           0.0
*       nsides
             0
*         ichf         iconc      pipetype          ipow        npipes
             1             0             0             0             1
*        radin            th         houtl         houtv         toutl
           0.0           0.0           0.0           0.0           0.0
*        toutv          pwin         pwoff         rpwmx         pwscl
           0.0           0.0           0.0           0.0           0.0
* dx    *    2.1333333   2.1333333   2.1333333e
* vol   *   9.72878E-3  9.72878E-3  9.72878E-3e
* fa    *   3.16692E-5  4.56037E-3  4.56037E-3  4.56037E-3e
* kfac  *         0.49         0.0         0.0         0.0e
* grav  *          1.0         1.0         1.0         1.0e
* hd    *      6.35E-3      0.0762      0.0762      0.0762e
* nff   *            1           1           1           1e
* alp   *          0.0         0.0         0.0e
* vl    *          0.0         0.0         0.0         0.0e
* vv    *          0.0         0.0         0.0         0.0e
* tl    *      378.149     378.149     378.149e
* tv    *      378.149     378.149     378.149e
* p     *      1.209E5     1.209E5     1.209E5e
* pa    *          0.0         0.0         0.0e
*
*
*******   type           num        userid                component name
pipe                      21             0                 CCDPHE Primary
*       ncells         nodes          jun1          jun2          epsw
             3             0            28            29           0.0
*       nsides
```

```
            0
*         ichf          iconc      pipetype          ipow        npipes
             1              0             0             0             1
*        radin            th         houtl         houtv         toutl
           0.0           0.0           0.0           0.0           0.0
*        toutv          pwin         pwoff         rpwmx         pwscl
           0.0           0.0           0.0           0.0           0.0
* dx    *    2.1333333   2.1333333   2.1333333e
* vol   *    6.7561E-5   6.7561E-5   6.7561E-5e
* fa    *   3.16692E-5  3.16692E-5  3.16692E-5  3.16692E-5e
* kfac  *          0.0         0.0         0.0         0.0e
* grav  *          1.0         1.0         1.0         1.0e
* hd    *      6.35E-3     6.35E-3     6.35E-3     6.35E-3e
* nff   *            1           1           1           1e
* alp   *          1.0         1.0         1.0e
* vl    *          0.0         0.0         0.0         0.0e
* vv    *          0.0         0.0         0.0         0.0e
* tl    *        293.0       293.0       293.0e
* tv    *        293.0       293.0       293.0e
* p     *      1.209E5     1.209E5     1.209E5e
* pa    *     101300.0    101300.0    101300.0e
*
*
*******   type           num        userid               component name
pipe                      31             0               CCDPHE Secondary
*       ncells         nodes          jun1          jun2          epsw
             3             0            31             1           0.0
*       nsides
             0
*         ichf          iconc      pipetype          ipow        npipes
             1              0             0             0             1
*        radin            th         houtl         houtv         toutl
           0.0           0.0           0.0           0.0           0.0
*        toutv          pwin         pwoff         rpwmx         pwscl
           0.0           0.0           0.0           0.0           0.0
* dx    *    2.1333333   2.1333333   2.1333333e
* vol   *   9.72878E-3  9.72878E-3  9.72878E-3e
* fa    *   5.06451E-4  5.06451E-4  5.06451E-4  5.06451E-4e
* kfac  *          0.0         0.0         0.0         0.0e
* grav  *          1.0         1.0         1.0         1.0e
* hd    *       0.0762      0.0762      0.0762      0.0762e
* nff   *            1           1           1           1e
* alp   *          0.0         0.0         0.0e
* vl    *          0.0         0.0         0.0         0.0e
* vv    *          0.0         0.0         0.0         0.0e
* tl    *        293.0       293.0       293.0e
* tv    *        293.0       293.0       293.0e
* p     *      1.013E5     1.013E5     1.013E5e
* pa    *          0.0         0.0         0.0e
*
*
*******   type           num        userid                   component name
vessel                    41             0                          unnamed
*         nasx          nrsx          ntsx          ncsr        ivssbf
            11             1             1             1             0
*         idcu          idcl          idcr          icru          icrl
             0             0             0             0             0
*         icrr         ilcsp         iucsp          iuhp         iconc
             0             0             0             0             0
*        igeom         nvent         nvvtb        nsgrid     vesstype
             0             0             0             0             0
*        shelv          epsw
           0.0           0.0
*   z    *  0.58181818   1.1636364   1.7454545   2.3272727s
*   z    *   2.9090909   3.4909091   4.0727273   4.6545455s
*   z    *   5.2363636   5.8181818         6.4e
*   r    *      0.0381e
*   t    *       360.0e
*         lisrl         lisrc         lisrf         ljuns          zfrac
            11             1             2            32
* level 1
```

```
*
*  cfzlyt *         0.0e
*  cfzlz  *         0.0e
*  cfzlxr *         0.0e
*  cfzvyt *         0.0e
*  cfzvz  *         0.0e
*  cfzvxr *         0.0e
*   frvol *         1.0e
*  frfayt *         1.0e
*  frfaz  *         1.0e
*  frfaxr *         0.5e
*    hdyt *      0.0381e
*    hdz  *     4.56E-3e
*    hdxr *     4.56E-3e
*   alpn  *         0.0e
*   vvnyt *         0.0e
*   vvnz  *         0.0e
*   vvnxr *         0.0e
*   vlnyt *         0.0e
*   vlnz  *         0.0e
*   vlnxr *         0.0e
*     tvn *     373.117e
*     tln *     373.117e
*      pn *     1.013E5e
*     pan *         0.0e
* level 2
*
*  cfzlyt *         0.0e
*  cfzlz  *         0.0e
*  cfzlxr *         0.0e
*  cfzvyt *         0.0e
*  cfzvz  *         0.0e
*  cfzvxr *         0.0e
*   frvol *         1.0e
*  frfayt *         1.0e
*  frfaz  *         1.0e
*  frfaxr *         0.5e
*    hdyt *      0.0381e
*    hdz  *     4.56E-3e
*    hdxr *     4.56E-3e
*   alpn  *        0.65e
*   vvnyt *         0.0e
*   vvnz  *         0.0e
*   vvnxr *         0.0e
*   vlnyt *         0.0e
*   vlnz  *         0.0e
*   vlnxr *         0.0e
*     tvn *     373.117e
*     tln *     373.117e
*      pn *     1.013E5e
*     pan *         0.0e
* level 3
*
*  cfzlyt *         0.0e
*  cfzlz  *         0.0e
*  cfzlxr *         0.0e
*  cfzvyt *         0.0e
*  cfzvz  *         0.0e
*  cfzvxr *         0.0e
*   frvol *         1.0e
*  frfayt *         1.0e
*  frfaz  *         1.0e
*  frfaxr *         0.5e
*    hdyt *      0.0381e
*    hdz  *     4.56E-3e
*    hdxr *     4.56E-3e
*   alpn  *         1.0e
*   vvnyt *         0.0e
*   vvnz  *         0.0e
*   vvnxr *         0.0e
*   vlnyt *         0.0e
```

```
*   vlnz  *         0.0e
*   vlnxr *         0.0e
*     tvn *     373.117e
*     tln *     373.117e
*      pn *     1.013E5e
*     pan *         0.0e
* level 4
*
*  cfzlyt *         0.0e
*  cfzlz  *         0.0e
*  cfzlxr *         0.0e
*  cfzvyt *         0.0e
*  cfzvz  *         0.0e
*  cfzvxr *         0.0e
*   frvol *         1.0e
*  frfayt *         1.0e
*  frfaz  *         1.0e
*  frfaxr *         0.5e
*    hdyt *      0.0381e
*    hdz  *     4.56E-3e
*    hdxr *     4.56E-3e
*   alpn  *         1.0e
*   vvnyt *         0.0e
*   vvnz  *         0.0e
*   vvnxr *         0.0e
*   vlnyt *         0.0e
*   vlnz  *         0.0e
*   vlnxr *         0.0e
*     tvn *     373.117e
*     tln *     373.117e
*      pn *     1.013E5e
*     pan *         0.0e
* level 5
*
*  cfzlyt *         0.0e
*  cfzlz  *         0.0e
*  cfzlxr *         0.0e
*  cfzvyt *         0.0e
*  cfzvz  *         0.0e
*  cfzvxr *         0.0e
*   frvol *         1.0e
*  frfayt *         1.0e
*  frfaz  *         1.0e
*  frfaxr *         0.5e
*    hdyt *      0.0381e
*    hdz  *     4.56E-3e
*    hdxr *     4.56E-3e
*   alpn  *         1.0e
*   vvnyt *         0.0e
*   vvnz  *         0.0e
*   vvnxr *         0.0e
*   vlnyt *         0.0e
*   vlnz  *         0.0e
*   vlnxr *         0.0e
*     tvn *     373.117e
*     tln *     373.117e
*      pn *     1.013E5e
*     pan *         0.0e
* level 6
*
*  cfzlyt *         0.0e
*  cfzlz  *         0.0e
*  cfzlxr *         0.0e
*  cfzvyt *         0.0e
*  cfzvz  *         0.0e
*  cfzvxr *         0.0e
*   frvol *         1.0e
*  frfayt *         1.0e
*  frfaz  *         1.0e
*  frfaxr *         0.5e
*    hdyt *      0.0381e
```

```
*    hdz  *     4.56E-3e
*    hdxr *     4.56E-3e
*   alpn  *         1.0e
*   vvnyt *         0.0e
*   vvnz  *         0.0e
*   vvnxr *         0.0e
*   vlnyt *         0.0e
*   vlnz  *         0.0e
*   vlnxr *         0.0e
*     tvn *     373.117e
*     tln *     373.117e
*      pn *     1.013E5e
*     pan *         0.0e
* level 7
*
*  cfzlyt *         0.0e
*  cfzlz  *         0.0e
*  cfzlxr *         0.0e
*  cfzvyt *         0.0e
*  cfzvz  *         0.0e
*  cfzvxr *         0.0e
*   frvol *         1.0e
*  frfayt *         1.0e
*  frfaz  *         1.0e
*  frfaxr *         0.5e
*    hdyt *      0.0381e
*    hdz  *     4.56E-3e
*    hdxr *     4.56E-3e
*   alpn  *         1.0e
*   vvnyt *         0.0e
*   vvnz  *         0.0e
*   vvnxr *         0.0e
*   vlnyt *         0.0e
*   vlnz  *         0.0e
*   vlnxr *         0.0e
*     tvn *     373.117e
*     tln *     373.117e
*      pn *     1.013E5e
*     pan *         0.0e
* level 8
*
*  cfzlyt *         0.0e
*  cfzlz  *         0.0e
*  cfzlxr *         0.0e
*  cfzvyt *         0.0e
*  cfzvz  *         0.0e
*  cfzvxr *         0.0e
*   frvol *         1.0e
*  frfayt *         1.0e
*  frfaz  *         1.0e
*  frfaxr *         0.5e
*    hdyt *      0.0381e
*    hdz  *     4.56E-3e
*    hdxr *     4.56E-3e
*   alpn  *         1.0e
*   vvnyt *         0.0e
*   vvnz  *         0.0e
*   vvnxr *         0.0e
*   vlnyt *         0.0e
*   vlnz  *         0.0e
*   vlnxr *         0.0e
*     tvn *     373.117e
*     tln *     373.117e
*      pn *     1.013E5e
*     pan *         0.0e
* level 9
*
*  cfzlyt *         0.0e
*  cfzlz  *         0.0e
*  cfzlxr *         0.0e
*  cfzvyt *         0.0e
```

```
*  cfzvz  *         0.0e
*  cfzvxr *         0.0e
*   frvol *         1.0e
*  frfayt *         1.0e
*  frfaz  *         1.0e
*  frfaxr *         0.5e
*    hdyt *      0.0381e
*    hdz  *     4.56E-3e
*    hdxr *     4.56E-3e
*   alpn  *         1.0e
*   vvnyt *         0.0e
*   vvnz  *         0.0e
*   vvnxr *         0.0e
*   vlnyt *         0.0e
*   vlnz  *         0.0e
*   vlnxr *         0.0e
*     tvn *     373.117e
*     tln *     373.117e
*      pn *     1.013E5e
*     pan *         0.0e
* level 10
*
*  cfzlyt *         0.0e
*  cfzlz  *         0.0e
*  cfzlxr *         0.0e
*  cfzvyt *         0.0e
*  cfzvz  *         0.0e
*  cfzvxr *         0.0e
*   frvol *         1.0e
*  frfayt *         1.0e
*  frfaz  *         1.0e
*  frfaxr *         0.5e
*    hdyt *      0.0381e
*    hdz  *     4.56E-3e
*    hdxr *     4.56E-3e
*   alpn  *         1.0e
*   vvnyt *         0.0e
*   vvnz  *         0.0e
*   vvnxr *         0.0e
*   vlnyt *         0.0e
*   vlnz  *         0.0e
*   vlnxr *         0.0e
*     tvn *     373.117e
*     tln *     373.117e
*      pn *     1.013E5e
*     pan *         0.0e
* level 11
*
*  cfzlyt *         0.0e
*  cfzlz  *    -1.0E-20e
*  cfzlxr *         0.0e
*  cfzvyt *         0.0e
*  cfzvz  *         0.0e
*  cfzvxr *         0.0e
*   frvol *         1.0e
*  frfayt *         1.0e
*  frfaz  *         1.0e
*  frfaxr *         0.5e
*    hdyt *      0.0381e
*    hdz  *    -4.56E-3e
*    hdxr *     4.56E-3e
*   alpn  *         1.0e
*   vvnyt *         0.0e
*   vvnz  *         0.0e
*   vvnxr *         0.0e
*   vlnyt *         0.0e
*   vlnz  *         0.0e
*   vlnxr *         0.0e
*     tvn *     373.117e
*     tln *     373.117e
*      pn *     1.013E5e
```

```
*     pan *         0.0e
*
*
*d: Hose Inlet
*******   type           num        userid                component name
fill                      51             0                     Hose Inlet
*         jun1          ifty          ioff
             1             2             0
*        twtold          rfmx        concin          felv
           0.0         1.0E20           0.0           0.0
*          dxin          volin         alpin          vlin          tlin
           0.1    5.064506E-4           0.0           0.0         293.0
*           pin          pain        flowin          vvin          tvin
       1.013E5           0.0       0.62957           0.0         293.0
*
*
*d: Hose Outlet
*******   type           num        userid                component name
break                     61             0                    Hose Outlet
*         jun1          ibty          isat          ioff      adjpress
            31             0             0             1             0
*          dxin          volin         alpin          tin           pin
           0.1    5.064506E-4           0.0         293.0       1.013E5
*         pain         concin          rbmx          poff          belv
           0.0           0.0        1.0E20           0.0           0.0
*
*
*******   type           num        userid                component name
pipe                      111             0                     Lower BOP
*        ncells         nodes          jun1          jun2          epsw
             6             0            27            28           0.0
*        nsides
             0
*          ichf         iconc      pipetype          ipow        npipes
             1             0             0             0             1
*         radin            th         houtl         houtv         toutl
           0.0           0.0           0.0           0.0           0.0
*         toutv          pwin         pwoff         rpwmx         pwscl
           0.0           0.0           0.0           0.0           0.0
* dx    *      0.10525     0.10525     0.10525     0.10525s
* dx    *      0.10525     0.10525e
* vol   *   3.33319E-6  3.33319E-6  3.33319E-6  3.33319E-6s
* vol   *   3.33319E-6  3.33319E-6e
* fa    *   3.16692E-5  3.16692E-5  3.16692E-5  3.16692E-5s
* fa    *   3.16692E-5  3.16692E-5  3.16692E-5e
* kfac  *         0.49         0.0         0.0         0.0s
* kfac  *          0.0         0.0         0.0e
* grav  *         -1.0 -0.70682518         0.0         0.0s
* grav  *   0.70710678         1.0         1.0e
* hd    *      6.35E-3     6.35E-3     6.35E-3     6.35E-3s
* hd    *      6.35E-3     6.35E-3     6.35E-3e
* nff   *            1           1           1           1s
* nff   *            1           1           1e
* alp   *          0.0         0.0         0.0         0.0s
* alp   *          0.0         0.0e
* vl    *          0.0         0.0         0.0         0.0s
* vl    *          0.0         0.0         0.0e
* vv    *          0.0         0.0         0.0         0.0s
* vv    *          0.0         0.0         0.0e
* tl    *        378.0       378.0       378.0       378.0s
* tl    *        378.0       378.0e
* tv    *      378.149     378.149     378.149     378.149s
* tv    *      378.149     378.149e
* p     *      1.209E5     1.209E5     1.209E5     1.209E5s
* p     *      1.209E5     1.209E5e
* pa    *          0.0         0.0         0.0         0.0s
* pa    *          0.0         0.0e
*
*
*******   type           num        userid                component name
pipe                      112             0                     Upper BOP
```

```
*       ncells         nodes          jun1          jun2          epsw
             6             0            26            23           0.0
*       nsides
             0
*         ichf         iconc      pipetype          ipow        npipes
             1             0             0             0             1
*        radin           th          houtl         houtv         toutl
           0.0          0.0           0.0           0.0           0.0
*        toutv          pwin         pwoff         rpwmx         pwscl
           0.0          0.0           0.0           0.0           0.0
* dx    *    0.0894667   0.0894667   0.0894667   0.0894667s
* dx    *    0.0894667   0.0894667e
* vol   *   2.83334E-6  2.83334E-6  2.83334E-6  2.83334E-6s
* vol   *   2.83334E-6  2.83334E-6e
* fa    *   3.16692E-5  3.16692E-5  3.16692E-5  3.16692E-5s
* fa    *   3.16692E-5  3.16692E-5  2.63022E-6e
* kfac  *          0.0         0.0         0.0         0.0s
* kfac  *          0.0         0.0        3.42e
* grav  *          1.0         1.0         1.0         0.0s
* grav  *          0.0        -1.0        -1.0e
* hd    *      6.35E-3     6.35E-3     6.35E-3     6.35E-3s
* hd    *      6.35E-3     6.35E-3     1.83E-3e
* nff   *            1           1           1           1s
* nff   *            1           1          1e
* alp   *          1.0         1.0         1.0         1.0s
* alp   *          1.0         1.0e
* vl    *          0.0         0.0         0.0         0.0s
* vl    *          0.0         0.0         0.0e
* vv    *          0.0         0.0         0.0         0.0s
* vv    *          0.0         0.0         0.0e
* tl    *        293.0       293.0       293.0       293.0s
* tl    *        293.0       293.0e
* tv    *        293.0       293.0       293.0       293.0s
* tv    *        293.0       293.0e
* p     *      1.013E5     1.013E5     1.013E5     1.013E5s
* p     *      1.013E5     1.013E5e
* pa    *          0.0         0.0         0.0         0.0s
* pa    *          0.0         0.0e
*
*
*d: Nozzle
* single junction
*******   type           num        userid                component name
pipe                     131             0                        Nozzle
*       ncells         nodes          jun1          jun2          epsw
             0             0            23            32           0.0
*         ichf         iconc      pipetype          ipow        npipes
             1             0             0             0             1
*        radin           th          houtl         houtv         toutl
           0.0          0.0           0.0           0.0           0.0
*        toutv          pwin         pwoff         rpwmx         pwscl
           0.0          0.0           0.0           0.0           0.0
* dx    *    f 0.0000e+00e
* vol   *    f 0.0000e+00e
* fa    *  f   2.63022E-6e
* kfac  *  f         3.42e
* grav  *  f         -1.0e
* hd    *  f      1.83E-3e
* nff   *  f            1e
* alp   *    f 0.0000e+00e
* vl    *  f          0.0e
* vv    *  f          0.0e
* tl    *    f 0.0000e+00e
* tv    *    f 0.0000e+00e
* p     *    f 0.0000e+00e
* pa    *    f 0.0000e+00e
*
*
*******   type           num        userid                component name
valve                    151             0                        unnamed
*       ncells         nodes         jun1         jun2         epsw
```

```
            0             0          29          26         0.0
*         ichf          iconc         ivty        ivps        nvtb2
            1             0           1           1           0
*         ivtr          ivsv        nvtb1        nvsv         nvrf
            0            30           6           0           0
*       ivtrov        ivtyov       ivtrlo   intlossoff       nkopen
            0             0           0           0           2
*         rvmx          rvov       fminov       fmaxov
          100.0           0.0         0.0         1.0
*        radin            th        houtl        houtv        toutl
            0.0           0.0         0.0         0.0         0.0
*        toutv         avlve        hvlve       favlve         xpos
            0.0   3.166922E-5      6.35E-3          0.0          0.0
* dx    *    f 0.0000e+00e
* vol   *    f 0.0000e+00e
* fa    *  f   3.16692E-5e
* kfac  *  f          0.0e
* grav  *  f          1.0e
* hd    *  f      6.35E-3e
* nff   *  f           1e
* alp   *    f 0.0000e+00e
* vl    *  f          0.0e
* vv    *  f          0.0e
* tl    *    f 0.0000e+00e
* tv    *    f 0.0000e+00e
* p     *    f 0.0000e+00e
* pa    *    f 0.0000e+00e
* vtb1  *         0.0         0.0s
* vtb1  *         1.0         0.0s
* vtb1  *         2.0         0.0s
* vtb1  *         3.0         0.0s
* vtb1  *         4.0         0.0s
* vtb1  *         5.0         1.0e
*
*
*****************************************
* Starting Heat Structure Section of Model *
*****************************************
*
*******   type           num        userid                component name
htstr                    101             1                       unnamed
*       nzhstr          ittc         hscyl         ichf
             11             0             1            1
*    nofuelrod         plane        liqlev        iaxcnd         pdrat
             1              3             1             0           0.0
*        nmwrx          nfci         nfcil         hdri          hdro
             0              0             1          0.0           0.0
*         nhot         nodes          fmon        nzmax       reflood
             0             11             0          210             0
*     dtxht(1)      dtxht(2)        dznht        hgapo
            0.0            0.0       1.0E-3       6300.0
*
*  idbcin *           2           2           2           2s
*  idbcin *           2           2           2           2s
*  idbcin *           2           2           2e
*  idbcon *           5           5           5           5s
*  idbcon *           5           5           5           5s
*  idbcon *           5           5           5e
* hcomon1 *          41           1           1           1e
* hcomon1 *          41           1           1           2e
* hcomon1 *          41           1           1           3e
* hcomon1 *          41           1           1           4e
* hcomon1 *          41           1           1           5e
* hcomon1 *          41           1           1           6e
* hcomon1 *          41           1           1           7e
* hcomon1 *          41           1           1           8e
* hcomon1 *          41           1           1           9e
* hcomon1 *          41           1           1          10e
* hcomon1 *          41           1           1          11e
* tsurfo2 *       293.0e
* tsurfo2 *       293.0e
```

```
* tsurfo2 *       293.0e
* tsurfo2 *       293.0e
* tsurfo2 *       293.0e
* tsurfo2 *       293.0e
* tsurfo2 *       293.0e
* tsurfo2 *       293.0e
* tsurfo2 *       293.0e
* tsurfo2 *       293.0e
* tsurfo2 *       293.0e
* dhtstrz *  0.39315152  0.19393939  0.39315152  0.19393939s
* dhtstrz *  0.39315152  0.19393939  0.39315152  0.19393939s
* dhtstrz *  0.39315152  0.19393939  0.39315152e
*   rdx   *          0.5e
*  radrd  *    0.038965 0.039222676 0.039265404    0.052045    0.056405s
*  radrd  *    0.060765    0.065125    0.069485    0.073845    0.078205s
*  radrd  *    0.082565e
*  matrd  *           9           9          52          52 s
*  matrd  *          52          52          52          52 s
*  matrd  *          52          52 e
*    nfax *           1           1           1           1s
*    nfax *           1           1           1           1s
*    nfax *           1           1           1e
*    rftn *       373.0       373.0       373.0       373.0s
*    rftn *       363.0       353.0       343.0       333.0s
*    rftn *       323.0       313.0       303.0       373.0s
*    rftn *       373.0       373.0       373.0       363.0s
*    rftn *       353.0       343.0       333.0       323.0s
*    rftn *       313.0       303.0       373.0       373.0s
*    rftn *       373.0       373.0       363.0       353.0s
*    rftn *       343.0       333.0       323.0       313.0s
*    rftn *       303.0       373.0       373.0       373.0s
*    rftn *       373.0       363.0       353.0       343.0s
*    rftn *       333.0       323.0       313.0       303.0s
*    rftn *       373.0       373.0       373.0       373.0s
*    rftn *       363.0       353.0       343.0       333.0s
*    rftn *       323.0       313.0       303.0       373.0s
*    rftn *       373.0       373.0       373.0       363.0s
*    rftn *       353.0       343.0       333.0       323.0s
*    rftn *       313.0       303.0       373.0       373.0s
*    rftn *       373.0       373.0       363.0       353.0s
*    rftn *       343.0       333.0       323.0       313.0s
*    rftn *       303.0       373.0       373.0       373.0s
*    rftn *       373.0       363.0       353.0       343.0s
*    rftn *       333.0       323.0       313.0       303.0s
*    rftn *       373.0       373.0       373.0       373.0s
*    rftn *       363.0       353.0       343.0       333.0s
*    rftn *       323.0       313.0       303.0       373.0s
*    rftn *       373.0       373.0       373.0       363.0s
*    rftn *       353.0       343.0       333.0       323.0s
*    rftn *       313.0       303.0       373.0       373.0s
*    rftn *       373.0       373.0       363.0       353.0s
*    rftn *       343.0       333.0       323.0       313.0s
*    rftn *       303.0e
*
*******   type           num        userid                component name
htstr                    121             1                        unnamed
*       nzhstr          ittc         hscyl          ichf
              6             0             1             1
*    nofuelrod         plane        liqlev        iaxcnd         pdrat
              1             3             1             0           0.0
*         nmwrx          nfci         nfcil          hdri          hdro
              0             0             1           0.0           0.0
*         nhot         nodes          fmon         nzmax       reflood
              0             6             0           100             0
*     dtxht(1)      dtxht(2)         dznht         hgapo
            0.0           0.0       1.0E-3        6300.0
*
*  idbcin *           2           2           2           2s
*  idbcin *           2           2e
*  idbcon *           5           5           5           5s
*  idbcon *           5           5e
```

```
* hcomon1 *         111           1           0           0e
* hcomon1 *         111           2           0           0e
* hcomon1 *         111           3           0           0e
* hcomon1 *         111           4           0           0e
* hcomon1 *         111           5           0           0e
* hcomon1 *         111           6           0           0e
* tsurfo2 *       293.0e
* tsurfo2 *       293.0e
* tsurfo2 *       293.0e
* tsurfo2 *       293.0e
* tsurfo2 *       293.0e
* tsurfo2 *       293.0e
* dhtstrz *     0.10525     0.10525     0.10525     0.10525s
* dhtstrz *     0.10525     0.10525e
*   rdx   *          1.0e
*  radrd  *    3.175E-3   3.5052E-3   3.8354E-3   4.1656E-3   4.4958E-3s
*  radrd  *    4.826E-3e
*  matrd  *          50          50          50          50 s
*  matrd  *          50 e
*    nfax *           1           1           1           1s
*    nfax *           1           1e
*    rftn *       378.0       378.0       378.0       378.0s
*    rftn *       378.0       378.0       378.0       378.0s
*    rftn *       378.0       378.0       378.0       378.0s
*    rftn *       378.0       378.0       378.0       378.0s
*    rftn *       378.0       378.0       378.0       378.0s
*    rftn *       378.0       378.0       378.0       378.0s
*    rftn *       378.0       378.0       378.0       378.0s
*    rftn *       378.0       378.0       378.0       378.0s
*    rftn *       378.0       378.0       378.0       378.0e
*
*******   type           num        userid                component name
htstr                    122             1                       unnamed
*       nzhstr          ittc         hscyl          ichf
              6             0             1             1
*    nofuelrod         plane        liqlev        iaxcnd         pdrat
              1             3             1             0           0.0
*        nmwrx          nfci         nfcil          hdri          hdro
              0             0             1           0.0           0.0
*         nhot         nodes          fmon         nzmax       reflood
              0             6             0           100             0
*     dtxht(1)      dtxht(2)         dznht         hgapo
            0.0           0.0        1.0E-3        6300.0
*
*  idbcin *           2           2           2           2s
*  idbcin *           2           2e
*  idbcon *           5           5           5           5s
*  idbcon *           5           5e
* hcomon1 *         112           1           0           0e
* hcomon1 *         112           2           0           0e
* hcomon1 *         112           3           0           0e
* hcomon1 *         112           4           0           0e
* hcomon1 *         112           5           0           0e
* hcomon1 *         112           6           0           0e
* tsurfo2 *       293.0e
* tsurfo2 *       293.0e
* tsurfo2 *       293.0e
* tsurfo2 *       293.0e
* tsurfo2 *       293.0e
* tsurfo2 *       293.0e
* dhtstrz *   0.0894667   0.0894667   0.0894667   0.0894667s
* dhtstrz *   0.0894667   0.0894667e
*   rdx   *          1.0e
*  radrd  *    3.175E-3   3.5052E-3   3.8354E-3   4.1656E-3   4.4958E-3s
*  radrd  *    4.826E-3e
*  matrd  *          50          50          50          50 s
*  matrd  *          50 e
*    nfax *           1           1           1           1s
*    nfax *           1           1e
*    rftn *       373.0       373.0       373.0       373.0s
*    rftn *       373.0       373.0       373.0       373.0s
```

```
*    rftn *       373.0       373.0       373.0       373.0s
*    rftn *       373.0       373.0       373.0       373.0s
*    rftn *       373.0       373.0       373.0       373.0s
*    rftn *       373.0       373.0       373.0       373.0s
*    rftn *       373.0       373.0       373.0       373.0s
*    rftn *       373.0       373.0       373.0       373.0s
*    rftn *       373.0       373.0       373.0       373.0e
*
*******   type           num        userid                component name
htstr                    132             1                        unnamed
*       nzhstr          ittc         hscyl          ichf
              3             0             1             1
*    nofuelrod         plane        liqlev        iaxcnd         pdrat
              1             3             1             0          0.0
*        nmwrx          nfci         nfcil          hdri          hdro
              0             0             1           0.0           0.0
*         nhot         nodes          fmon         nzmax       reflood
              0            10             0           100             0
*     dtxht(1)      dtxht(2)         dznht         hgapo
            0.0           0.0        1.0E-3        6300.0
*
*  idbcin *           2           2           2e
*  idbcon *           5           5           5e
* hcomon1 *          31           1           0           0e
* hcomon1 *          31           2           0           0e
* hcomon1 *          31           3           0           0e
* tsurfo2 *       293.0e
* tsurfo2 *       293.0e
* tsurfo2 *       293.0e
* dhtstrz *      0.6196      0.6196      0.6196e
*   rdx   *          1.0e
*  radrd  *      0.0127 0.013205178 0.013710356 0.014215533 0.014720711s
*  radrd  * 0.015225889 0.015731067 0.016236244 0.016741422   0.0172466e
*  matrd  *          51          51          51          51 s
*  matrd  *          51          51          51          51 s
*  matrd  *          51 e
*    nfax *           1           1           1e
*    rftn *       293.0       293.0       293.0       293.0s
*    rftn *       293.0       293.0       293.0       293.0s
*    rftn *       293.0       293.0       293.0       293.0s
*    rftn *       293.0       293.0       293.0       293.0s
*    rftn *       293.0       293.0       293.0       293.0s
*    rftn *       293.0       293.0       293.0       293.0s
*    rftn *       293.0       293.0       293.0       293.0s
*    rftn *       293.0       293.0       293.0e
*
*******   type           num        userid                component name
htstr                    141             1                        unnamed
*       nzhstr          ittc         hscyl          ichf
              3             0             1             1
*    nofuelrod         plane        liqlev        iaxcnd         pdrat
              1             3             1             0          0.0
*        nmwrx          nfci         nfcil          hdri          hdro
              0             0             1           0.0           0.0
*         nhot         nodes          fmon         nzmax       reflood
              0            10             0           100             0
*     dtxht(1)      dtxht(2)         dznht         hgapo
            0.0           0.0        1.0E-3        6300.0
*
*  idbcin *           2           2           2e
*  idbcon *           2           2           2e
* hcomon1 *          21           1           0           0e
* hcomon1 *          21           2           0           0e
* hcomon1 *          21           3           0           0e
* hcomon2 *          31           1           0           0e
* hcomon2 *          31           2           0           0e
* hcomon2 *          31           3           0           0e
* dhtstrz *      0.6196      0.6196      0.6196e
*   rdx   *          1.0e
*  radrd  *    3.175E-3  3.35844E-3  3.54189E-3  3.72533E-3  3.90878E-3s
*  radrd  *  4.09222E-3  4.27567E-3  4.45911E-3  4.64256E-3    4.826E-3e
```

```
*  matrd  *          50          50          50          50 s
*  matrd  *          50          50          50          50 s
*  matrd  *          50 e
*    nfax *           1           1           1e
*    rftn *       293.0       293.0       293.0       293.0s
*    rftn *       293.0       293.0       293.0       293.0s
*    rftn *       293.0       293.0       293.0       293.0s
*    rftn *       293.0       293.0       293.0       293.0s
*    rftn *       293.0       293.0       293.0       293.0s
*    rftn *       293.0       293.0       293.0       293.0s
*    rftn *       293.0       293.0       293.0       293.0s
*    rftn *       293.0       293.0e
*
*******   type           num        userid                component name
htstr                    161             1                       unnamed
*       nzhstr          ittc         hscyl          ichf
             3             0             1             1
*    nofuelrod         plane        liqlev        iaxcnd         pdrat
             1             3             1             0           0.0
*        nmwrx          nfci         nfcil          hdri          hdro
             0             0             1           0.0           0.0
*         nhot         nodes          fmon         nzmax       reflood
             0            11             0           100             0
*     dtxht(1)      dtxht(2)         dznht         hgapo
           0.0           0.0       1.0E-3        6300.0
*
*  idbcin *           2           2           2e
*  idbcon *           5           5           5e
* hcomon1 *          11           1           0           0e
* hcomon1 *          11           2           0           0e
* hcomon1 *          11           3           0           0e
* tsurfo2 *       293.0e
* tsurfo2 *       293.0e
* tsurfo2 *       293.0e
* dhtstrz *  0.58709091  0.58709091  0.58709091e
*   rdx   *         1.0e
*  radrd  *    0.038965    0.043325      0.0445    0.052045    0.056405s
*  radrd  *    0.060765    0.065125    0.069485    0.073845    0.078205s
*  radrd  *    0.082565e
*  matrd  *           9           9          52          52 s
*  matrd  *          52          52          52          52 s
*  matrd  *          52          52 e
*    nfax *           1           1           1e
*    rftn *       378.0       378.0       378.0       368.0s
*    rftn *       358.0       348.0       338.0       328.0s
*    rftn *       318.0       308.0       298.0       378.0s
*    rftn *       378.0       378.0       368.0       358.0s
*    rftn *       348.0       338.0       328.0       318.0s
*    rftn *       308.0       298.0       378.0       378.0s
*    rftn *       378.0       368.0       358.0       348.0s
*    rftn *       338.0       328.0       318.0       308.0s
*    rftn *       298.0e
*
*******   type           num        userid                component name
htstr                    171             1                       unnamed
*       nzhstr          ittc         hscyl          ichf
            33             0             1             1
*    nofuelrod         plane        liqlev        iaxcnd         pdrat
             1             3             1             0           0.0
*        nmwrx          nfci         nfcil          hdri          hdro
             0             0             1           0.0           0.0
*         nhot         nodes          fmon         nzmax       reflood
             0            11             0           210             0
*     dtxht(1)      dtxht(2)         dznht         hgapo
           0.0           0.0       1.0E-3        6300.0
*
*  idbcin *           2           2           2           2s
*  idbcin *           2           2           2           2s
*  idbcin *           2           2           2           0s
*  idbcin *           0           0           0           0s
*  idbcin *           0           0           0           0s
```

```
*  idbcin *          0           0           0           0s
*  idbcin *          0           0           0           0s
*  idbcin *          0           0           0           0s
*  idbcin *          0e
*  idbcon *          5           5           5           5s
*  idbcon *          5           5           5           5s
*  idbcon *          5           5           5           5s
*  idbcon *          5           5           5           5s
*  idbcon *          5           5           5           5s
*  idbcon *          5           5           5           5s
*  idbcon *          5           5           5           5s
*  idbcon *          5           5           5           5s
*  idbcon *          5e
* hcomon1 *         41           1           1           1e
* hcomon1 *         41           1           1           2e
* hcomon1 *         41           1           1           3e
* hcomon1 *         41           1           1           4e
* hcomon1 *         41           1           1           5e
* hcomon1 *         41           1           1           6e
* hcomon1 *         41           1           1           7e
* hcomon1 *         41           1           1           8e
* hcomon1 *         41           1           1           9e
* hcomon1 *         41           1           1          10e
* hcomon1 *         41           1           1          11e
*qflxbco1 *        0.0e
*qflxbco1 *        0.0e
*qflxbco1 *        0.0e
*qflxbco1 *        0.0e
*qflxbco1 *        0.0e
*qflxbco1 *        0.0e
*qflxbco1 *        0.0e
*qflxbco1 *        0.0e
*qflxbco1 *        0.0e
*qflxbco1 *        0.0e
*qflxbco1 *        0.0e
*qflxbco1 *        0.0e
*qflxbco1 *        0.0e
*qflxbco1 *        0.0e
*qflxbco1 *        0.0e
*qflxbco1 *        0.0e
*qflxbco1 *        0.0e
*qflxbco1 *        0.0e
*qflxbco1 *        0.0e
*qflxbco1 *        0.0e
*qflxbco1 *        0.0e
*qflxbco1 *        0.0e
* tsurfo2 *      293.0e
* tsurfo2 *      293.0e
* tsurfo2 *      293.0e
* tsurfo2 *      293.0e
* tsurfo2 *      293.0e
* tsurfo2 *      293.0e
* tsurfo2 *      293.0e
* tsurfo2 *      293.0e
* tsurfo2 *      293.0e
* tsurfo2 *      293.0e
* tsurfo2 *      293.0e
* tsurfo2 *      293.0e
* tsurfo2 *      293.0e
* tsurfo2 *      293.0e
* tsurfo2 *      293.0e
* tsurfo2 *      293.0e
* tsurfo2 *      293.0e
* tsurfo2 *      293.0e
* tsurfo2 *      293.0e
* tsurfo2 *      293.0e
* tsurfo2 *      293.0e
* tsurfo2 *      293.0e
* tsurfo2 *      293.0e
* tsurfo2 *      293.0e
* tsurfo2 *      293.0e
```

```
* tsurfo2 *       293.0e
* tsurfo2 *       293.0e
* tsurfo2 *       293.0e
* tsurfo2 *       293.0e
* tsurfo2 *       293.0e
* tsurfo2 *       293.0e
* tsurfo2 *       293.0e
* tsurfo2 *       293.0e
* dhtstrz *  0.39315152  0.19393939  0.39315152  0.19393939s
* dhtstrz *  0.39315152  0.19393939  0.39315152  0.19393939s
* dhtstrz *  0.39315152  0.19393939  0.39315152  0.19393939s
* dhtstrz *  0.39315152  0.19393939  0.39315152  0.19393939s
* dhtstrz *  0.39315152  0.19393939  0.39315152  0.19393939s
* dhtstrz *  0.39315152  0.19393939  0.19393939  0.19393939s
* dhtstrz *  0.19393939  0.19393939  0.19393939  0.19393939s
* dhtstrz *  0.19393939  0.19393939  0.19393939  0.19393939s
* dhtstrz *  0.19393939e
*   rdx   *         0.25e
*  radrd  *    0.038965 0.039222676 0.039265404    0.052045    0.056405s
*  radrd  *    0.060765    0.065125    0.069485    0.073845    0.078205s
*  radrd  *    0.082565e
*  matrd  *          9           9          52          52 s
*  matrd  *         52          52          52          52 s
*  matrd  *         52          52 e
*    nfax *          1           1           1           1s
*    nfax *          1           1           1           1s
*    nfax *          1           1           1           1s
*    nfax *          1           1           1           1s
*    nfax *          1           1           1           1s
*    nfax *          1           1           1           1s
*    nfax *          1           1           1           1s
*    nfax *          1           1           1           1s
*    nfax *          1e
*    rftn *      373.0       373.0       373.0       373.0s
*    rftn *      363.0       353.0       343.0       333.0s
*    rftn *      323.0       313.0       303.0       373.0s
*    rftn *      373.0       373.0       373.0       363.0s
*    rftn *      353.0       343.0       333.0       323.0s
*    rftn *      313.0       303.0       373.0       373.0s
*    rftn *      373.0       373.0       363.0       353.0s
*    rftn *      343.0       333.0       323.0       313.0s
*    rftn *      303.0       373.0       373.0       373.0s
*    rftn *      373.0       363.0       353.0       343.0s
*    rftn *      333.0       323.0       313.0       303.0s
*    rftn *      373.0       373.0       373.0       373.0s
*    rftn *      363.0       353.0       343.0       333.0s
*    rftn *      323.0       313.0       303.0       373.0s
*    rftn *      373.0       373.0       373.0       363.0s
*    rftn *      353.0       343.0       333.0       323.0s
*    rftn *      313.0       303.0       373.0       373.0s
*    rftn *      373.0       373.0       363.0       353.0s
*    rftn *      343.0       333.0       323.0       313.0s
*    rftn *      303.0       373.0       373.0       373.0s
*    rftn *      373.0       363.0       353.0       343.0s
*    rftn *      333.0       323.0       313.0       303.0s
*    rftn *      373.0       373.0       373.0       373.0s
*    rftn *      363.0       353.0       343.0       333.0s
*    rftn *      323.0       313.0       303.0       373.0s
*    rftn *      373.0       373.0       373.0       363.0s
*    rftn *      353.0       343.0       333.0       323.0s
*    rftn *      313.0       303.0       373.0       373.0s
*    rftn *      373.0       373.0       363.0       353.0s
*    rftn *      343.0       333.0       323.0       313.0s
*    rftn *      303.0       373.0       373.0       373.0s
*    rftn *      373.0       363.0       353.0       343.0s
*    rftn *      333.0       323.0       313.0       303.0s
*    rftn *      373.0       373.0       373.0       373.0s
*    rftn *      363.0       353.0       343.0       333.0s
*    rftn *      323.0       313.0       303.0       373.0s
*    rftn *      373.0       373.0       373.0       363.0s
*    rftn *      353.0       343.0       333.0       323.0s
```

```
*    rftn *       313.0       303.0       373.0       373.0s
*    rftn *       373.0       373.0       363.0       353.0s
*    rftn *       343.0       333.0       323.0       313.0s
*    rftn *       303.0       373.0       373.0       373.0s
*    rftn *       373.0       363.0       353.0       343.0s
*    rftn *       333.0       323.0       313.0       303.0s
*    rftn *       373.0       373.0       373.0       373.0s
*    rftn *       363.0       353.0       343.0       333.0s
*    rftn *       323.0       313.0       303.0       373.0s
*    rftn *       373.0       373.0       373.0       363.0s
*    rftn *       353.0       343.0       333.0       323.0s
*    rftn *       313.0       303.0       373.0       373.0s
*    rftn *       373.0       373.0       363.0       353.0s
*    rftn *       343.0       333.0       323.0       313.0s
*    rftn *       303.0       373.0       373.0       373.0s
*    rftn *       373.0       363.0       353.0       343.0s
*    rftn *       333.0       323.0       313.0       303.0s
*    rftn *       373.0       373.0       373.0       373.0s
*    rftn *       363.0       353.0       343.0       333.0s
*    rftn *       323.0       313.0       303.0       373.0s
*    rftn *       373.0       373.0       373.0       363.0s
*    rftn *       353.0       343.0       333.0       323.0s
*    rftn *       313.0       303.0       373.0       373.0s
*    rftn *       373.0       373.0       363.0       353.0s
*    rftn *       343.0       333.0       323.0       313.0s
*    rftn *       303.0       373.0       373.0       373.0s
*    rftn *       373.0       363.0       353.0       343.0s
*    rftn *       333.0       323.0       313.0       303.0s
*    rftn *       373.0       373.0       373.0       373.0s
*    rftn *       363.0       353.0       343.0       333.0s
*    rftn *       323.0       313.0       303.0       373.0s
*    rftn *       373.0       373.0       373.0       363.0s
*    rftn *       353.0       343.0       333.0       323.0s
*    rftn *       313.0       303.0       373.0       373.0s
*    rftn *       373.0       373.0       363.0       353.0s
*    rftn *       343.0       333.0       323.0       313.0s
*    rftn *       303.0       373.0       373.0       373.0s
*    rftn *       373.0       363.0       353.0       343.0s
*    rftn *       333.0       323.0       313.0       303.0s
*    rftn *       373.0       373.0       373.0       373.0s
*    rftn *       363.0       353.0       343.0       333.0s
*    rftn *       323.0       313.0       303.0       373.0s
*    rftn *       373.0       373.0       373.0       363.0s
*    rftn *       353.0       343.0       333.0       323.0s
*    rftn *       313.0       303.0       373.0       373.0s
*    rftn *       373.0       373.0       363.0       353.0s
*    rftn *       343.0       333.0       323.0       313.0s
*    rftn *       303.0       373.0       373.0       373.0s
*    rftn *       373.0       363.0       353.0       343.0s
*    rftn *       333.0       323.0       313.0       303.0s
*    rftn *       373.0       373.0       373.0       373.0s
*    rftn *       363.0       353.0       343.0       333.0s
*    rftn *       323.0       313.0       303.0e
*
*******   type           num        userid                component name
htstr                    181             1                       unnamed
*       nzhstr          ittc         hscyl          ichf
            33             0             1             1
*    nofuelrod         plane        liqlev        iaxcnd         pdrat
             1             3             1             0           0.0
*        nmwrx          nfci         nfcil          hdri          hdro
             0             0             1           0.0           0.0
*         nhot         nodes          fmon         nzmax       reflood
             0            11             0           210             0
*     dtxht(1)     dtxht(2)         dznht         hgapo
           0.0           0.0       1.0E-3        6300.0
*
*  idbcin *           2           2           2           2s
*  idbcin *           2           2           2           2s
*  idbcin *           2           2           2           0s
*  idbcin *           0           0           0           0s
```

```
*  idbcin *          0           0           0           0s
*  idbcin *          0           0           0           0s
*  idbcin *          0           0           0           0s
*  idbcin *          0           0           0           0s
*  idbcin *          0e
*  idbcon *          5           5           5           5s
*  idbcon *          5           5           5           5s
*  idbcon *          5           5           5           5s
*  idbcon *          5           5           5           5s
*  idbcon *          5           5           5           5s
*  idbcon *          5           5           5           5s
*  idbcon *          5           5           5           5s
*  idbcon *          5           5           5           5s
*  idbcon *          5e
* hcomon1 *         41           1           1           1e
* hcomon1 *         41           1           1           2e
* hcomon1 *         41           1           1           3e
* hcomon1 *         41           1           1           4e
* hcomon1 *         41           1           1           5e
* hcomon1 *         41           1           1           6e
* hcomon1 *         41           1           1           7e
* hcomon1 *         41           1           1           8e
* hcomon1 *         41           1           1           9e
* hcomon1 *         41           1           1          10e
* hcomon1 *         41           1           1          11e
*qflxbco1 *        0.0e
*qflxbco1 *        0.0e
*qflxbco1 *        0.0e
*qflxbco1 *        0.0e
*qflxbco1 *        0.0e
*qflxbco1 *        0.0e
*qflxbco1 *        0.0e
*qflxbco1 *        0.0e
*qflxbco1 *        0.0e
*qflxbco1 *        0.0e
*qflxbco1 *        0.0e
*qflxbco1 *        0.0e
*qflxbco1 *        0.0e
*qflxbco1 *        0.0e
*qflxbco1 *        0.0e
*qflxbco1 *        0.0e
*qflxbco1 *        0.0e
*qflxbco1 *        0.0e
*qflxbco1 *        0.0e
*qflxbco1 *        0.0e
*qflxbco1 *        0.0e
*qflxbco1 *        0.0e
* tsurfo2 *      293.0e
* tsurfo2 *      293.0e
* tsurfo2 *      293.0e
* tsurfo2 *      293.0e
* tsurfo2 *      293.0e
* tsurfo2 *      293.0e
* tsurfo2 *      293.0e
* tsurfo2 *      293.0e
* tsurfo2 *      293.0e
* tsurfo2 *      293.0e
* tsurfo2 *      293.0e
* tsurfo2 *      293.0e
* tsurfo2 *      293.0e
* tsurfo2 *      293.0e
* tsurfo2 *      293.0e
* tsurfo2 *      293.0e
* tsurfo2 *      293.0e
* tsurfo2 *      293.0e
* tsurfo2 *      293.0e
* tsurfo2 *      293.0e
* tsurfo2 *      293.0e
* tsurfo2 *      293.0e
* tsurfo2 *      293.0e
* tsurfo2 *      293.0e
```

```
* tsurfo2 *       293.0e
* tsurfo2 *       293.0e
* tsurfo2 *       293.0e
* tsurfo2 *       293.0e
* tsurfo2 *       293.0e
* tsurfo2 *       293.0e
* tsurfo2 *       293.0e
* tsurfo2 *       293.0e
* tsurfo2 *       293.0e
* dhtstrz *  0.39315152  0.19393939  0.39315152  0.19393939s
* dhtstrz *  0.39315152  0.19393939  0.39315152  0.19393939s
* dhtstrz *  0.39315152  0.19393939  0.39315152  0.19393939s
* dhtstrz *  0.39315152  0.19393939  0.39315152  0.19393939s
* dhtstrz *  0.39315152  0.19393939  0.39315152  0.19393939s
* dhtstrz *  0.39315152  0.19393939  0.19393939  0.19393939s
* dhtstrz *  0.19393939  0.19393939  0.19393939  0.19393939s
* dhtstrz *  0.19393939  0.19393939  0.19393939  0.19393939s
* dhtstrz *  0.19393939e
*   rdx   *        0.125e
*  radrd  *    0.038965 0.039222676 0.039265404    0.052045    0.056405s
*  radrd  *    0.060765    0.065125    0.069485    0.073845    0.078205s
*  radrd  *    0.082565e
*  matrd  *          9           9          52          52 s
*  matrd  *         52          52          52          52 s
*  matrd  *         52          52 e
*    nfax *          1           1           1           1s
*    nfax *          1           1           1           1s
*    nfax *          1           1           1           1s
*    nfax *          1           1           1           1s
*    nfax *          1           1           1           1s
*    nfax *          1           1           1           1s
*    nfax *          1           1           1           1s
*    nfax *          1           1           1           1s
*    nfax *          1e
*    rftn *      373.0       373.0       373.0       373.0s
*    rftn *      363.0       353.0       343.0       333.0s
*    rftn *      323.0       313.0       303.0       373.0s
*    rftn *      373.0       373.0       373.0       363.0s
*    rftn *      353.0       343.0       333.0       323.0s
*    rftn *      313.0       303.0       373.0       373.0s
*    rftn *      373.0       373.0       363.0       353.0s
*    rftn *      343.0       333.0       323.0       313.0s
*    rftn *      303.0       373.0       373.0       373.0s
*    rftn *      373.0       363.0       353.0       343.0s
*    rftn *      333.0       323.0       313.0       303.0s
*    rftn *      373.0       373.0       373.0       373.0s
*    rftn *      363.0       353.0       343.0       333.0s
*    rftn *      323.0       313.0       303.0       373.0s
*    rftn *      373.0       373.0       373.0       363.0s
*    rftn *      353.0       343.0       333.0       323.0s
*    rftn *      313.0       303.0       373.0       373.0s
*    rftn *      373.0       373.0       363.0       353.0s
*    rftn *      343.0       333.0       323.0       313.0s
*    rftn *      303.0       373.0       373.0       373.0s
*    rftn *      373.0       363.0       353.0       343.0s
*    rftn *      333.0       323.0       313.0       303.0s
*    rftn *      373.0       373.0       373.0       373.0s
*    rftn *      363.0       353.0       343.0       333.0s
*    rftn *      323.0       313.0       303.0       373.0s
*    rftn *      373.0       373.0       373.0       363.0s
*    rftn *      353.0       343.0       333.0       323.0s
*    rftn *      313.0       303.0       373.0       373.0s
*    rftn *      373.0       373.0       363.0       353.0s
*    rftn *      343.0       333.0       323.0       313.0s
*    rftn *      303.0       373.0       373.0       373.0s
*    rftn *      373.0       363.0       353.0       343.0s
*    rftn *      333.0       323.0       313.0       303.0s
*    rftn *      373.0       373.0       373.0       373.0s
*    rftn *      363.0       353.0       343.0       333.0s
*    rftn *      323.0       313.0       303.0       373.0s
*    rftn *      373.0       373.0       373.0       363.0s
```

```
*    rftn *       353.0       343.0       333.0       323.0s
*    rftn *       313.0       303.0       373.0       373.0s
*    rftn *       373.0       373.0       363.0       353.0s
*    rftn *       343.0       333.0       323.0       313.0s
*    rftn *       303.0       373.0       373.0       373.0s
*    rftn *       373.0       363.0       353.0       343.0s
*    rftn *       333.0       323.0       313.0       303.0s
*    rftn *       373.0       373.0       373.0       373.0s
*    rftn *       363.0       353.0       343.0       333.0s
*    rftn *       323.0       313.0       303.0       373.0s
*    rftn *       373.0       373.0       373.0       363.0s
*    rftn *       353.0       343.0       333.0       323.0s
*    rftn *       313.0       303.0       373.0       373.0s
*    rftn *       373.0       373.0       363.0       353.0s
*    rftn *       343.0       333.0       323.0       313.0s
*    rftn *       303.0       373.0       373.0       373.0s
*    rftn *       373.0       363.0       353.0       343.0s
*    rftn *       333.0       323.0       313.0       303.0s
*    rftn *       373.0       373.0       373.0       373.0s
*    rftn *       363.0       353.0       343.0       333.0s
*    rftn *       323.0       313.0       303.0       373.0s
*    rftn *       373.0       373.0       373.0       363.0s
*    rftn *       353.0       343.0       333.0       323.0s
*    rftn *       313.0       303.0       373.0       373.0s
*    rftn *       373.0       373.0       363.0       353.0s
*    rftn *       343.0       333.0       323.0       313.0s
*    rftn *       303.0       373.0       373.0       373.0s
*    rftn *       373.0       363.0       353.0       343.0s
*    rftn *       333.0       323.0       313.0       303.0s
*    rftn *       373.0       373.0       373.0       373.0s
*    rftn *       363.0       353.0       343.0       333.0s
*    rftn *       323.0       313.0       303.0       373.0s
*    rftn *       373.0       373.0       373.0       363.0s
*    rftn *       353.0       343.0       333.0       323.0s
*    rftn *       313.0       303.0       373.0       373.0s
*    rftn *       373.0       373.0       363.0       353.0s
*    rftn *       343.0       333.0       323.0       313.0s
*    rftn *       303.0       373.0       373.0       373.0s
*    rftn *       373.0       363.0       353.0       343.0s
*    rftn *       333.0       323.0       313.0       303.0s
*    rftn *       373.0       373.0       373.0       373.0s
*    rftn *       363.0       353.0       343.0       333.0s
*    rftn *       323.0       313.0       303.0       373.0s
*    rftn *       373.0       373.0       373.0       363.0s
*    rftn *       353.0       343.0       333.0       323.0s
*    rftn *       313.0       303.0       373.0       373.0s
*    rftn *       373.0       373.0       363.0       353.0s
*    rftn *       343.0       333.0       323.0       313.0s
*    rftn *       303.0       373.0       373.0       373.0s
*    rftn *       373.0       363.0       353.0       343.0s
*    rftn *       333.0       323.0       313.0       303.0s
*    rftn *       373.0       373.0       373.0       373.0s
*    rftn *       363.0       353.0       343.0       333.0s
*    rftn *       323.0       313.0       303.0e
*
*******   type           num        userid                component name
htstr                    191             1                       unnamed
*       nzhstr          ittc         hscyl          ichf
            33             0             1             1
*    nofuelrod         plane        liqlev        iaxcnd         pdrat
             1             3             1             0           0.0
*        nmwrx          nfci         nfcil          hdri          hdro
             0             0             1           0.0           0.0
*         nhot         nodes          fmon         nzmax       reflood
             0            11             0           210             0
*     dtxht(1)      dtxht(2)         dznht         hgapo
           0.0           0.0        1.0E-3        6300.0
*
*  idbcin *           2           2           2           2s
*  idbcin *           2           2           2           2s
*  idbcin *           2           2           2           0s
```

```
*  idbcin *         0           0           0           0s
*  idbcin *         0           0           0           0s
*  idbcin *         0           0           0           0s
*  idbcin *         0           0           0           0s
*  idbcin *         0           0           0           0s
*  idbcin *         0e
*  idbcon *         5           5           5           5s
*  idbcon *         5           5           5           5s
*  idbcon *         5           5           5           5s
*  idbcon *         5           5           5           5s
*  idbcon *         5           5           5           5s
*  idbcon *         5           5           5           5s
*  idbcon *         5           5           5           5s
*  idbcon *         5           5           5           5s
*  idbcon *         5e
* hcomon1 *        41           1           1           1e
* hcomon1 *        41           1           1           2e
* hcomon1 *        41           1           1           3e
* hcomon1 *        41           1           1           4e
* hcomon1 *        41           1           1           5e
* hcomon1 *        41           1           1           6e
* hcomon1 *        41           1           1           7e
* hcomon1 *        41           1           1           8e
* hcomon1 *        41           1           1           9e
* hcomon1 *        41           1           1          10e
* hcomon1 *        41           1           1          11e
*qflxbco1 *       0.0e
*qflxbco1 *       0.0e
*qflxbco1 *       0.0e
*qflxbco1 *       0.0e
*qflxbco1 *       0.0e
*qflxbco1 *       0.0e
*qflxbco1 *       0.0e
*qflxbco1 *       0.0e
*qflxbco1 *       0.0e
*qflxbco1 *       0.0e
*qflxbco1 *       0.0e
*qflxbco1 *       0.0e
*qflxbco1 *       0.0e
*qflxbco1 *       0.0e
*qflxbco1 *       0.0e
*qflxbco1 *       0.0e
*qflxbco1 *       0.0e
*qflxbco1 *       0.0e
*qflxbco1 *       0.0e
*qflxbco1 *       0.0e
*qflxbco1 *       0.0e
*qflxbco1 *       0.0e
* tsurfo2 *     293.0e
* tsurfo2 *     293.0e
* tsurfo2 *     293.0e
* tsurfo2 *     293.0e
* tsurfo2 *     293.0e
* tsurfo2 *     293.0e
* tsurfo2 *     293.0e
* tsurfo2 *     293.0e
* tsurfo2 *     293.0e
* tsurfo2 *     293.0e
* tsurfo2 *     293.0e
* tsurfo2 *     293.0e
* tsurfo2 *     293.0e
* tsurfo2 *     293.0e
* tsurfo2 *     293.0e
* tsurfo2 *     293.0e
* tsurfo2 *     293.0e
* tsurfo2 *     293.0e
* tsurfo2 *     293.0e
* tsurfo2 *     293.0e
* tsurfo2 *     293.0e
* tsurfo2 *     293.0e
* tsurfo2 *     293.0e
```

```
* tsurfo2 *       293.0e
* tsurfo2 *       293.0e
* tsurfo2 *       293.0e
* tsurfo2 *       293.0e
* tsurfo2 *       293.0e
* tsurfo2 *       293.0e
* tsurfo2 *       293.0e
* tsurfo2 *       293.0e
* tsurfo2 *       293.0e
* tsurfo2 *       293.0e
* dhtstrz *  0.39315152  0.19393939  0.39315152  0.19393939s
* dhtstrz *  0.39315152  0.19393939  0.39315152  0.19393939s
* dhtstrz *  0.39315152  0.19393939  0.39315152  0.19393939s
* dhtstrz *  0.39315152  0.19393939  0.39315152  0.19393939s
* dhtstrz *  0.39315152  0.19393939  0.39315152  0.19393939s
* dhtstrz *  0.39315152  0.19393939  0.19393939  0.19393939s
* dhtstrz *  0.19393939  0.19393939  0.19393939  0.19393939s
* dhtstrz *  0.19393939  0.19393939  0.19393939  0.19393939s
* dhtstrz *  0.19393939e
*   rdx   *        0.125e
*  radrd  *    0.038965 0.039222676 0.039265404    0.052045    0.056405s
*  radrd  *    0.060765    0.065125    0.069485    0.073845    0.078205s
*  radrd  *    0.082565e
*  matrd  *           9           9          52          52 s
*  matrd  *          52          52          52          52 s
*  matrd  *          52          52 e
*    nfax *           1           1           1           1s
*    nfax *           1           1           1           1s
*    nfax *           1           1           1           1s
*    nfax *           1           1           1           1s
*    nfax *           1           1           1           1s
*    nfax *           1           1           1           1s
*    nfax *           1           1           1           1s
*    nfax *           1           1           1           1s
*    nfax *           1e
*    rftn *       373.0       373.0       373.0       373.0s
*    rftn *       363.0       353.0       343.0       333.0s
*    rftn *       323.0       313.0       303.0       373.0s
*    rftn *       373.0       373.0       373.0       363.0s
*    rftn *       353.0       343.0       333.0       323.0s
*    rftn *       313.0       303.0       373.0       373.0s
*    rftn *       373.0       373.0       363.0       353.0s
*    rftn *       343.0       333.0       323.0       313.0s
*    rftn *       303.0       373.0       373.0       373.0s
*    rftn *       373.0       363.0       353.0       343.0s
*    rftn *       333.0       323.0       313.0       303.0s
*    rftn *       373.0       373.0       373.0       373.0s
*    rftn *       363.0       353.0       343.0       333.0s
*    rftn *       323.0       313.0       303.0       373.0s
*    rftn *       373.0       373.0       373.0       363.0s
*    rftn *       353.0       343.0       333.0       323.0s
*    rftn *       313.0       303.0       373.0       373.0s
*    rftn *       373.0       373.0       363.0       353.0s
*    rftn *       343.0       333.0       323.0       313.0s
*    rftn *       303.0       373.0       373.0       373.0s
*    rftn *       373.0       363.0       353.0       343.0s
*    rftn *       333.0       323.0       313.0       303.0s
*    rftn *       373.0       373.0       373.0       373.0s
*    rftn *       363.0       353.0       343.0       333.0s
*    rftn *       323.0       313.0       303.0       373.0s
*    rftn *       373.0       373.0       373.0       363.0s
*    rftn *       353.0       343.0       333.0       323.0s
*    rftn *       313.0       303.0       373.0       373.0s
*    rftn *       373.0       373.0       363.0       353.0s
*    rftn *       343.0       333.0       323.0       313.0s
*    rftn *       303.0       373.0       373.0       373.0s
*    rftn *       373.0       363.0       353.0       343.0s
*    rftn *       333.0       323.0       313.0       303.0s
*    rftn *       373.0       373.0       373.0       373.0s
*    rftn *       363.0       353.0       343.0       333.0s
*    rftn *       323.0       313.0       303.0       373.0s
```

```
*    rftn *       373.0       373.0       373.0       363.0s
*    rftn *       353.0       343.0       333.0       323.0s
*    rftn *       313.0       303.0       373.0       373.0s
*    rftn *       373.0       373.0       363.0       353.0s
*    rftn *       343.0       333.0       323.0       313.0s
*    rftn *       303.0       373.0       373.0       373.0s
*    rftn *       373.0       363.0       353.0       343.0s
*    rftn *       333.0       323.0       313.0       303.0s
*    rftn *       373.0       373.0       373.0       373.0s
*    rftn *       363.0       353.0       343.0       333.0s
*    rftn *       323.0       313.0       303.0       373.0s
*    rftn *       373.0       373.0       373.0       363.0s
*    rftn *       353.0       343.0       333.0       323.0s
*    rftn *       313.0       303.0       373.0       373.0s
*    rftn *       373.0       373.0       363.0       353.0s
*    rftn *       343.0       333.0       323.0       313.0s
*    rftn *       303.0       373.0       373.0       373.0s
*    rftn *       373.0       363.0       353.0       343.0s
*    rftn *       333.0       323.0       313.0       303.0s
*    rftn *       373.0       373.0       373.0       373.0s
*    rftn *       363.0       353.0       343.0       333.0s
*    rftn *       323.0       313.0       303.0       373.0s
*    rftn *       373.0       373.0       373.0       363.0s
*    rftn *       353.0       343.0       333.0       323.0s
*    rftn *       313.0       303.0       373.0       373.0s
*    rftn *       373.0       373.0       363.0       353.0s
*    rftn *       343.0       333.0       323.0       313.0s
*    rftn *       303.0       373.0       373.0       373.0s
*    rftn *       373.0       363.0       353.0       343.0s
*    rftn *       333.0       323.0       313.0       303.0s
*    rftn *       373.0       373.0       373.0       373.0s
*    rftn *       363.0       353.0       343.0       333.0s
*    rftn *       323.0       313.0       303.0       373.0s
*    rftn *       373.0       373.0       373.0       363.0s
*    rftn *       353.0       343.0       333.0       323.0s
*    rftn *       313.0       303.0       373.0       373.0s
*    rftn *       373.0       373.0       363.0       353.0s
*    rftn *       343.0       333.0       323.0       313.0s
*    rftn *       303.0       373.0       373.0       373.0s
*    rftn *       373.0       363.0       353.0       343.0s
*    rftn *       333.0       323.0       313.0       303.0s
*    rftn *       373.0       373.0       373.0       373.0s
*    rftn *       363.0       353.0       343.0       333.0s
*    rftn *       323.0       313.0       303.0       373.0s
*    rftn *       373.0       373.0       373.0       363.0s
*    rftn *       353.0       343.0       333.0       323.0s
*    rftn *       313.0       303.0       373.0       373.0s
*    rftn *       373.0       373.0       363.0       353.0s
*    rftn *       343.0       333.0       323.0       313.0s
*    rftn *       303.0       373.0       373.0       373.0s
*    rftn *       373.0       363.0       353.0       343.0s
*    rftn *       333.0       323.0       313.0       303.0s
*    rftn *       373.0       373.0       373.0       373.0s
*    rftn *       363.0       353.0       343.0       333.0s
*    rftn *       323.0       313.0       303.0e
********************************************
* Finished Heat Structure Section of Model *
********************************************
*
*
*
end
*
*****************
* Timestep Data *
*****************
*        dtmin        dtmax         tend        rtwfp
       1.0E-6          1.0       7000.0         10.0
*        edint        gfint       dmpint       sedint
        100.0          1.0        100.0          1.0
*
```

```
*       endflag
           -1.0
```

Appendix H: Summary of Plot Parameters

Description	Test Instrument	TRACE	Fig. Number
Boiler pressure	MicroDAQ LOGiT	PIPE 11:3	10,15,20,25,30,43,44,46, 54,57,58
Condenser pressure	MicroDAQ LOGiT	PIPE 1:11	10,15,20,25,30,43,46,48, 49,54,57,58
Differential pressure	Omega PX409-015WDUV	N/A	14,19,24,29,34,43
Boiler temperature			
Centerline			
01	Pico TC-08, Type J	PIPE 11:1	13,18,23,28,33,44,52
11	Pico TC-08, Type J	PIPE 11:2	13,18,23,28,33,44,52
21	Pico TC-08, Type J	PIPE 11:3	13,18,23,28,33,44,52
Surface			
01	Pico TC-08, Type J	HTSTR 161: 1	13,18,23,28,33
11	Pico TC-08, Type J	HTSTR 161: 2	13,18,23,28,33
21	Pico TC-08, Type J	HTSTR 161: 3	13,18,23,28,33
Condenser temperature			
Centerline			
01	Pico TC-08, Type J	PIPE 1: 1	9,11,16,21,26,31,50,59
03	Pico TC-08, Type J	PIPE 1: 2	11,16,21,26,31,50,59
05	Pico TC-08, Type J	PIPE 1: 3	11,16,21,26,31,50,59
07	Pico TC-08, Type J	PIPE 1: 4	11,16,21,26,31,50,59
09	Pico TC-08, Type J	PIPE 1: 5	11,16,21,26,31,50,59
11	Pico TC-08, Type J	PIPE 1: 6	11,16,21,26,31,50,59
13	Pico TC-08, Type J	PIPE 1: 7	11,16,21,26,31,50,59
15	Pico TC-08, Type J	PIPE 1: 8	11,16,21,26,31,50,59
17	Pico TC-08, Type J	PIPE 1: 9	11,16,21,26,31,50,59
19	Pico TC-08, Type J	PIPE 1: 10	11,16,21,26,31,50,59
21	Pico TC-08, Type J	PIPE 1: 11	11,16,21,26,31,50,59
Surface			
01	Pico TC-08, Type J	HTSTR 101: 1	12,17,22,27,32,51
03	Pico TC-08, Type J	HTSTR 101: 2	12,17,22,27,32,51
05	Pico TC-08, Type J	HTSTR 101: 3	12,17,22,27,32,51
07	Pico TC-08, Type J	HTSTR 101: 4	12,17,22,27,32,51
09	Pico TC-08, Type J	HTSTR 101: 5	12,17,22,27,32,51
11	Pico TC-08, Type J	HTSTR 101: 6	12,17,22,27,32,51
13	Pico TC-08, Type J	HTSTR 101: 7	12,17,22,27,32,51
15	Pico TC-08, Type J	HTSTR 101: 8	12,17,22,27,32,51
17	Pico TC-08, Type J	HTSTR 101: 9	12,17,22,27,32,51
19	Pico TC-08, Type J	HTSTR 101: 10	12,17,22,27,32,51
21	Pico TC-08, Type J	HTSTR 101: 11	12,17,22,27,32,51

REFERENCES

REFERENCES

Abramson, P. B., 1985, Guide Book to Light Water Reactor Safety Analysis, Hemisphere, New York.

Applied Programming Technology, 2007a. TRACE V5.0 User's Manual, Vol. 1: Input Specifications, prepared for the U.S. NRC, Washington D.C.

Applied Programming Technology, 2007b. TRACE V5.0 Theory Manual, Vol. 1: Field Equations, Solution Methods, and Physical Models, prepared for the U.S. NRC, Washington D.C.

Bankoff, S. G., 1980. Some Condensation Studies Pertinent to LWR Safety. Int. J. Multiphase Flow 6, 51-67.

Batet, L., Reventos, F., 2001. Analysis of PANDA Experiments P3 and P6 Using RELAP5/MOD3.2, NUREG/IA-0196.

Beard, J. A., 2006. ESBWR Overview, GE Energy/Nuclear. Available online: http://www.ne.doe.gov/np2010/pdfs/esbwrOverview.pdf

Block, J. A., 1980. Condensation-driven Fluid Motion. Int. J. Multiphase Flow 6, 113-129.

Choi, K. Y., Chung, H. J., No, H. C., 2002, Direct-contact Condensation Heat Transer Model in RELAP5/MOD3.2 With/Without Noncondensable Gases for Horizontally Stratified Flow. Nucl. Eng. Des. 211 (2-3), 139-151.

Di Marzo, M., Almenas, K. K., Hsu, Y. Y., Wang, Z., 1988. The Phenomenology of a Small Break LOCA in a Complex Thermal Hydraulic Loop. Nucl. Eng. Des. 110, 107-116.

Duffey, R. B., Sursock, J. P., 1987. Natural Circulation Phenomena Relevant to Small Breaks and Transients. Nucl. Eng. Des. 102, 115-128.

Geissler, G. O., et al., 1987. MIST Test Group 30 Mapping Tests, BAW-1950, Babcock & Wilcox Company.

Hass, P. M., Knee, H. E., 1982. PKL Test on Energy Transfer Mechanisms During Small-break LOCAs, Nuclear Safety, 23, 146-154.

Heisler, M. P., 1947. Temperature Charts for Induction and Constant Temperature Heating. Trans. ASME, 69, 227-36.

Hijikata, K., Chen, S. J., Tien, C. L., 1984. Non-condensable Gas Effect on Condensation in a Two-phase Closed Thermosyphon. Int. J. Heat Mass Trans. 27(8), 1319-25.

Hochreiter, L. E., 1985. FLECHT SEASET Program Final Report, NUREG/CR-4167, U.S. NRC.

Hsu, Y. Y., et al., 1987. Observation from the UMCP 2X4 Loop Test Results Simulating B&W Power Plant Behavior, Proc. XV Water Reactor Safety Research Info. Meeting, NUREG/CP-0091, 349-371.

Incropera, F. P., Dewitt, D. P., 2002. Fundamentals of Heat and Mass Transfer, 5th ed., Ch. 5, pp. 256-260, Wiley: New York.

Information Systems Laboratory, 2010. TRACE Users Workshop Course Notes, prepared for the U.S. NRC, Potomac, MD.

Jaczko, G. B., 2011. Written Statement to the Environment and Public Works Committee and the Clean Air and Nuclear Safety Subcommittee, United States Senate, June 16th. Available online: http://www.nrc.gov/reading-rm/doc-collections/congress-docs/congress-testimony/2011.

Kirchner, W., Bankoff, S. G., 1985. Condensation Effects in Reactor Transients. Nucl. Sci. Eng. 89, 310-321.

Kloppers, J. C., Kroger, D. G., 2005. Influence of Temperature Inversions on Wet-Cooling Tower Performance. Applied Thermal Eng. 25, 1325-1336.

Kuhn, S. Z., Schrock, V. E., and Peterson, P. F., 1994. Final Report on U.C. Berkeley Single Tube Condensation Studies, UCB-NE-4201.

Locke, G. S. H., 1992. The Tubular Thermosyphon: Variations on a Theme, Oxford Univ. Press, New York.

Loomis, G. G., 1987. Summary of Semiscale Program, NUREG/CR-4945 EGG-2509, U.S. NRC.

Massoud, M., 2005. Engineering Thermofluids, Springer, New York.

Moon, Y. M., Park, H. S., Bang, Y. S., 2000. Assessment of the RELAP5/MOD3.2 for Reflux Condensation Experiment, NUREG/IA-0181, U.S. NRC.

Nalezny, C. L., 1985. Summary of the NRC's LOFT Program Research Findings, NUREG/CR-3005, U.S. NRC.

NRC Reactor Safety Code User Information Exchange Website, 2011a. http://www.nrccodes.com, accessed 15 July 2011.

NRC Website, 2011b. http://www.nrc.gov/aboutnrc/regulatory/research/comp-codes.html#th, accessed 15 May 2011.

Nuclear Energy Institute Website, 2011. http://www.nei.org/resourcesandstats /nuclear_statistics/usnuclearpowerplants/, accessed 15 May 2011.

Nuclear Energy Research Advisory Committee Report, 2002. A Technological Roadmap for Generation IV Nuclear Energy Systems, GIF-002-00, U.S. DOE.

Stadenmeier, J. L., 2011. Personal conversation with Joe Stadenmeier, senior engineer, during U.S. NRC Code Development Branch visit to U.S. Naval Academy to tour MANOTEA, July 16, 2011.

Schulz, T. L., 2006. Westinghouse AP1000 Advanced Passive Plant, Nucl. Eng. Des. 236, 1547-1557.

Steele, J. H., Thorpe, S. A., Turekian, K. K., 2009. Elements of Physical Oceanography, Academic Press, Waltham, MA.

Tagami, T., 1965. Interim Report on Safety Assessment and Facilities, Establishment Project, National Japanese Atomic Energy Research Agency.

Uchida, H., Oyama, A., Togo, Y., 1965. Evaluation of Post-incident Cooling Systems of Light-water Power Reactors. Proc. Int. Conf. on Peaceful Uses of Atomic Energy, 13, 93-102.

Wang, Z., Almenas, K., di Marzo, M., Hsu, Y. Y., Unal, C., 1992. Impact of Rapid Condensation of Large Vapor Spaces on Natural Circulation in Integral Systems. Nucl. Eng. Des. 133, 285-300.

Woods, B. G., Collins, B., 2009. RELAP-3D Modeling of PWR Steam Generator Condensation Experiments at the Oregon State University APEX Facility. Nucl. Eng. Des. 239 (10), 1925-1932.

Young, M. W., Sursock, J. P., 1987. Coordination of Safety Research for the Babcock and Wilcox Integral System Test Program. NUREG-1163, U.S. NRC.